

UNCLASSIFIED

AD NUMBER

AD921349

LIMITATION CHANGES

TO:

Approved for public release; distribution is unlimited.

FROM:

Distribution authorized to U.S. Gov't. agencies only; Test and Evaluation; JUL 1974. Other requests shall be referred to Armament Development Test Center, Eglin AFB, FL 32542.

AUTHORITY

AFATL ltr 3 Jan 1977

THIS PAGE IS UNCLASSIFIED

AEDC-TR-74-71
AFATL-TR-74-108

204.2



EFFECTS OF THE SCANA SHAPE NO. 1 TURRET ON SEPARATION OF GUIDED MK-84 WEAPONS AND THE SUU-30H/B DISPENSER FROM THE F-111E AIRCRAFT AT TRANSONIC SPEEDS

Gary R. Mattasits
ARO, Inc.

PROPULSION WIND TUNNEL FACILITY
ARNOLD ENGINEERING DEVELOPMENT CENTER
AIR FORCE SYSTEMS COMMAND
ARNOLD AIR FORCE STATION, TENNESSEE 37389

July 1974

Final Report for Period March 12 - 15, 1974

Distribution limited to U.S. Government agencies only; this report contains information on test and evaluation of military hardware; July 1974; other requests for this document must be referred to Air Force Armament Laboratory (DLJC), Eglin AFB, FL 32542.

This document has been approved for public release

per AFATL Hq. 3 Jan 77

TAB 77-6 (18 Mar 77)

210000-74-0-0001

Prepared for

JTKnator

AIR FORCE ARMAMENT LABORATORY (DLJC)
EGLIN AFB, FLORIDA 32542

NOTICES

When U. S. Government drawings specifications, or other data are used for any purpose other than a definitely related Government procurement operation, the Government thereby incurs no responsibility nor any obligation whatsoever, and the fact that the Government may have formulated, furnished, or in any way supplied the said drawings, specifications, or other data, is not to be regarded by implication or otherwise, or in any manner licensing the holder or any other person or corporation, or conveying any rights or permission to manufacture, use, or sell any patented invention that may in any way be related thereto.

Qualified users may obtain copies of this report from the Defense Documentation Center.

References to named commercial products in this report are not to be considered in any sense as an endorsement of the product by the United States Air Force or the Government.

APPROVAL STATEMENT

This technical report has been reviewed and is approved.



LAMAR R. KISSLING
Lt Colonel, USAF
Chief Air Force Test Director, PWT
Directorate of Test



FRANK J. PASSARELLO
Colonel, USAF
Director of Test

UNCLASSIFIED

SECURITY CLASSIFICATION OF THIS PAGE (When Data Entered)

REPORT DOCUMENTATION PAGE		READ INSTRUCTIONS BEFORE COMPLETING FORM
1. REPORT NUMBER AEDC-TR-74-71 AFATL-TR-74-108	2. GOVT ACCESSION NO.	3. RECIPIENT'S CATALOG NUMBER
4. TITLE (and Subtitle) EFFECTS OF THE SCANA SHAPE NO. 1 TURRET ON SEPARATION OF GUIDED MK-84 WEAPONS AND THE SUU-30H/B DISPENSER FROM THE F-111E AIRCRAFT AT TRANSONIC SPEEDS		5. TYPE OF REPORT & PERIOD COVERED Final Report, March 12 to 15, 1974
7. AUTHOR(s) Gary R. Mattasits, ARO, Inc.		6. PERFORMING ORG. REPORT NUMBER
9. PERFORMING ORGANIZATION NAME AND ADDRESS Arnold Engineering Development Center Arnold Air Force Station, Tennessee 37389		8. CONTRACT OR GRANT NUMBER(s)
11. CONTROLLING OFFICE NAME AND ADDRESS Air Force Armament Laboratory (DLJC) Eglin AFB, Florida 32542		10. PROGRAM ELEMENT, PROJECT, TASK AREA & WORK UNIT NUMBERS PE 64709F, Project 1210 PE 27231F, Project 3169
14. MONITORING AGENCY NAME & ADDRESS (if different from Controlling Office)		12. REPORT DATE July 1974
		13. NUMBER OF PAGES 92
		15. SECURITY CLASS. (of this report) UNCLASSIFIED
		15a. DECLASSIFICATION/DOWNGRADING SCHEDULE N/A
16. DISTRIBUTION STATEMENT (of this Report) Distribution limited to U.S. Government agencies only; this report contains information on test and evaluation of military hardware; July 1974; other requests for this docu- ment must be referred to Air Force Armament Laboratory (DLJC), Eglin AFB, Florida 32542.		
17. DISTRIBUTION STATEMENT (of the abstract entered in Block 20, if different from Report)		
18. SUPPLEMENTARY NOTES Available in DDC		
19. KEY WORDS (Continue on reverse side if necessary and identify by block number) F-111E aircraft guided bombs Super HOBOS MK-84 captive trajectory tests SCANA aerodynamic loading aircraft turrets transonic flow aerodynamic characteristics wind tunnel tests		
20. ABSTRACT (Continue on reverse side if necessary and identify by block number) A test was conducted in the Aerodynamic Wind Tunnel (4T) to evaluate the effects of the SCANA (shape No. 1) modification to the F-111 fuselage on store separation characteristics and to determine store aerodynamic coefficients when located at, or near, the in- board and outboard pivot pylons of the F-111 aircraft. Data were obtained at Mach numbers from 0.40 to 1.30 to assess the influence of the aircraft angle of attack, wing-sweep angle, and the presence of the SCANA turret. Trajectory data were obtained on 1/24-scale		

DD FORM 1 JAN 73 1473

EDITION OF 1 NOV 65 IS OBSOLETE

UNCLASSIFIED

SECURITY CLASSIFICATION OF THIS PAGE (When Data Entered)

UNCLASSIFIED

SECURITY CLASSIFICATION OF THIS PAGE(When Data Entered)

20. ABSTRACT (Continued)

models of the MK-84 LGB and MK-84 EOGB guided bombs and the SUU-30 H/B dispenser munition. Aerodynamic loads survey data were obtained on the MK-84 EOGB and the MK-84 Super HOBOS (with and without extended tips) at the carriage position and at 2-ft vertical increments (full-scale) from carriage. This report contains a description of the test, information to identify the test conditions and configurations for all data taken, and sufficient plotted data to show the various effects on the store model trajectories and aerodynamic loads. Test results indicate no significant alteration in store trajectories when the SCANA turret is added to the F-111E aircraft. A slight decrease in the negative pitch and outboard yaw rates occurred at the highest wing sweep angle. Increasing the aircraft angle of attack produced the expected effects of increasing the normal-force coefficient and decreasing the pitching-moment coefficient.

AFSC
Arnold AFB Tenn

UNCLASSIFIED

SECURITY CLASSIFICATION OF THIS PAGE(When Data Entered)

PREFACE

The work reported herein was done by the Arnold Engineering Development Center (AEDC), Air Force Systems Command (AFSC) and sponsored by the Air Force Armament Laboratory (AFATL/DLJC/M. B. Hume), AFSC, under Program Element 64709F, Project 1210, and Program Element 27231F, Project 3169.

The test results presented were obtained by ARO, Inc. (a subsidiary of Sverdrup & Parcel and Associates, Inc.), contract operator of the AEDC, AFSC, Arnold Air Force Station, Tennessee. The test was conducted from March 12 through 15, 1974, under ARO Project No. PA469. The manuscript (ARO Control No. ARO-PWT-74-44) was submitted for publication on May 24, 1974.

CONTENTS

	<u>Page</u>
1.0 INTRODUCTION	7
2.0 APPARATUS	
2.1 Test Facility	7
2.2 Test Articles	8
2.3 Instrumentation	9
3.0 TEST DESCRIPTION	
3.1 Test Conditions	9
3.2 Data Acquisition	10
3.3 Corrections	11
3.4 Precision of Data	11
4.0 RESULTS AND DISCUSSION	
4.1 Captive Trajectory Data	12
4.2 Aerodynamic Loads Survey Data	14
5.0 SUMMARY OF RESULTS	14

ILLUSTRATIONS

Figure

1. Isometric Drawing of a Typical Store Separation Installation and a Block Diagram of the Computer Control Loop	17
2. Schematic of the Tunnel Test Section Showing Model Location	18
3. Details and Dimensions of the SCANA (Shape No. 1) Turret	19
4. Sketch of the F-111E Model Showing the Locations of the SCANA (Shape No. 1) Turret and the Pylon Positions for Various Wing Sweep Angles	20
5. Photograph of the F-111E Model Installed in the Wind Tunnel	21
6. Details and Dimensions of the Pylon Models	22
7. Details and Dimensions of the MK-84 LGB Model	23
8. Details and Dimensions of the MK-84 EOGB Model	24
9. Details and Dimensions of the SUU-30 H/B Model	25
10. Details and Dimensions of the BRU-3A/A Model	26
11. Details and Dimensions of the MK-84 Super HOBOS Model	27
12. Effects of the SCANA (Shape No. 1) Turret on Trajectory Data for the MK-84 LGB with Canards; $\Lambda_{LE} = 26$ deg, Configuration 1	28

<u>Figure</u>	<u>Page</u>
13. Effects of the SCANA (Shape No. 1) Turret on Trajectory Data for the MK-84 LGB with Canards; $\Lambda_{LE} = 45$ deg, Configuration 3	30
14. Effects of the SCANA (Shape No. 1) Turret on Trajectory Data for the MK-84 LGB with Canards; $\Lambda_{LE} = 60$ deg, Configuration 1	31
15. Effects of the Canards on Trajectory Data for the MK-84 LGB; SCANA Off, $\Lambda_{LE} = 26$ deg, Configuration 1	37
16. Effects of the Canards on Trajectory Data for the MK-84 LGB; SCANA Off, $\Lambda_{LE} = 60$ deg, Configuration 1	40
17. Effects of the Wing Sweep Angle on Trajectory Data for the MK-84 LGB; Canards Off, SCANA Off, Configuration 1	43
18. Effects of Mach Number on Trajectory Data for the MK-84 LGB; Canards On, SCANA On, $\Lambda_{LE} = 26$ deg, Configuration 2	45
19. Effects of Mach Number on Trajectory Data for the MK-84 LGB; Canards On, SCANA On, $\Lambda_{LE} = 45$ deg, Configuration 3	46
20. Effects of the Carriage Position on Trajectory Data for the MK-84 LGB; Canards On, SCANA On, $\Lambda_{LE} = 26$ deg, Configuration 2	47
21. Effects of the Carriage Position on Trajectory Data for the MK-84 LGB; Canards On, SCANA On, $\Lambda_{LE} = 45$ deg, Configuration 3	48
22. Effects of Climb Angle on Trajectory Data for the MK-84 LGB; Canards On, SCANA Off, $\Lambda_{LE} = 45$ deg, Configuration 3	50
23. Effects of the Carriage Position on Trajectory Data for the MK-84 EOGB; SCANA On, $\Lambda_{LE} = 60$ deg, Configuration 4	51
24. Effects of the Wing Sweep Angle on Trajectory Data for the MK-84 EOGB; SCANA On, Configuration 4	55
25. Effects of Climb Angle on Trajectory Data for the MK-84 EOGB; SCANA On, $\Lambda_{LE} = 45$ deg, Configuration 4	58
26. Effects of the SCANA (Shape No. 1) Turret on Trajectory Data for the SUU-30 H/B; CG Forward, BRU Sta. 2, $\Lambda_{LE} = 45$ deg, Configuration 7	61
27. Effects of Mach Number on Trajectory Data for the SUU-30 H/B; CG Forward, BRU Sta. 2, $\Lambda_{LE} = 45$ deg, Configuration 7	63
28. Effects of the CG Position on Trajectory Data for the SUU-30 H/B; BRU Sta. 2, $\Lambda_{LE} = 45$ deg, Configuration 7	64
29. Effects of the Carriage Position on Trajectory Data for the SUU-30 H/B; CG Forward, $\Lambda_{LE} = 45$ deg	66
30. Effect of Mach Number on Aerodynamic Coefficients for the MK-84 EOGB; SCANA On, Configuration 4	67

<u>Figure</u>	<u>Page</u>
31. Effects of the Carriage Position on Aerodynamic Coefficients for the MK-84 EOGB; SCANA On, $\Lambda_{LE} = 45$ deg, Configuration 4	71
32. Effect of Wing Tip Extensions on Aerodynamic Coefficients for the MK-84 Super HOBOS; SCANA On, $\Lambda_{LE} = 45$ deg	75
33. Free-Stream Data for the MK-84 Super HOBOS, $M_\infty = 0.80$	79

TABLES

1. Identification of Test Conditions	
a. Trajectory	80
b. Aerodynamic Loads Survey	86
2. Identification of Full-Scale Store Parameters	89
3. Store Positions and Orientations for the Aerodynamic Loads Survey Data	89
 NOMENCLATURE	 90

1.0 INTRODUCTION

As part of a program to provide a self-contained target acquisition and weapon guidance capability for the F-111 aircraft, a turret protrusion (SCANA) was added to the underside of the F-111 fuselage. The test described in this report was conducted in the Aerodynamic Wind Tunnel (4T) of the Propulsion Wind Tunnel Facility primarily to assess the influence of the SCANA turret on the separation characteristics of various externally carried weapons. In addition, aerodynamic coefficients were measured on two guided-bomb versions of the MK-84 bomb at and near the carriage position for use in computer simulation programs concerned with weapon guidance and control requirements.

The test was conducted using 1/24-scale models of the F-111E aircraft and various weapons. Captive trajectory data were obtained for the MK-84 LGB, MK-84 EOGB, and SUU-30 H/B. The SUU-30 H/B was separated from the BRU-3A/A multiple-carriage rack on the left-wing inboard pylon of the F-111E aircraft model. The MK-84 LGB and MK-84 EOGB were separated from single-carriage positions on the pivot pylons (wing pylon positions 3, 4, 5, and 6). Trajectory data were obtained at Mach numbers from 0.40 to 1.30, simulated altitudes from sea level to 18,000 ft, wing sweep angles of 26, 45, and 60 deg, simulated climb angles of 0 and -45 deg, and aircraft angles of attack from 0 to 7 deg.

Aerodynamic loads survey data were obtained for the MK-84 EOGB on both inboard and outboard pivot pylons of the F-111E aircraft model. Data for the MK-84 Super HOBOS (with and without extended tips) were obtained on the outboard pivot pylon only. These surveys were used to determine store aerodynamic coefficients at the carriage position and at a 2-ft increment (full-scale) from carriage. These data were obtained at Mach numbers from 0.70 to 0.95, wing sweep angles of 45 and 60 deg, and aircraft angles of attack from 0 to 6 deg.

2.0 APPARATUS

2.1 TEST FACILITY

The Aerodynamic Wind Tunnel (4T) is a closed-loop, continuous flow, variable-density tunnel in which the Mach number can be varied from 0.1 to 1.3. At all Mach numbers, the stagnation pressure can be varied from 300 to 3700 psfa. The test section is 4 ft square and 12.5 ft long with perforated, variable porosity (0.5- to 10-percent open) walls. It is completely enclosed in a plenum chamber from which the air can be evacuated, allowing part of the tunnel airflow to be removed through the perforated walls of the test section.

For store separation and grid survey testing, two separate and independent support systems are used to support the models. The parent aircraft model is inverted in the test section and supported by an offset sting attached to the main pitch sector. The store model is supported by the captive trajectory support (CTS) which extends down from the tunnel top wall and provides store movement (six degrees of freedom) independent of the parent-aircraft model. An isometric drawing of a typical store separation installation is shown in Fig. 1.

Also shown in Fig. 1 is a block diagram of the computer control loop used during captive trajectory testing. The analog system and the digital computer work as an integrated unit and, utilizing required input information, control the store movement during a trajectory. Store positioning is accomplished by use of six individual d-c electric motors. Maximum translational travel of the CTS is ± 15 in. from the tunnel centerline in the lateral and vertical directions and 36 in. in the axial direction. Maximum angular displacements are ± 45 deg in pitch and yaw and ± 360 deg in roll. A more complete description of the test facility can be found in the Test Facilities Handbook.¹ A schematic showing the test section details and the location of the models in the tunnel is shown in Fig. 2.

2.2 TEST ARTICLES

2.2.1 Aircraft Model

During both phases of the test, 1/24-scale models of the F-111E aircraft and the stores were used. The aircraft model was equipped with a manually adjustable wing which permitted the wing leading-edge-sweep angle to be varied from 0 to 72.5 deg. The F-111 model was also equipped with a removable SCANA (shape No. 1) turret, details and dimensions of which are presented in Fig. 3. A sketch showing the F-111 aircraft model with attached SCANA turret is presented in Fig. 4. A photograph of a typical F-111 model installation is shown in Fig. 5. During the test, leading-edge-sweep angles of 26, 45, and 60 deg were employed. To permit the pylons and stores to remain parallel to the aircraft centerline, the pylons were repositioned at each wing station for the various sweep angles. A sketch showing one of the pylons is presented in Fig. 6.

2.2.2 Captive Trajectory Store Models

Store models used during the trajectory portion of the test were 1/24-scale models of the MK-84 (with and without canards), the MK-84 EOGB, and the SUU-30 H/B. Details

¹Test Facilities Handbook (Tenth Edition). "Propulsion Wind Tunnel Facility, Vol. 4." Arnold Engineering Development Center, May 1974.

and dimensions of these models are presented in Figs. 7, 8, and 9, respectively. The SUU-30 H/B store model was tested with the BRU-3 A/A multiple-carriage rack, details and dimensions of which are shown in Fig. 10.

2.2.3 Aerodynamic Loads Survey Models

Store models used during the loads survey testing were 1/24-scale models of the MK-84 EOGB, Fig. 8, and MK-84 Super HOBOS. The Super HOBOS model was equipped with two sets of wings: one with retracted tips, which simulated the store at and near carriage, and one with extended tips, which simulated the store during gliding flight. Details and dimensions of the MK-84 Super HOBOS model, with retracted and extended tips, are presented in Fig. 11.

2.3 INSTRUMENTATION

A 0.40-in.-diam, six-component, internal strain-gage balance was used to measure aerodynamic loads acting on the MK-84 LGB, MK-84 EOGB, and MK-84 Super HOBOS store models. A 0.16-in.-diam, four-component, internal strain-gage balance was used to measure aerodynamic loads acting on the SUU-30 H/B store model. Translational and angular positions of the store models were obtained from the CTS analog inputs.

The instrumented pylons and BRU-3 A/A were equipped with a spring-loaded plunger (touch wire), extending approximately 0.050 in. below the pylon or rack surface, to provide an indication of when this store was in its carriage position. This system was electrically wired to give a visual indication on the control console when contact between the store model and touch wire was made. The system was also electrically connected to automatically stop the CTS movement if the store model or sting support contacted the parent aircraft or its support structure.

3.0 TEST DESCRIPTION

3.1 TEST CONDITIONS

3.1.1 Captive Trajectory Phase

Store separation data were obtained at Mach numbers from 0.40 to 1.30 and at simulated pressure altitudes from sea level to 18,000 ft. The dynamic pressure ranged from 300 to 500 psf and the aircraft-model angle of attack varied from 0 to 7 deg. Tunnel conditions were held constant at the desired Mach number and dynamic pressure while data for each trajectory were obtained. The trajectories were terminated manually when sufficient data were obtained, when the CTS reached a travel limit, or when the store or support sting contacted the aircraft or its support structure. A summary of all trajectory test conditions is presented in Table 1a.

3.1.2 Aerodynamic Loads Survey Phase

Grid survey data were obtained at Mach numbers from 0.70 to 0.95. The dynamic pressure was 500 psf and the aircraft-model angle of attack was varied from 0 to 6 deg. Tunnel conditions were held constant at the desired Mach number and dynamic pressure while data for each grid survey were obtained. A summary of all loads survey test conditions is presented in Table 1b.

3.2 DATA ACQUISITION

To obtain data, test conditions were established in the tunnel and the parent model was positioned at the desired angle of attack. The store model was then oriented to a position corresponding to the store carriage location. After the store was set at the desired initial position, operational control of the CTS was switched to the digital computer which controlled the store movement during data acquisition through commands to the CTS analog system (see block diagram, Fig. 1). Data from the wind tunnel, consisting of measured model forces and moments, wind tunnel operating conditions, and CTS rig positions, were input to the digital computer.

3.2.1 Captive Trajectory Phase

The digital computer was programmed to solve the six-degree-of-freedom equations to calculate the angular and linear displacements of the store relative to the parent aircraft pylon. In general, the program involves using the last two successive measured values of each static aerodynamic coefficient to predict the magnitude of the coefficients over the next time interval of the trajectory. These predicted values are used to calculate the new position and attitude of the store at the end of the time interval. The CTS is then commanded to move the store model to this new position and the aerodynamic loads are measured. If these new measurements agree with the predicted values, the process is continued over another time interval of the same magnitude. If the measured and predicted values do not agree within the desired precision, the calculation is redone over a time interval one-half the previous value. This process is repeated until a complete trajectory has been obtained.

In applying the wind tunnel data to the calculations of the full-scale store trajectories, the measured forces and moments are reduced to coefficient form and then applied with proper full-scale store dimensions and flight dynamic pressure. Dynamic pressure was calculated using a flight velocity equal to the free-stream velocity component plus the components of store velocity relative to the aircraft, and a density corresponding to the simulated altitude.

The initial portion of each launch trajectory incorporated simulated ejector forces in addition to the measured aerodynamic forces acting on the store. The ejector force functions for the stores are presented in Table 2. The ejector force was considered to act perpendicular to the rack or pylon mounting surface. The locations of the applied ejector forces and other full-scale store parameters used in the trajectory calculations are listed in Table 2.

3.2.2 Aerodynamic Loads Survey

Preselected positions of the store model center of gravity (cg) relative to the initial carriage position were programmed into the computer. The grid program performed the calculations which commanded the CTS rig to position the store model at the preselected positions, in a specified sequence, for any or all of the six degrees of freedom. Store positions and orientations at which data were obtained are listed in Table 3.

3.3 CORRECTIONS

Balance, sting, and support deflections caused by the aerodynamic loads on the store models were accounted for in the data reduction program to calculate the true store-model angles. Corrections were also made for model weight tares to calculate the net aerodynamic forces on the store model.

3.4 PRECISION OF DATA

3.4.1 Captive Trajectory Data

The trajectory data are subject to errors resulting from uncertainties in tunnel conditions, balance measurements, extrapolation tolerances, and CTS positioning accuracies. Maximum errors in CTS positioning were ± 0.05 in. for translational setting, ± 0.15 deg in pitch and yaw, and ± 1.0 deg in roll. Extrapolation tolerances in the trajectory integration procedure were ± 0.1 for all aerodynamic coefficients. Estimates of the uncertainties in the trajectory data attributable to balance precision limitations were made for the individual store models at a given time in the trajectory and were found to be the following:

Store	t, sec	ΔX_p	ΔY_p	ΔZ_p	$\Delta \theta$	$\Delta \psi$	$\Delta \phi$
MK-84 LGB	0.20	0.014	0.007	0.010	0.2	0.1	0.6
MK-84 EOGB	0.20	0.013	0.005	0.009	0.2	0.1	0.5
SUU-30 H/B	0.20	--	0.024	0.028	0.7	0.7	--

During certain trajectories, balance shifts in the roll gage made it impossible to accurately define the true aerodynamic roll characteristics of the MK-84 LGB. These data, therefore, have not been presented.

3.4.2 Aerodynamic Loads Survey Data

Estimated uncertainties in model positioning resulting from the ability of the CTS to set on a specified value were ± 0.05 in. for translational settings, ± 0.15 deg in pitch and yaw, and ± 1.0 deg in roll.

Uncertainties in the force and moment data were calculated taking into consideration the probable inaccuracies in the balance measurements and tunnel conditions. The uncertainties in the coefficients are based on a 95-percent confidence level, ignoring bias errors, and are as follows:

<u>Store</u>	<u>ΔC_N</u>	<u>ΔC_y</u>	<u>ΔC_Λ</u>	<u>ΔC_ℓ</u>	<u>ΔC_m</u>	<u>ΔC_n</u>
MK-84 EOGB	± 0.014	± 0.009	± 0.020	± 0.004	± 0.025	± 0.015
MK-84 Super HOBOS	± 0.014	± 0.009	± 0.021	± 0.004	± 0.023	± 0.014

The Mach number was held within ± 0.005 of the quoted Mach number, with an estimated uncertainty of ± 0.003 . Uncertainty in setting the aircraft model angle of attack was estimated to be ± 0.1 deg.

4.0 RESULTS AND DISCUSSION

4.1 CAPTIVE TRAJECTORY DATA

4.1.1 MK-84 LGB

Data for the MK-84 LGB are shown in Figs. 12 through 22. Effects of the SCANA turret are presented in Figs. 12 through 14 and indicate that the presence of the SCANA (shape No. 1) turret tends to slightly decrease the negative pitch rate and outboard yaw rate of the store at wing station 3. In general, no effects in the linear displacements were encountered.

Presented in Figs. 15 and 16 are the canard effects. The addition of canards to the store had a major effect on all angular displacements. The addition of canards produced an increase in the magnitude of the store pitch rate and outboard yaw rate. Variations in linear displacements were found to be minor, with a small outboard shift in the lateral position when canards were added.

Effects of wing sweep, Λ_{LE} , are presented in Fig. 17. The negative pitch and outboard yaw rates were decreased slightly at the highest wing sweep angle.

Mach number effects are presented in Figs. 18 and 19. The changes in pitch direction and yaw rate shown in Fig. 18 were due to a combination of reduced aircraft angle of

attack and increased dynamic pressure, although the data in Fig. 19 show that increasing Mach number alone would produce a more downward pitch motion.

The effects of the carriage position are shown in Figs. 20 and 21. The outboard yawing motion and pitch rate increased and decreased, respectively, as the store was moved to the inboard pivot pylon. The presence of the BRU-3 A/A with dummy SUU-30 H/B stores on the inboard left wing pylon had only small effects, affecting only the pitch rate. Little, if any, difference in the linear displacements can be seen by varying the carriage position.

Climb angle effects are shown in Fig. 22. No variations in angular displacement rates were noted. Changes in the store vertical and longitudinal displacement rates were due to the rotation of the store weight component at $\bar{\theta} = -45$ deg.

4.1.2 MK-84 EOGB

Data for the MK-84 EOGB are presented in Figs. 23 through 25. Effects of the carriage position are shown in Fig. 23. The outboard yawing motion and inboard lateral movement increased as the store moved from the outboard to the inboard pivot pylon. The negative pitch rate increased slightly at the inboard position for subsonic Mach numbers. The effect of the BRU-3 A/A with dummy SUU-30 H/B stores on trajectory data is shown by the increase of the nose down pitch rate.

Mach number effects can be seen by comparing Figs. 23a, b, c, and d. Of the linear displacements, only the longitudinal movement was affected. As M_{∞} increased, the increase in drag caused an increase in aft motion. The downward pitching and outboard yawing motion also increased with increasing Mach number.

Figure 24 shows the effect caused by the wing sweep angle. The only significant effect was a reduction in the downward pitching motion at the highest wing sweep angle.

The effects of climb angle caused no variations in angular displacements (Fig. 25). Changes in the store vertical and longitudinal displacement rates were due to the rotation of the store weight component.

4.1.3 SUU-30 H/B

Data for the SUU-30 H/B are shown in Figs. 26 through 29. The effects of the SCANA (shape No. 1) turret are presented in Fig. 26. No effect on trajectory data was noted.

Mach number effects are given in Fig. 27. Major effects caused by increasing M_{∞} can be seen in the angular displacements where the nose down pitch and outboard yaw rates were greatly increased.

Presented in Fig. 28 are the effects of varying the cg position. No effect was indicated in the data.

The effects of store location on the BRU-3 A/A are shown in Fig. 29. Movement of the store from BRU station 2 (bottom) to station 6 (inboard shoulder) resulted in an increase in the outboard yawing motion and an inboard rather than outboard lateral motion.

4.2 AERODYNAMIC LOADS SURVEY DATA

4.2.1 MK-84 EOGB

Data for the MK-84 EOGB are presented in Figs. 30 and 31. Mach number effects were primarily in the side-force coefficient at the lower aircraft angles of attack. This shift may also have been partially caused by the change in the wing-sweep angle. Increasing the aircraft angle of attack had the expected effect of increasing the normal-force coefficient and decreasing the pitching-moment coefficient, with some minor shifts occurring in the side-force and yawing-moment coefficients. No significant variations were observed between the data obtained near pylon 5 and pylon 6 except for minor changes near the carriage position.

4.2.2 MK-84 Super HOBOS

Presented in Figs. 32 and 33 are the data obtained for the MK-84 Super HOBOS. The data show a significant change in the forces and moments when the wing tips are extended.

Free-stream data are presented in Fig. 33 for reference and show that the store was unstable with retracted tips and neutrally stable with extended tips at low angles of attack.

5.0 SUMMARY OF RESULTS

The results of this investigation may be summarized as follows:

1. The presence of the SCANA (shape No. 1) turret had only a minor effect, slightly decreasing the nose down pitch and outboard yaw rates of the MK-84 LGB at wing station 3.
2. The addition of canards to the MK-84 EOGB had major effects on all angular displacements.

3. Increasing the wing-sweep angle produced minor decreases in the nose down pitch rate for both the MK-84 LGB and EOGB. A minor increase in the outboard yaw rate was also noted for the MK-84 LGB.
4. Increasing Mach number produced an increase in both the nose down pitch and outboard yaw rates on all stores.
5. Store angular displacements were not affected by varying the aircraft climb angle.
6. Variation of the cg position for the SUU-30 H/B did not affect the trajectory data.
7. Wing tip extension on the MK-84 Super HOBOS had a major influence on all force and moment coefficients.
8. Increasing the aircraft angle of attack increased the normal-force coefficient and decreased the pitching-moment coefficient of the MK-84 EOGB.

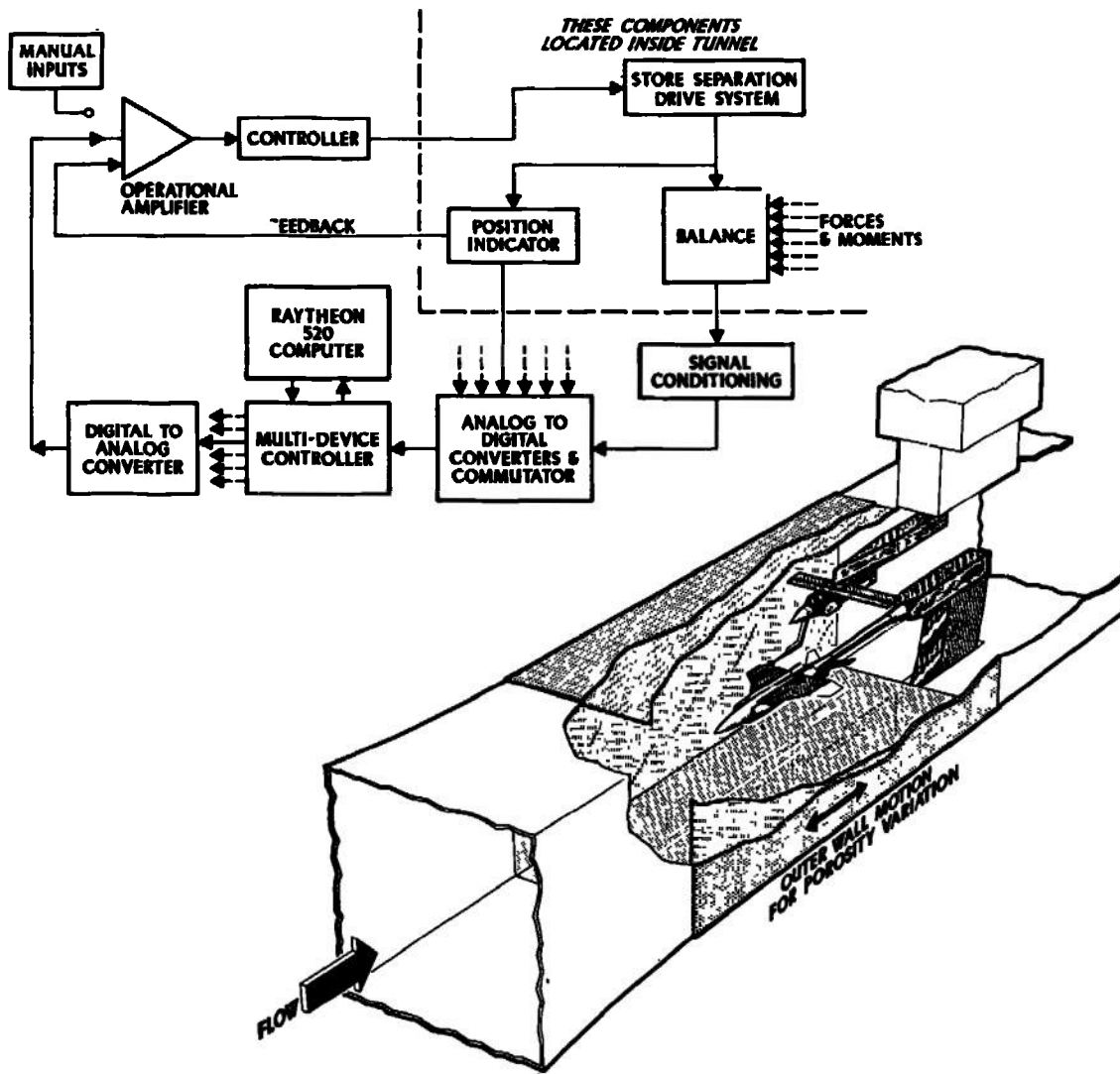
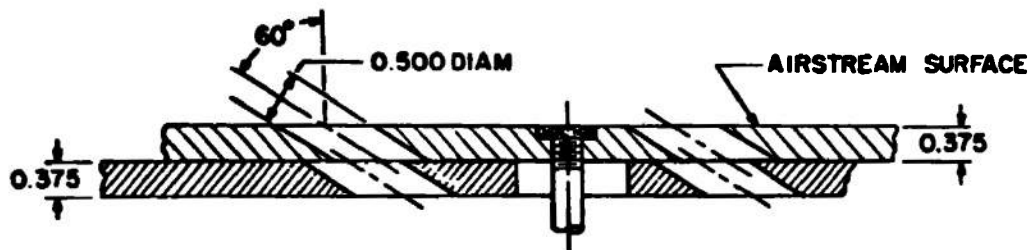


Figure 1. Isometric drawing of a typical store separation installation and a block diagram of the computer control loop.



TYPICAL PERFORATED WALL CROSS SECTION

TUNNEL STATIONS AND DIMENSIONS IN INCHES

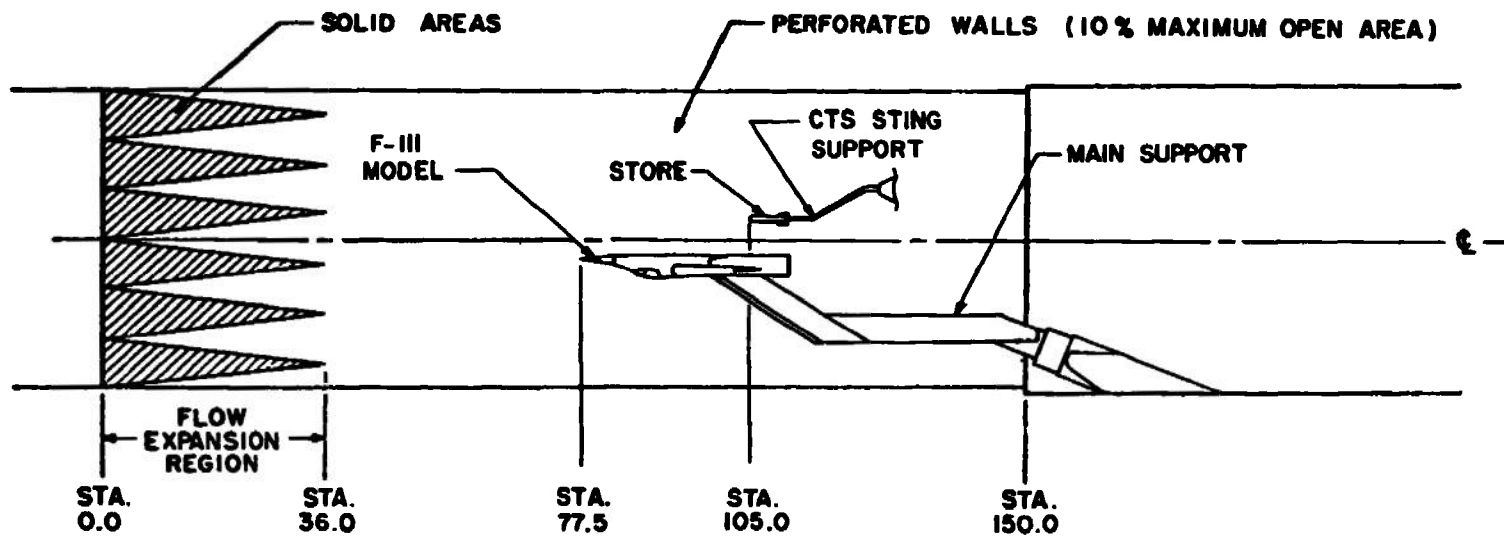
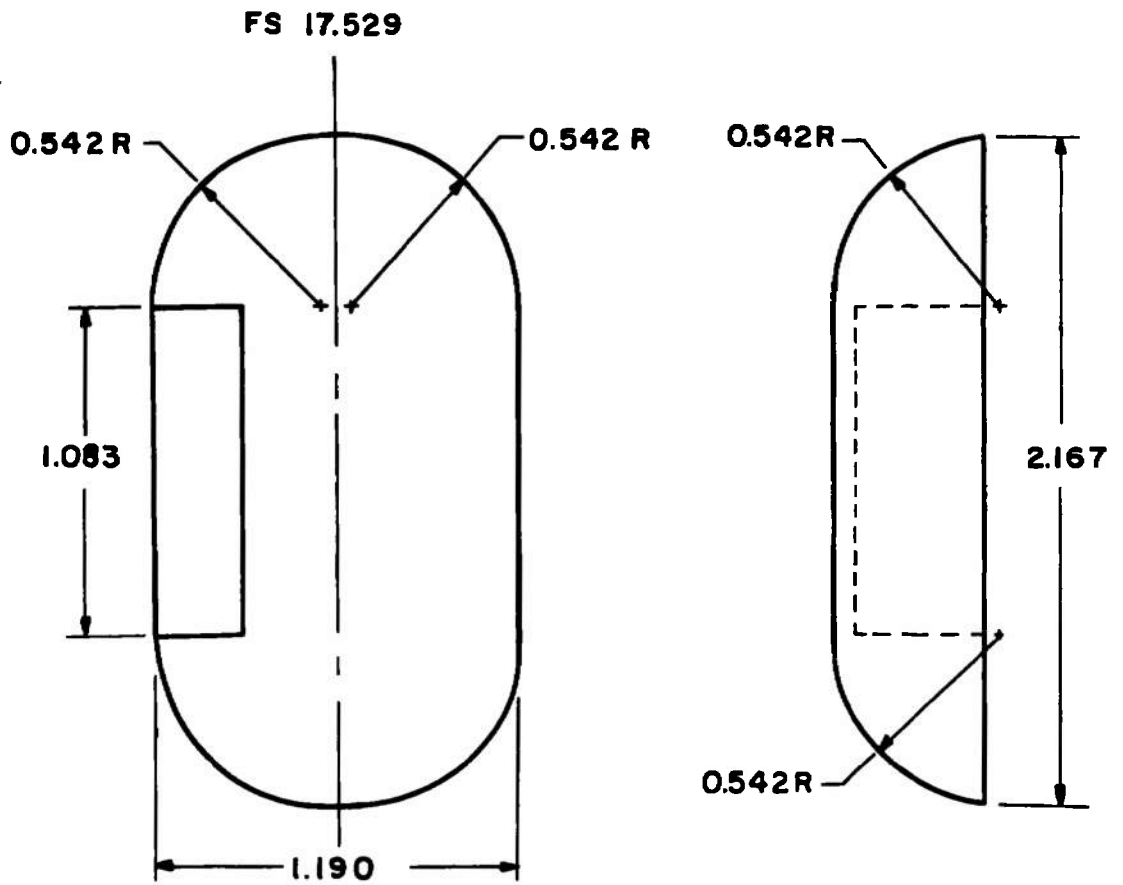


Figure 2. Schematic of the tunnel test section showing model location.



ALL DIMENSIONS IN INCHES

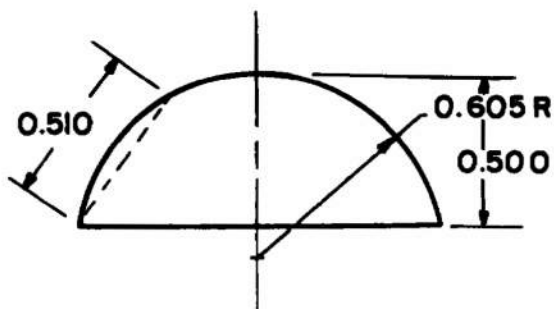


Figure 3. Details and dimensions of the SCANA (shape No. 1) turret.

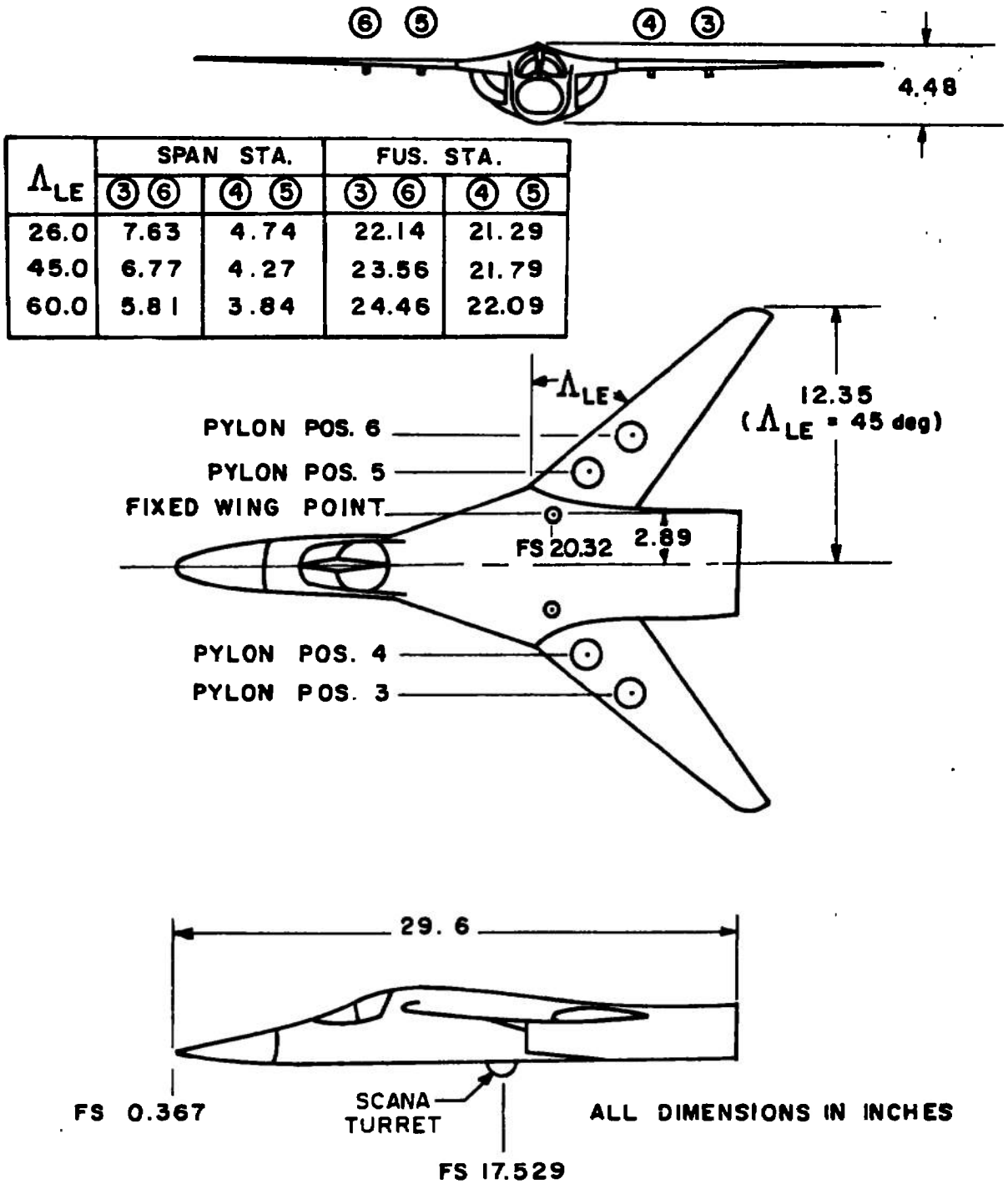


Figure 4. Sketch of the F-111E model showing the locations of the SCANA (shape No. 1) turret and the pylon positions for various wing sweep angles.

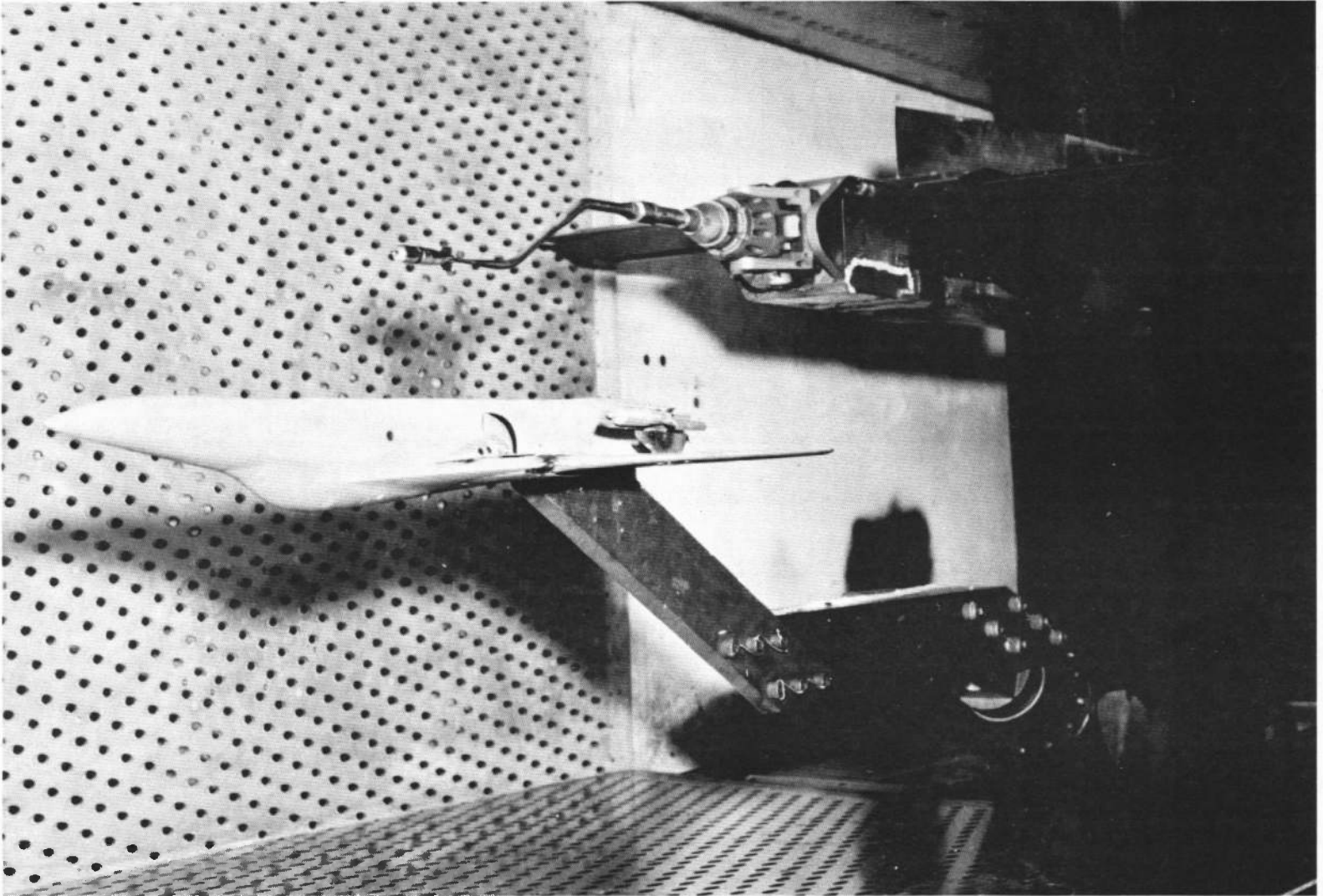


Figure 5. Photograph of the F-111E model installed in the wind tunnel.

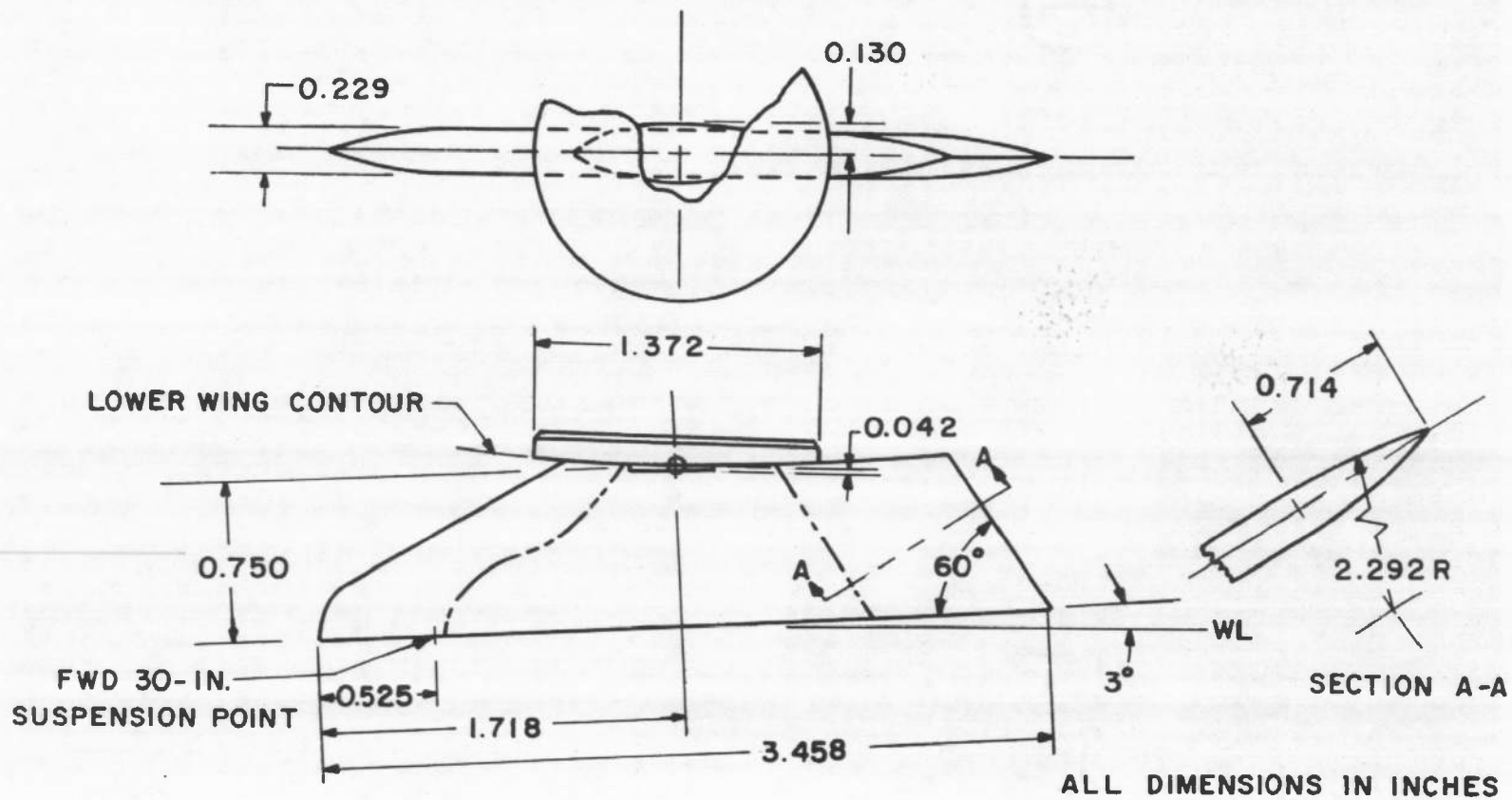
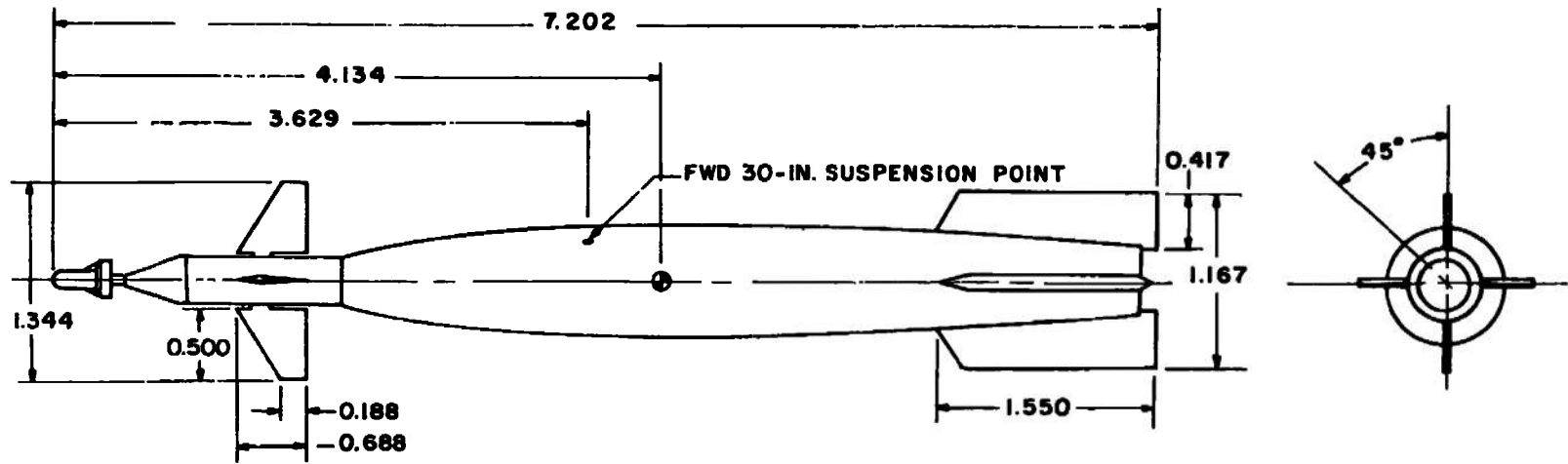


Figure 6. Details and dimensions of the pylon models.



ALL DIMENSIONS IN INCHES

Figure 7. Details and dimensions of the MK-84 LGB model.

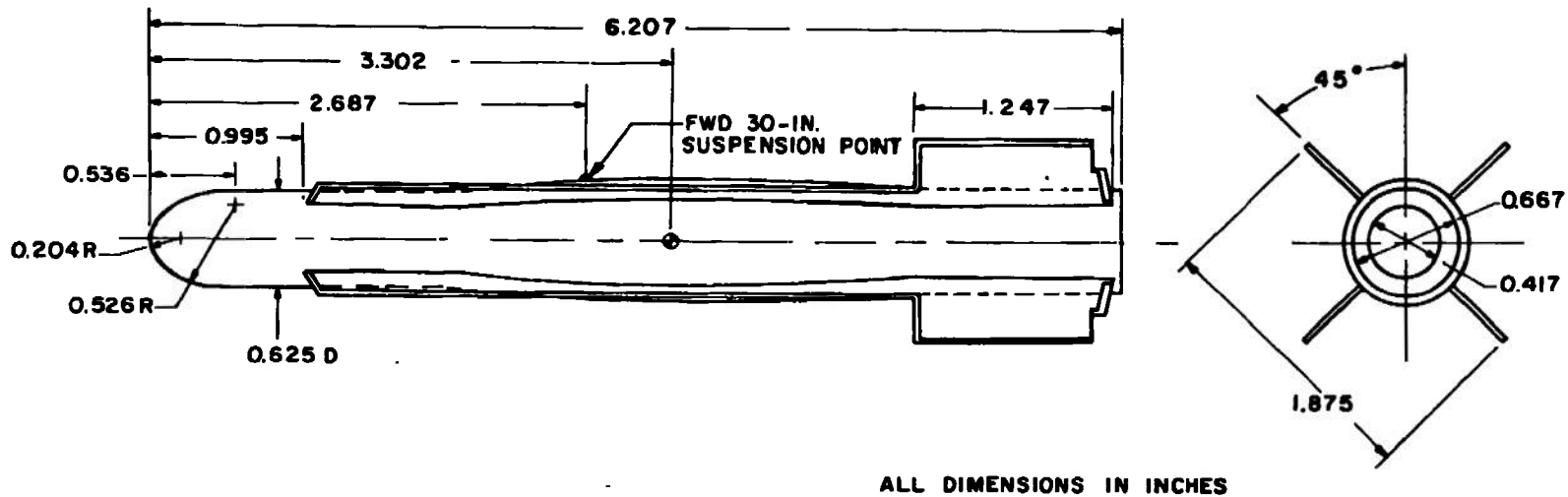


Figure 8. Details and dimensions of the MK-84 EOGB model.

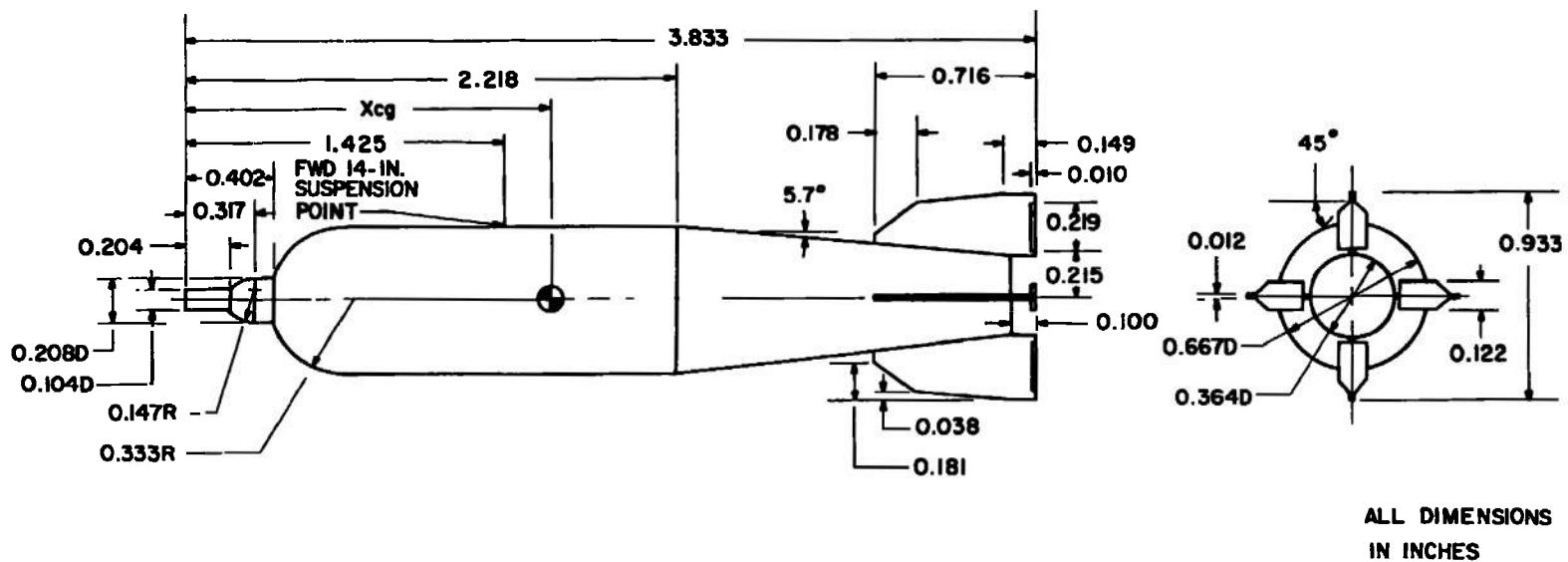
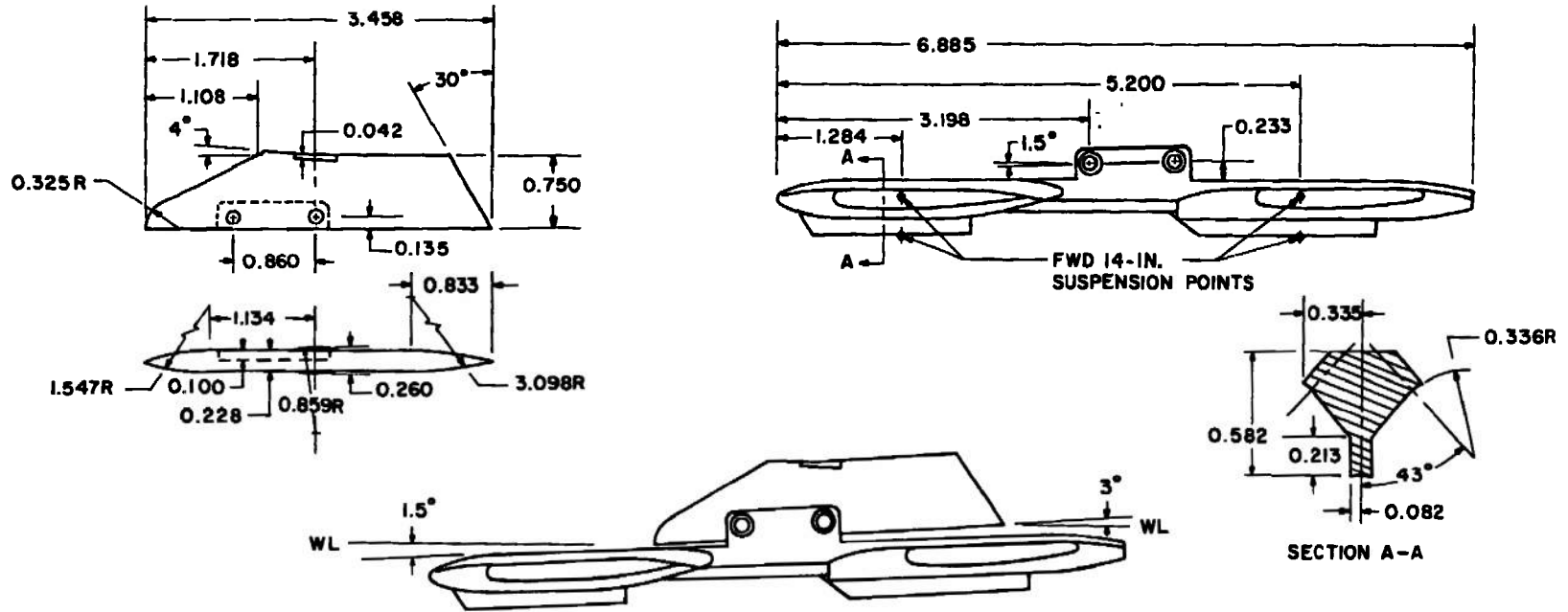
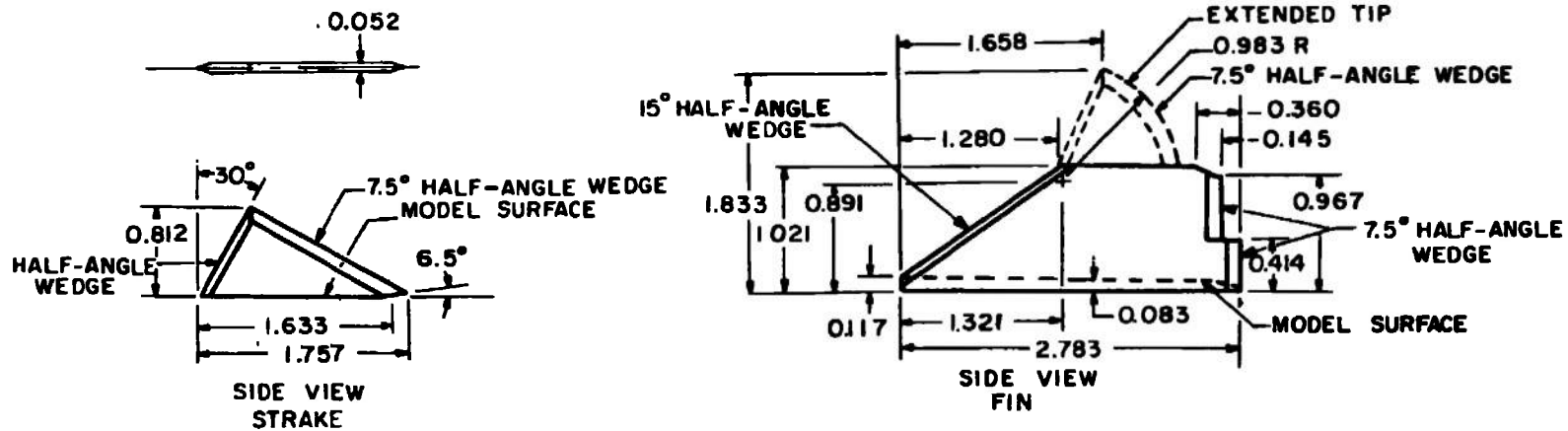


Figure 9. Details and dimensions of the SUU-30 H/B model.



ALL DIMENSIONS IN INCHES

Figure 10. Details and dimensions of the BRU-3A/A model.



ALL DIMENSIONS IN INCHES

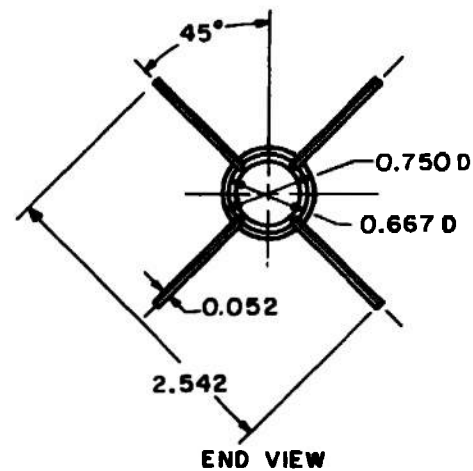
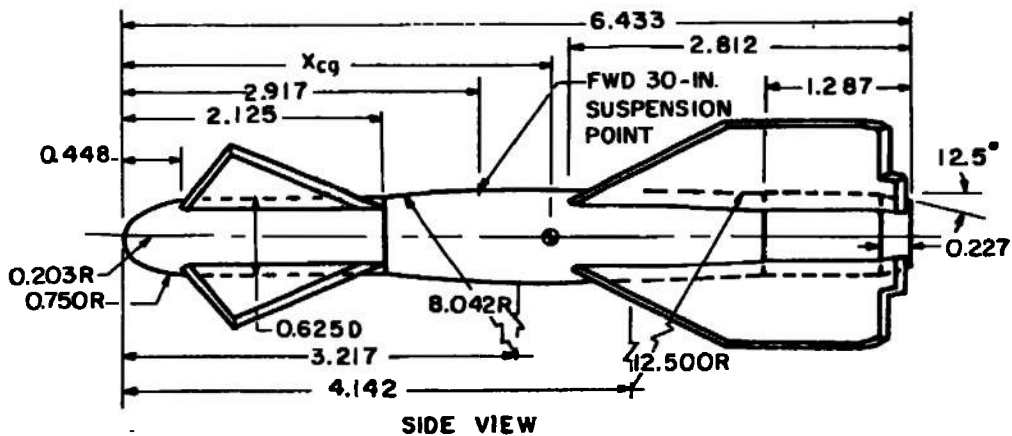
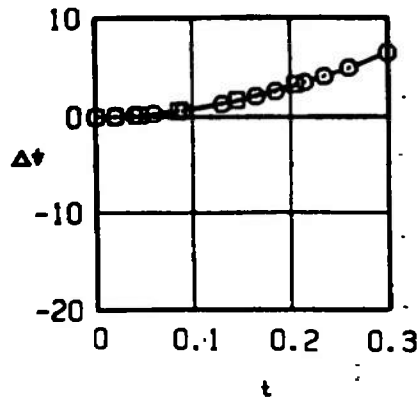
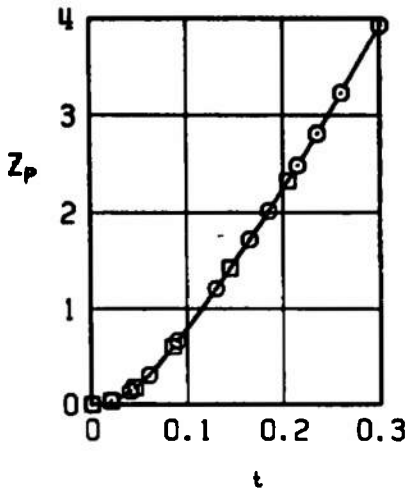
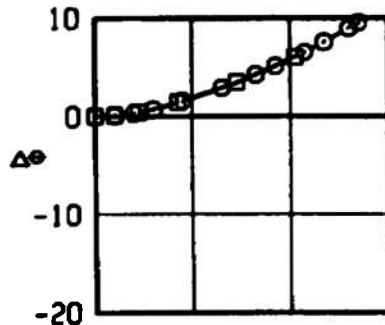
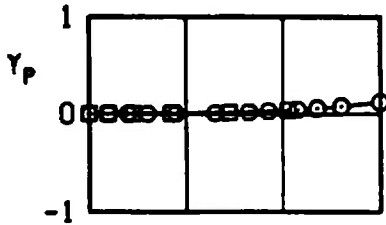
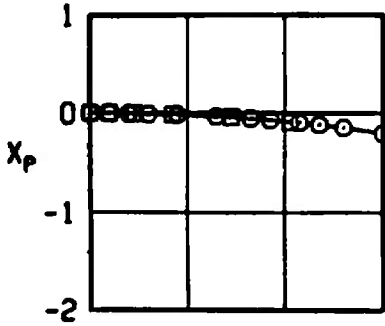


Figure 11. Details and dimensions of the MK-84 Super HOBOS model.

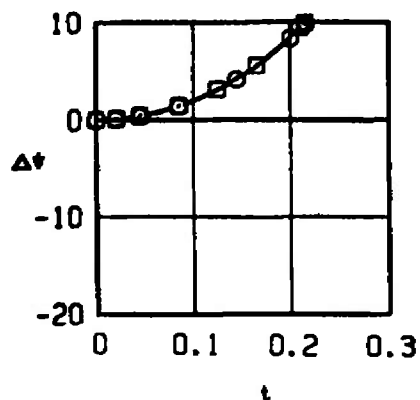
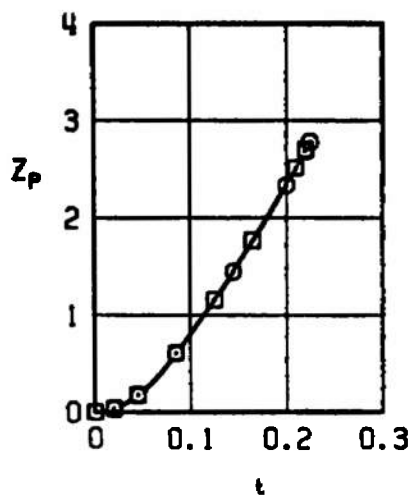
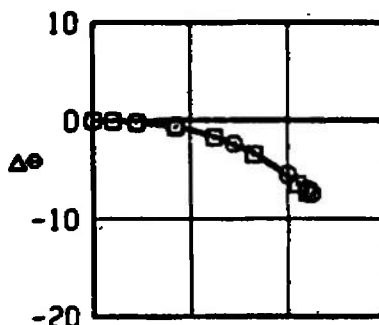
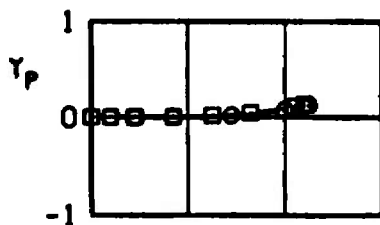
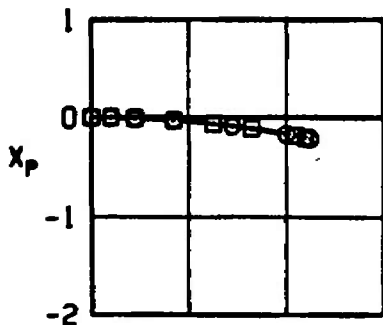
SYMBOL	α_p	M_∞	PYLON NO.	SCANA
○	7	0.40	5	OFF
□	7	0.40	5	ON



a. $M_\infty = 0.40, \alpha_p = 7$

Figure 12. Effects of the SCANA (shape No. 1) turret on trajectory data for the MK-84 LGB with canards; $\Delta_{LE} = 26$ deg, configuration 1.

SYMBOL	a_p	M_∞	PYLON NO.	SCANA
○	2	0.75	5	OFF
□	2	0.75	5	ON



b. $M_\infty = 0.75, a_p = 2$
 Figure 12. Concluded.

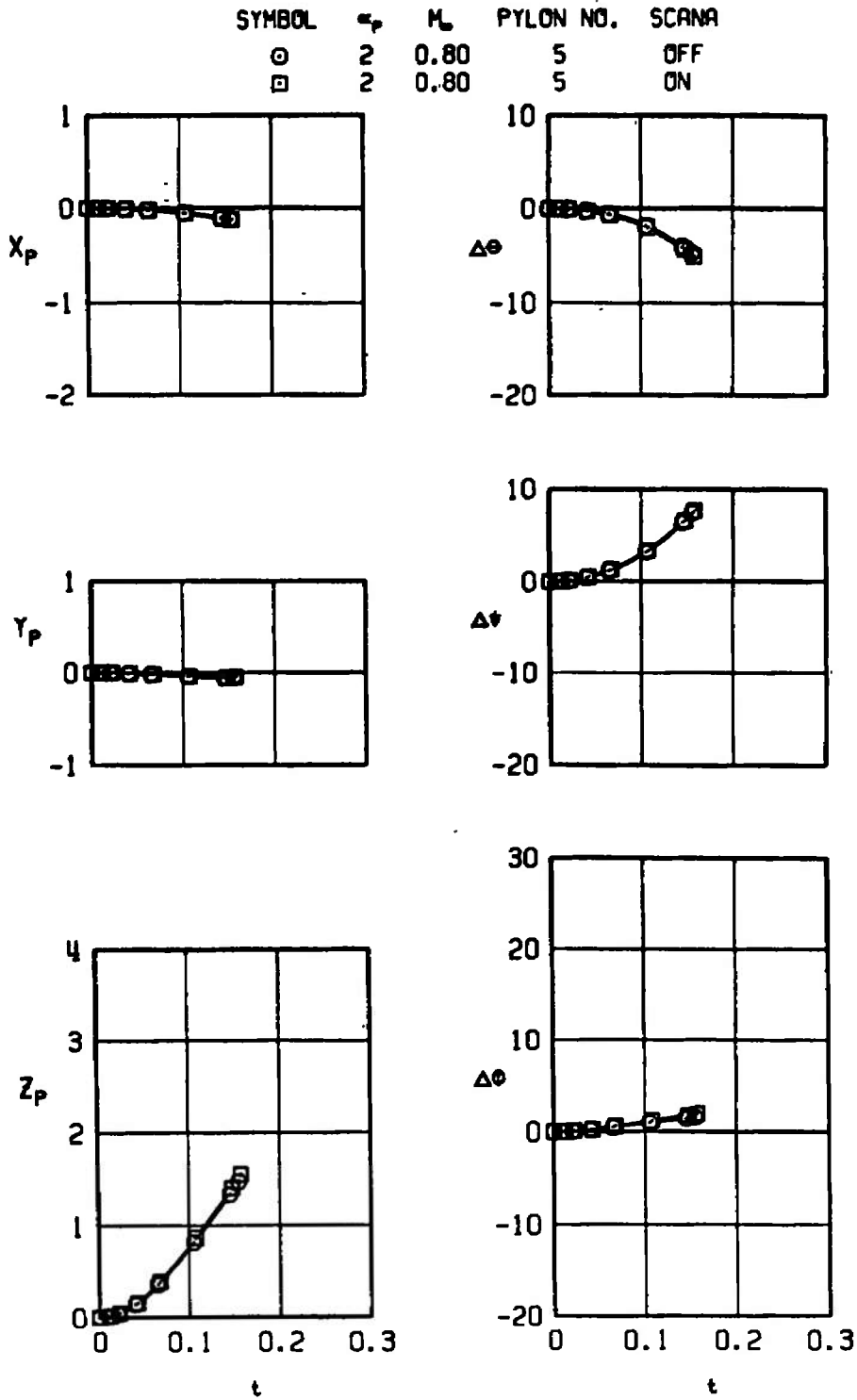
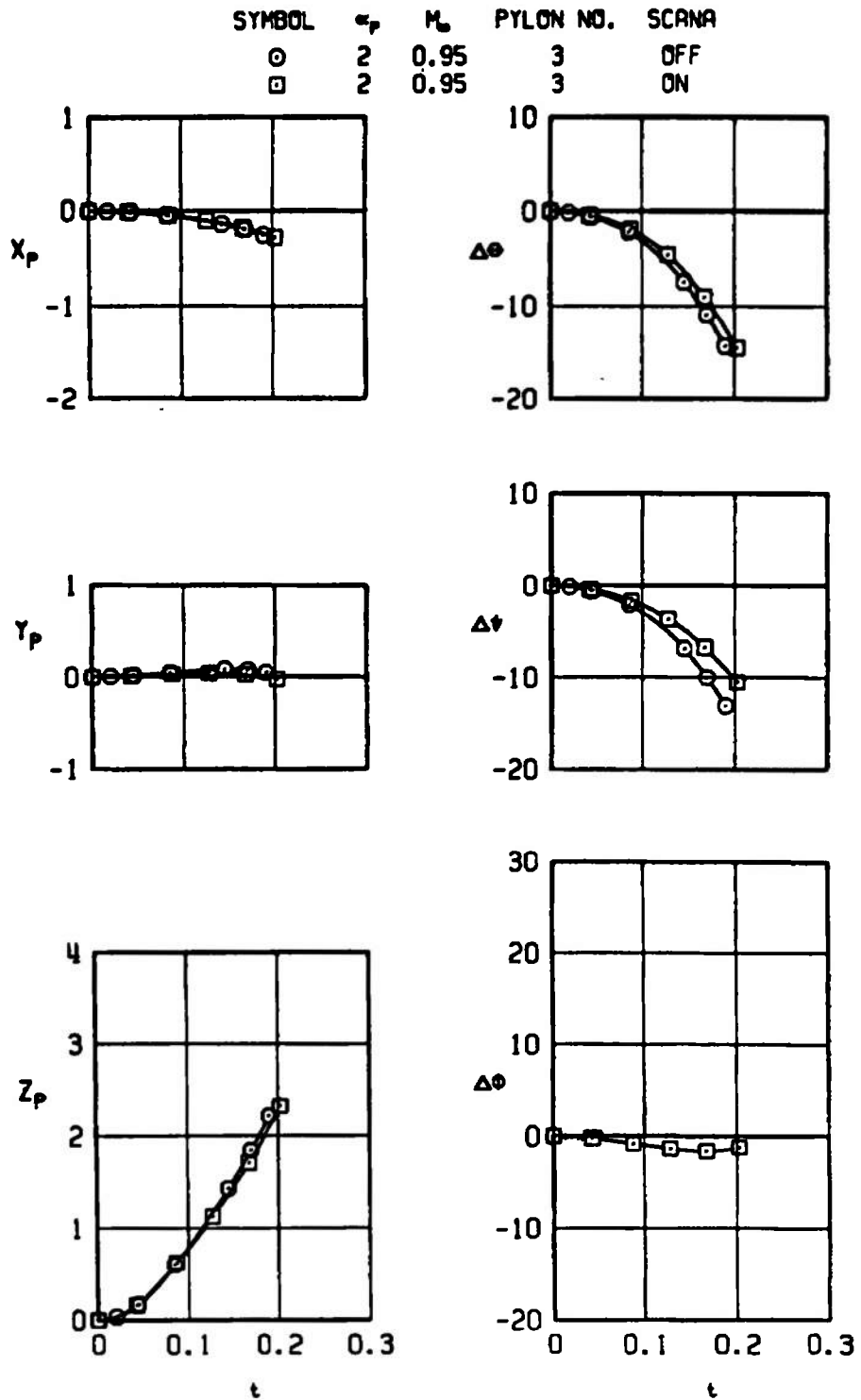
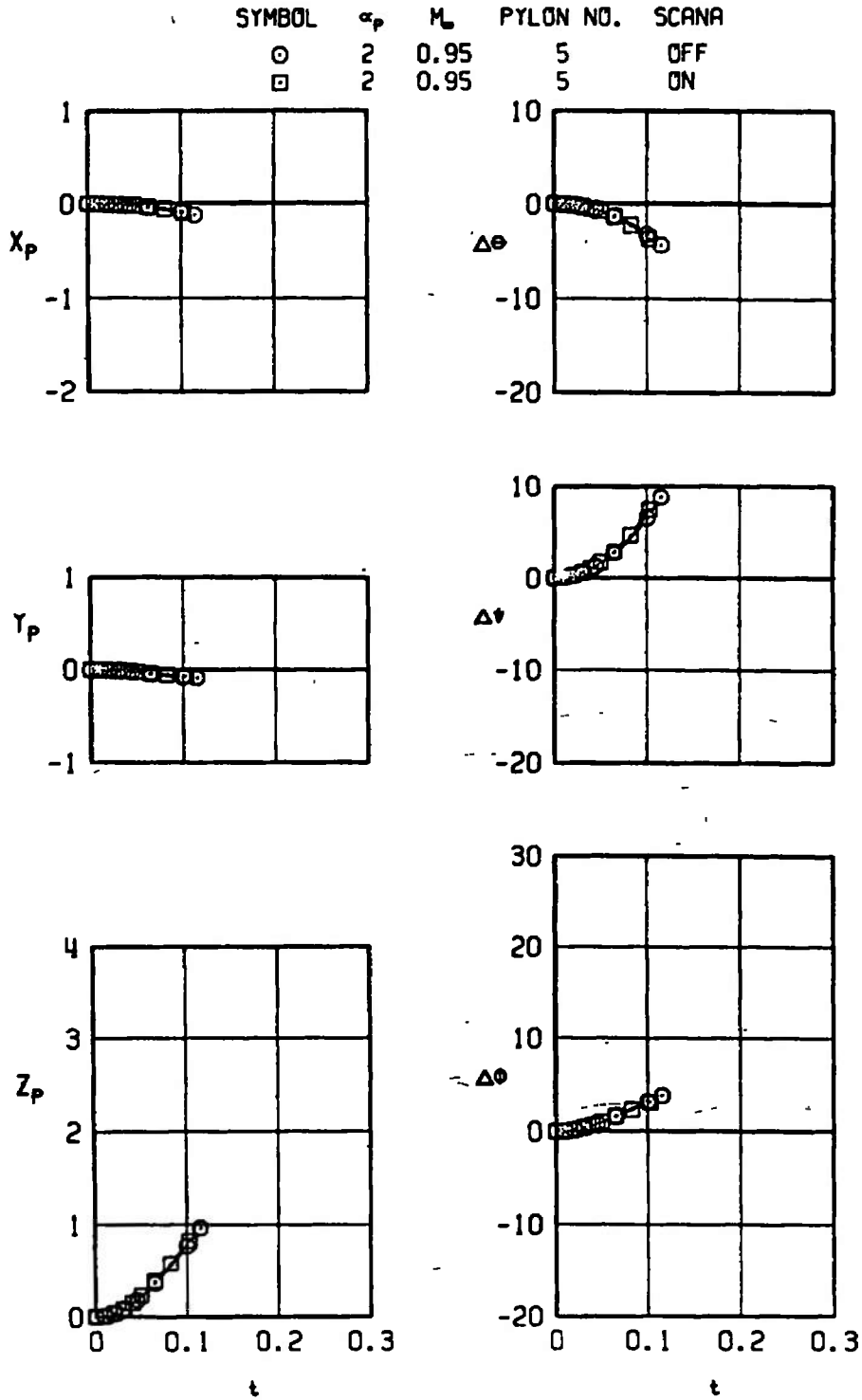


Figure 13. Effects of the SCANA (shape No. 1) turret on trajectory data for the MK-84 LGB with canards; $\Delta_{LE} = 45$ deg, configuration 3.

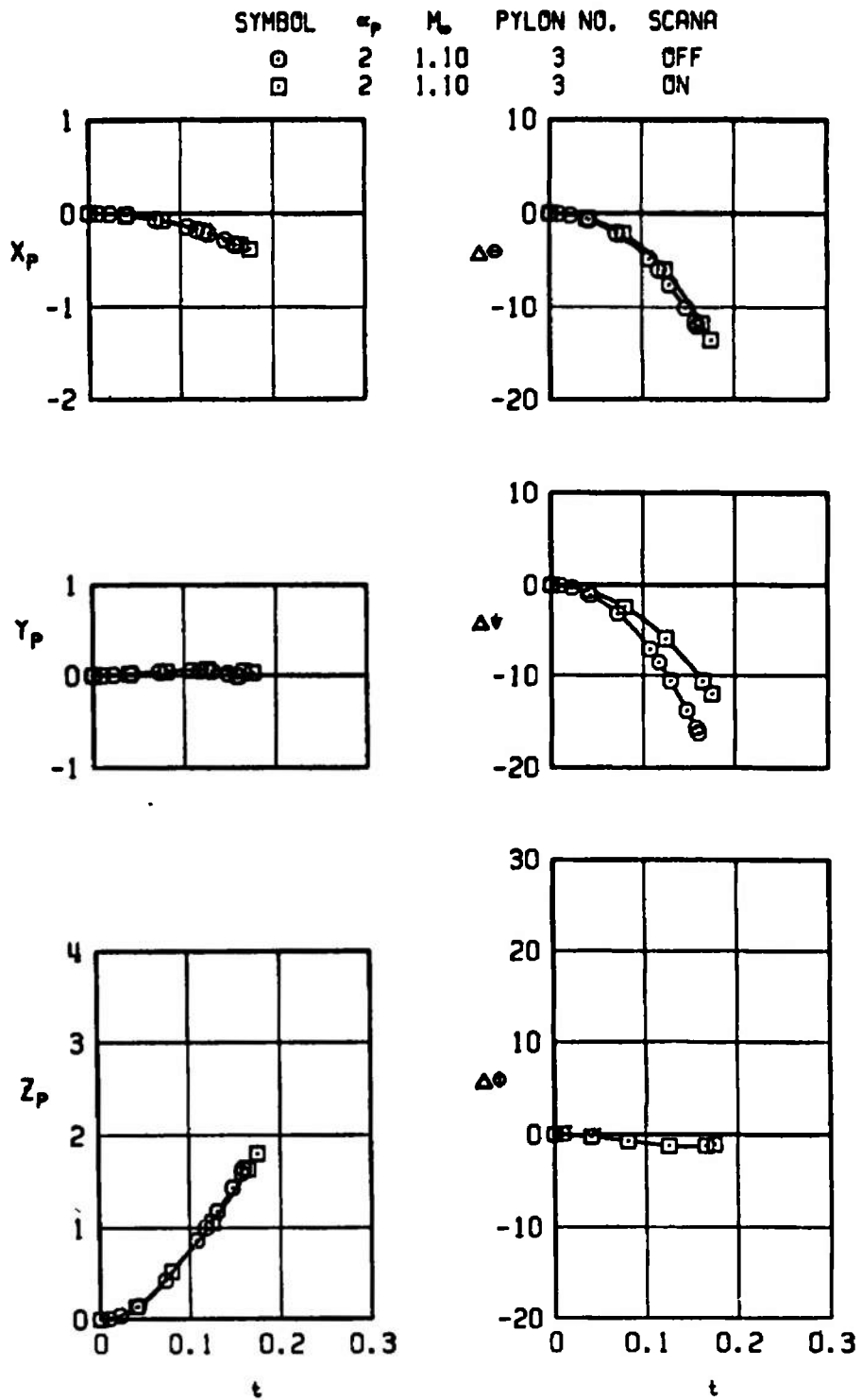


a. $M_\infty = 0.95$, pylon No. 3

Figure 14. Effects of the SCANA (shape No. 1) turret on trajectory data for the MK-84 LGB with canards; $\Lambda_{LE} = 60$ deg, configuration 1.

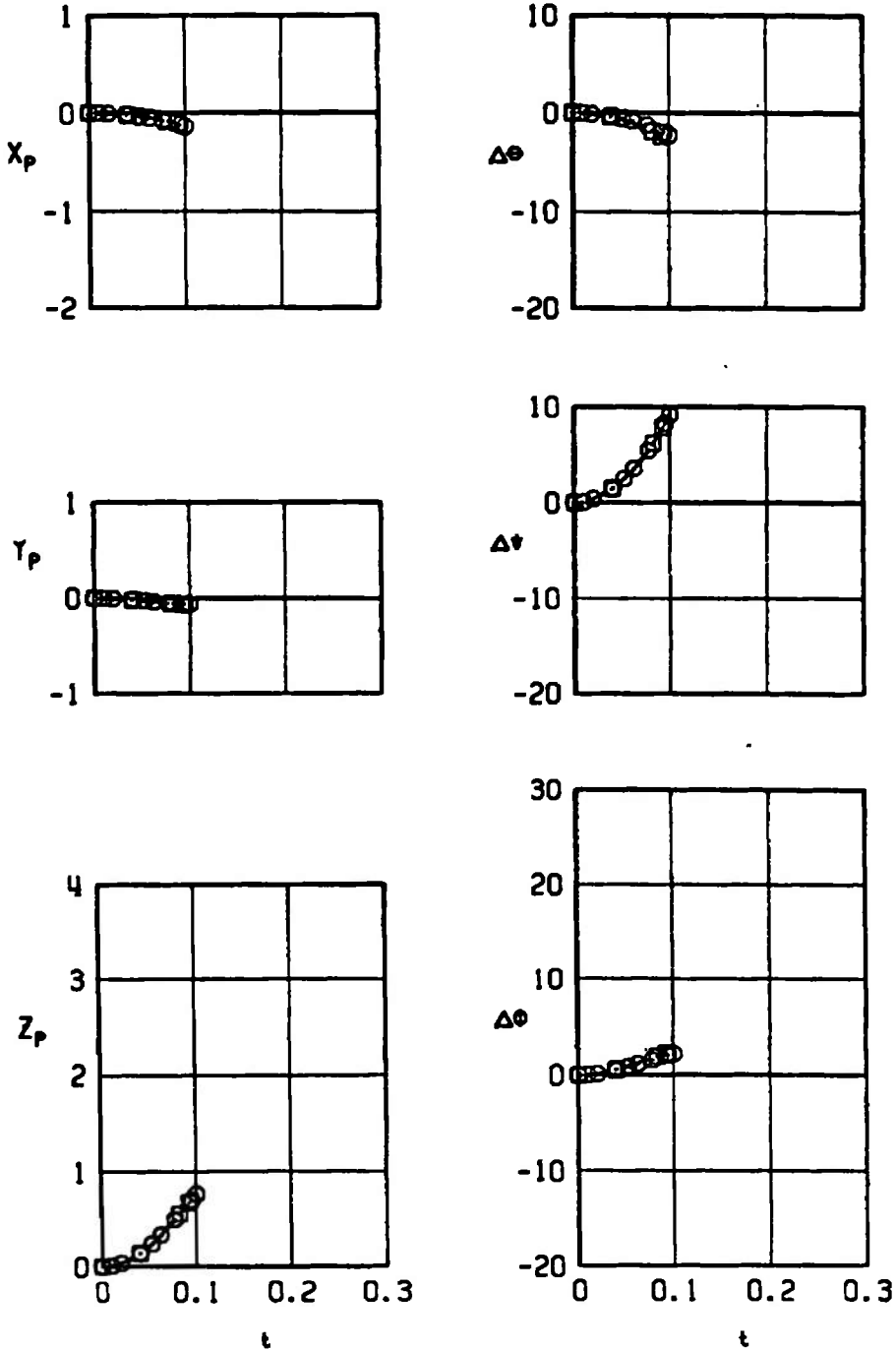


b. $M_e = 0.95$, pylon No. 5
 Figure 14. Continued.

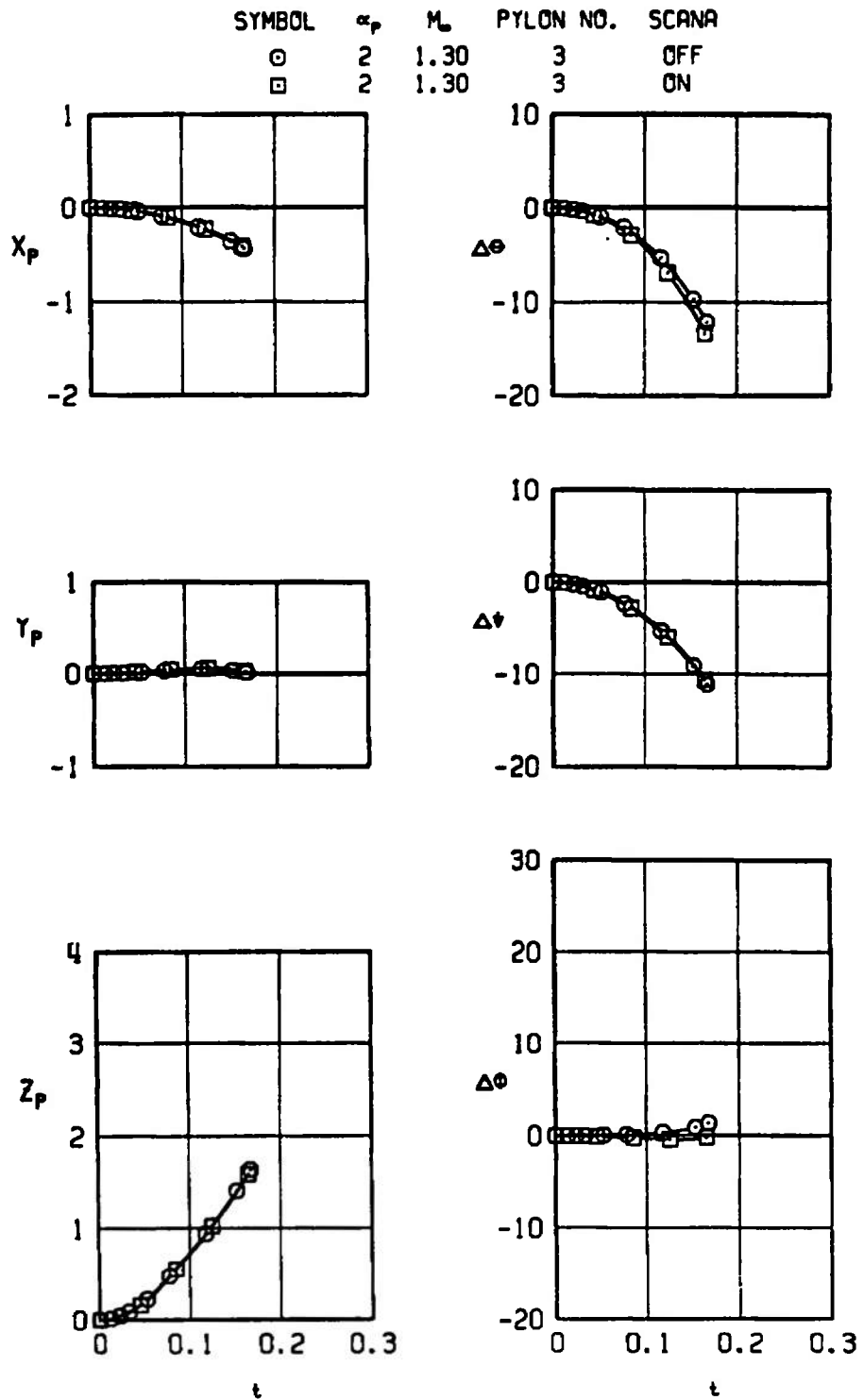


c. $M_\infty = 1.10$, pylon No. 3
 Figure 14. Continued.

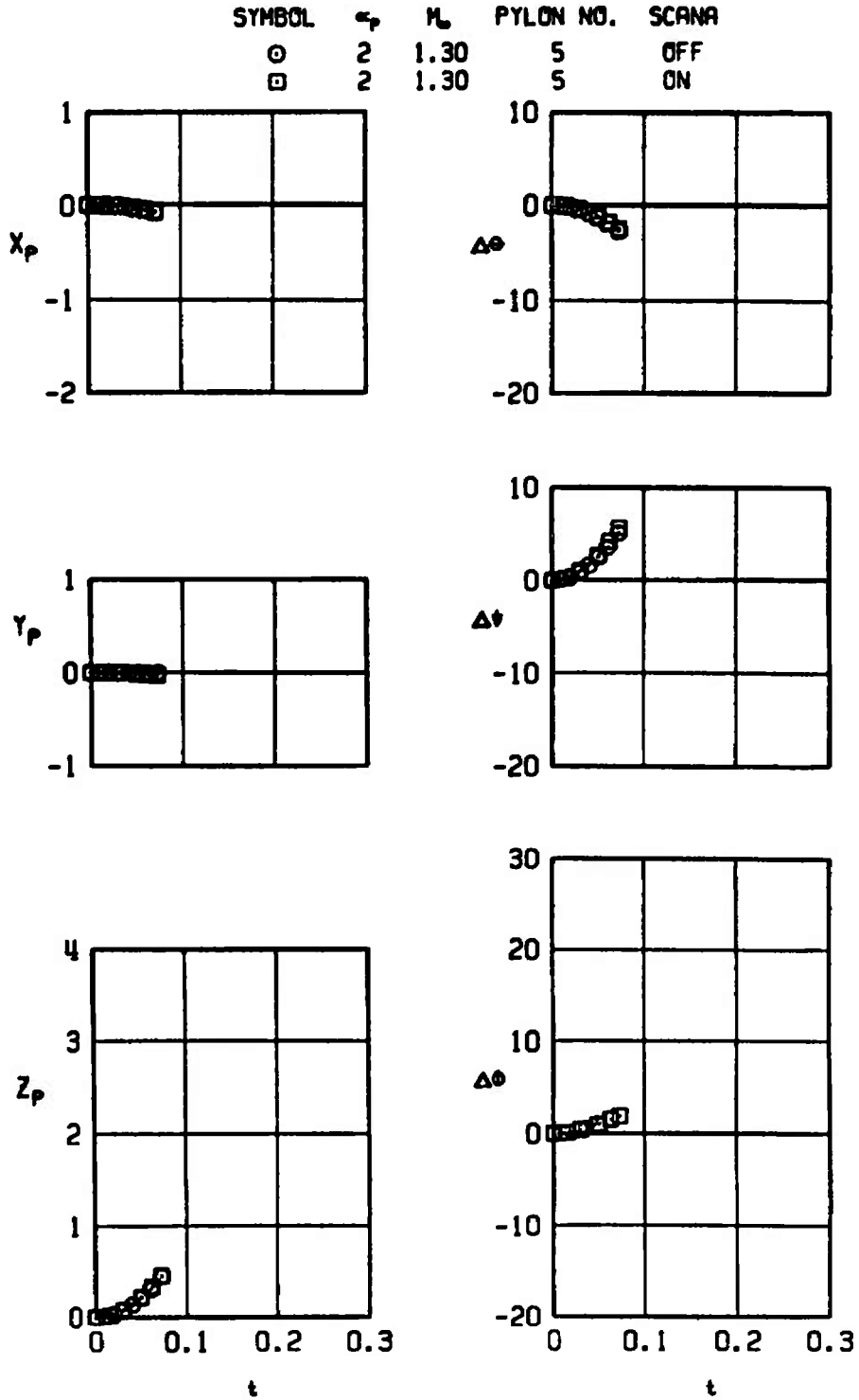
SYMBOL	α_p	M_∞	PYLON NO.	SCANA
○	2	1.10	5	OFF
□	2	1.10	5	ON



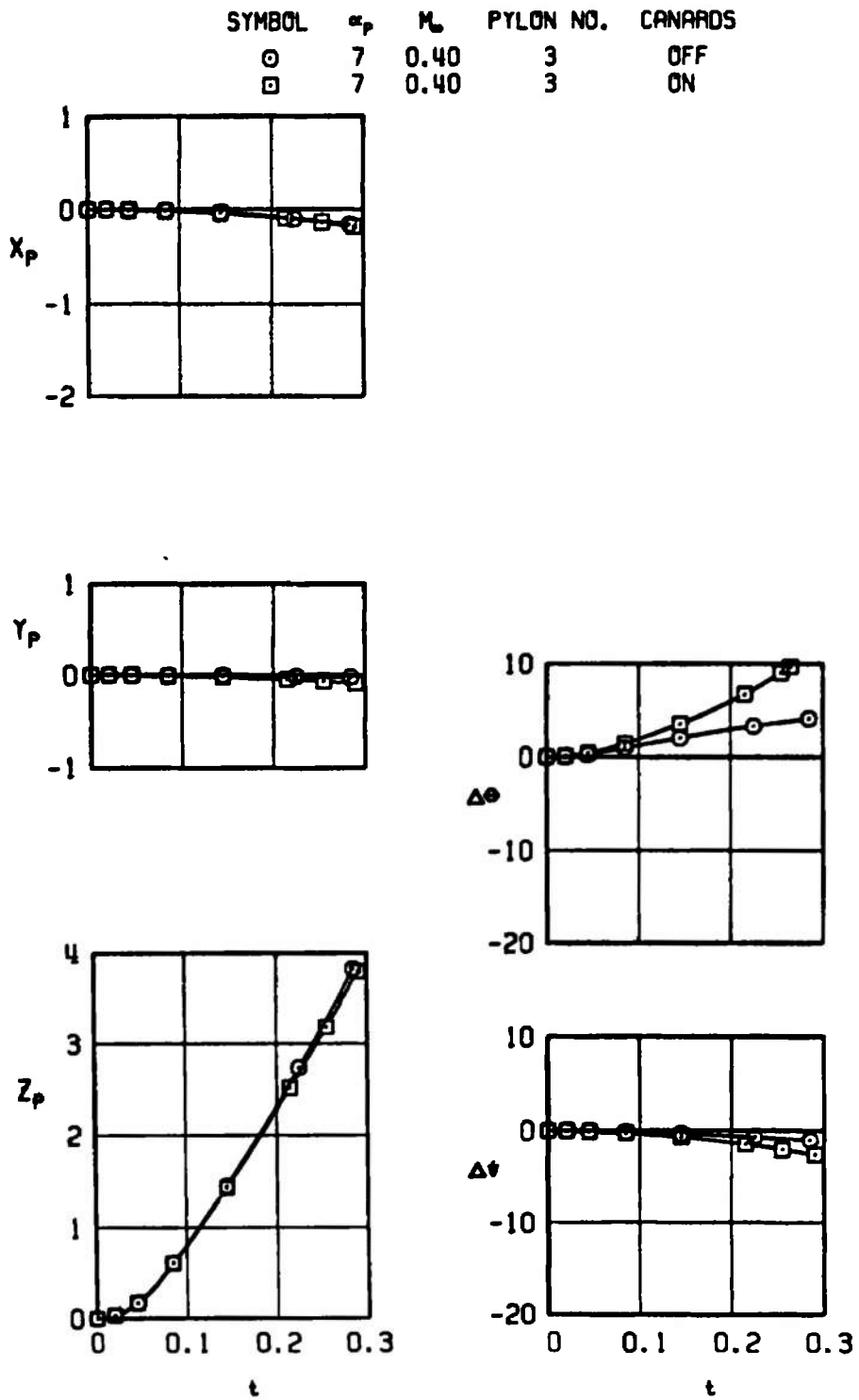
d. $M_\infty = 1.10$, pylon No. 5
Figure 14. Continued.



e. $M_\infty = 1.30$, pylon No. 3
 Figure 14. Continued.



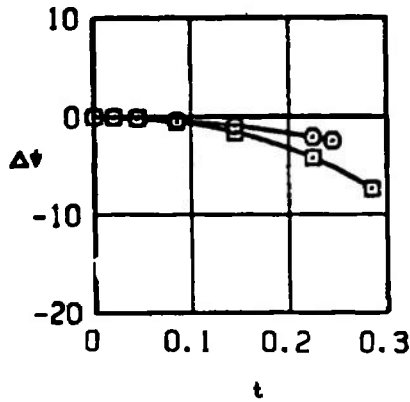
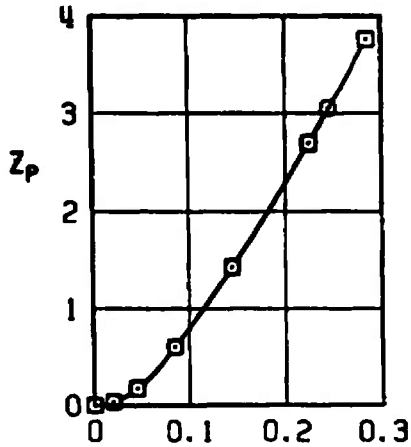
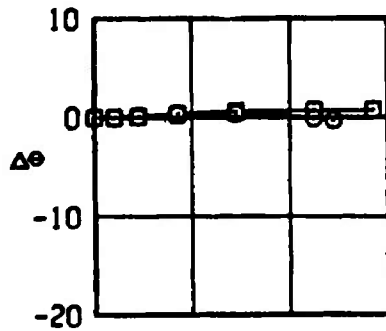
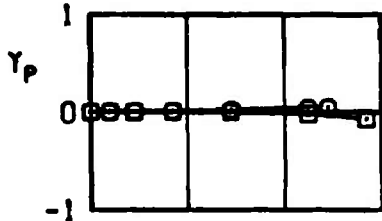
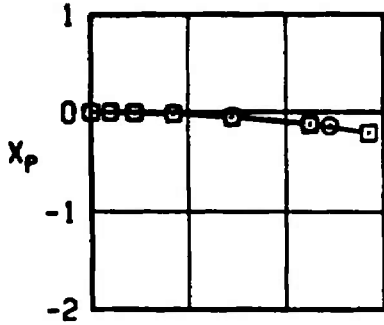
f. $M_\infty = 1.30$, pylon No. 5
 Figure 14. Concluded.



a. $M_\infty = 0.40, \alpha_p = 7$

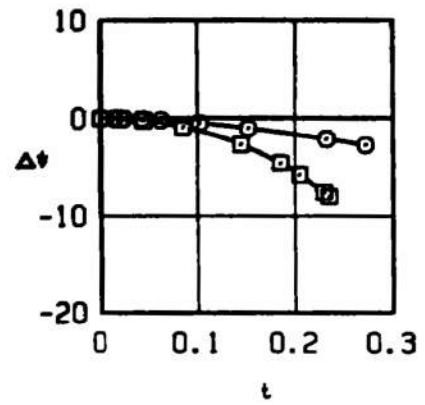
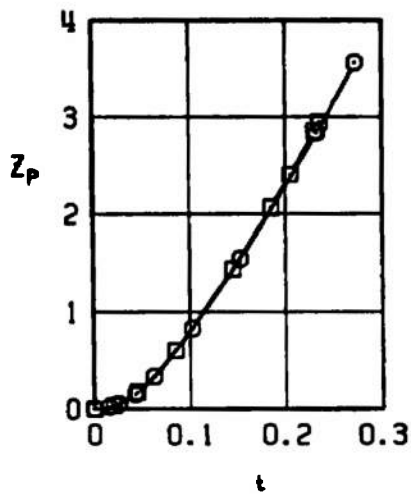
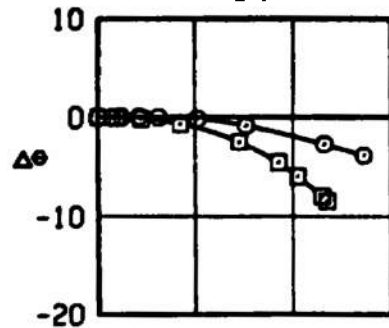
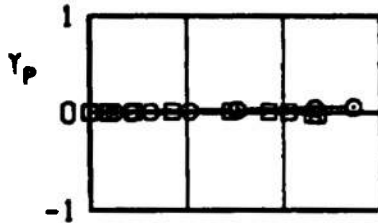
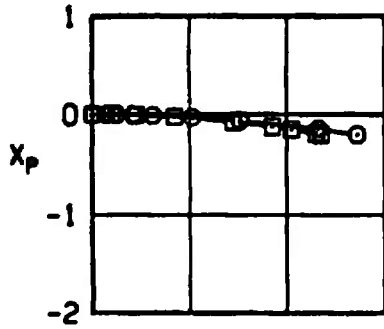
Figure 15. Effects of the canards on trajectory data for the MK-84 LGB; SCANA off, $\Delta_{LE} = 26$ deg, configuration 1.

SYMBOL	α_p	M_∞	PYLON NO.	CANARDS
○	3	0.60	3	OFF
□	3	0.60	3	ON



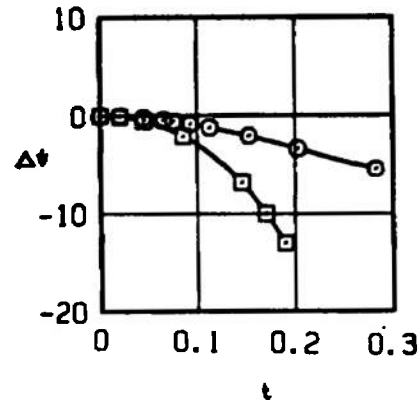
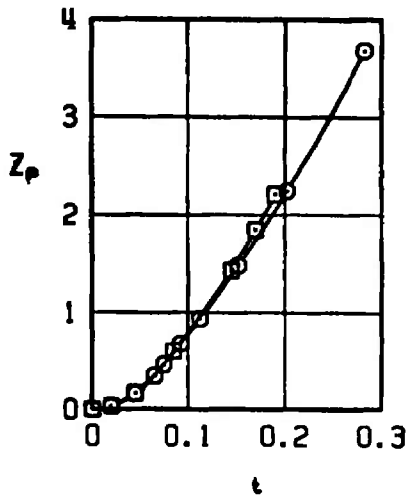
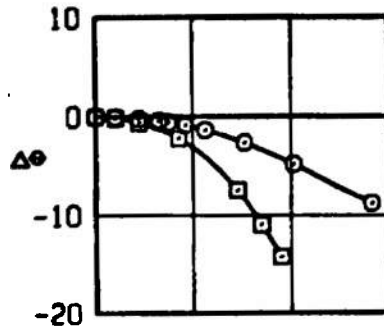
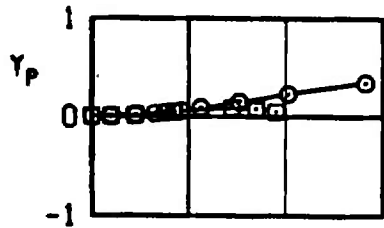
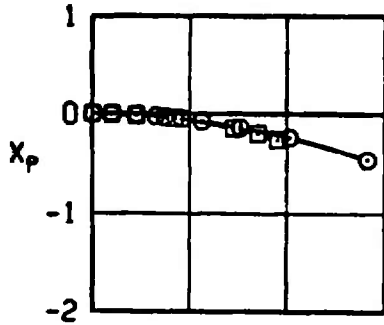
b. $M_\infty = 0.60, \alpha_p = 3$
Figure 15. Continued.

SYMBOL	α_p	M_∞	PYLON NO.	CANARDS
○	2	0.75	3	OFF
□	2	0.75	3	ON



c. $M_\infty = 0.75, \alpha_p = 2$
 Figure 15. Concluded.

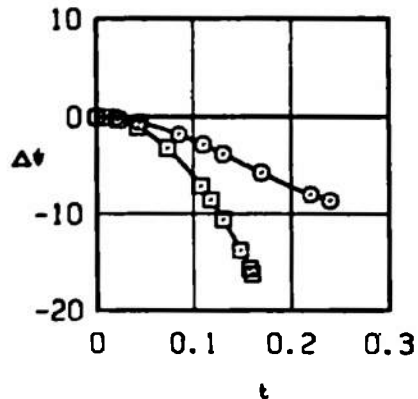
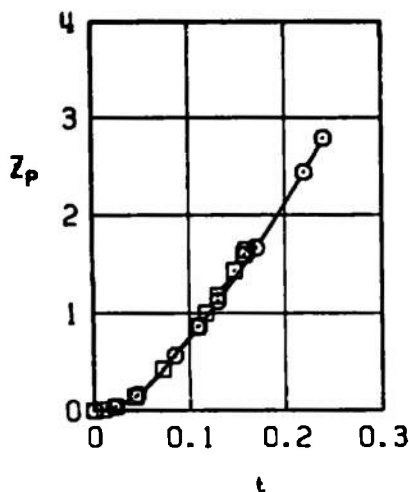
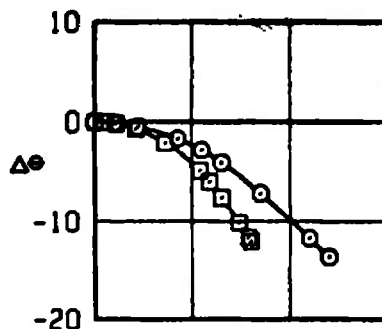
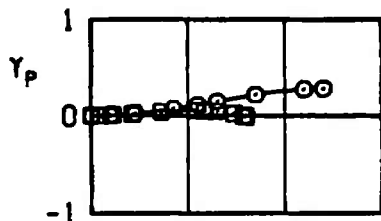
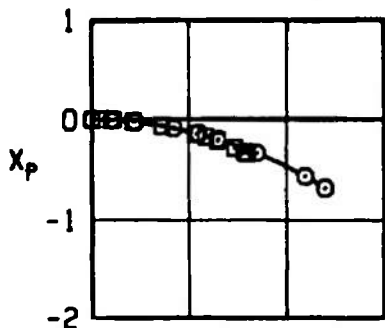
SYMBOL	α_p	M_∞	PYLON NO.	CANARDS
○	2	0.95	3	OFF
□	2	0.95	3	ON



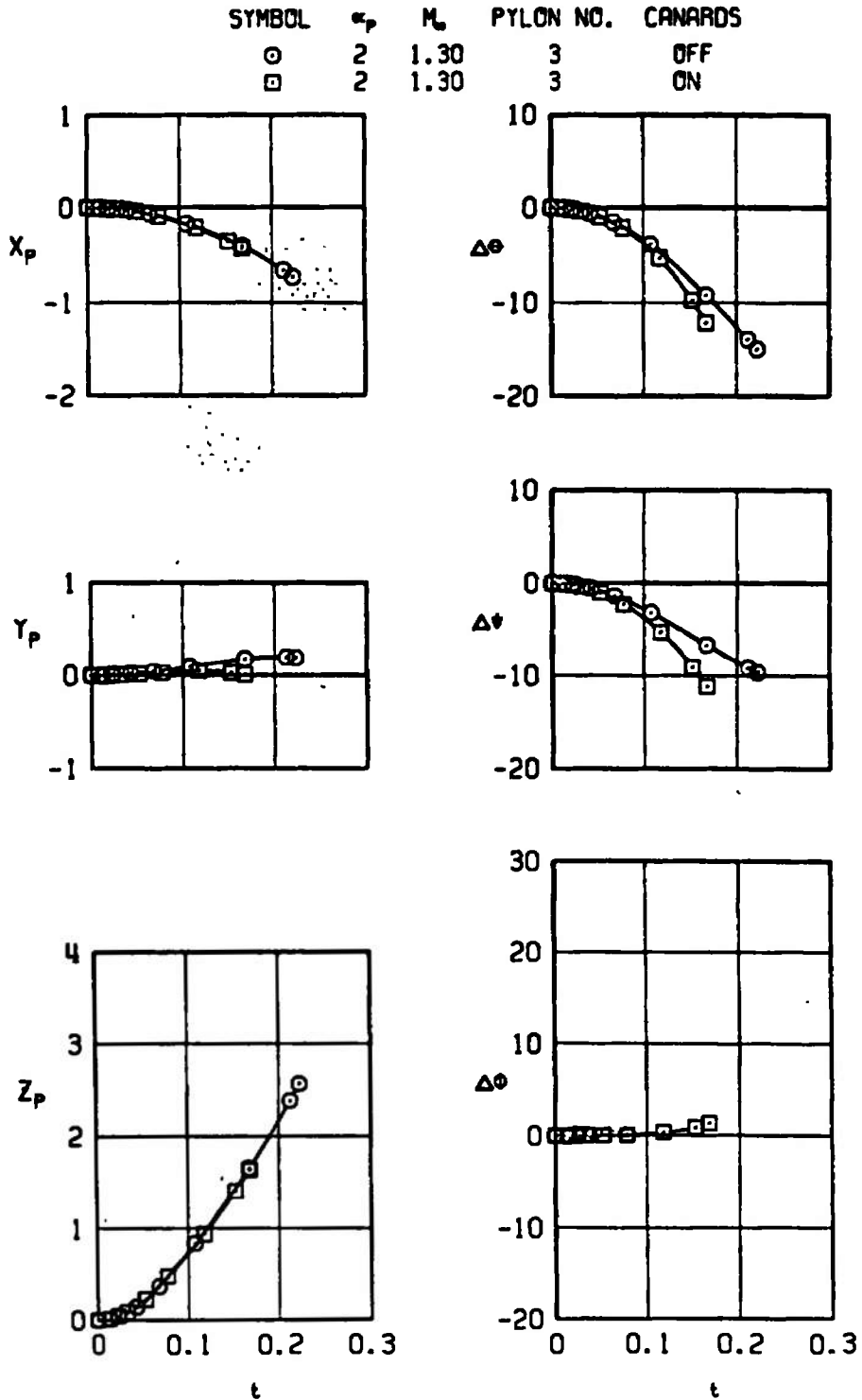
a. $M_\infty = 0.95, \alpha_p = 2$

Figure 16. Effects of the canards on trajectory data for the MK-84 LGB; SCANA off, $\Delta_{LE} = 60$ deg, configuration 1.

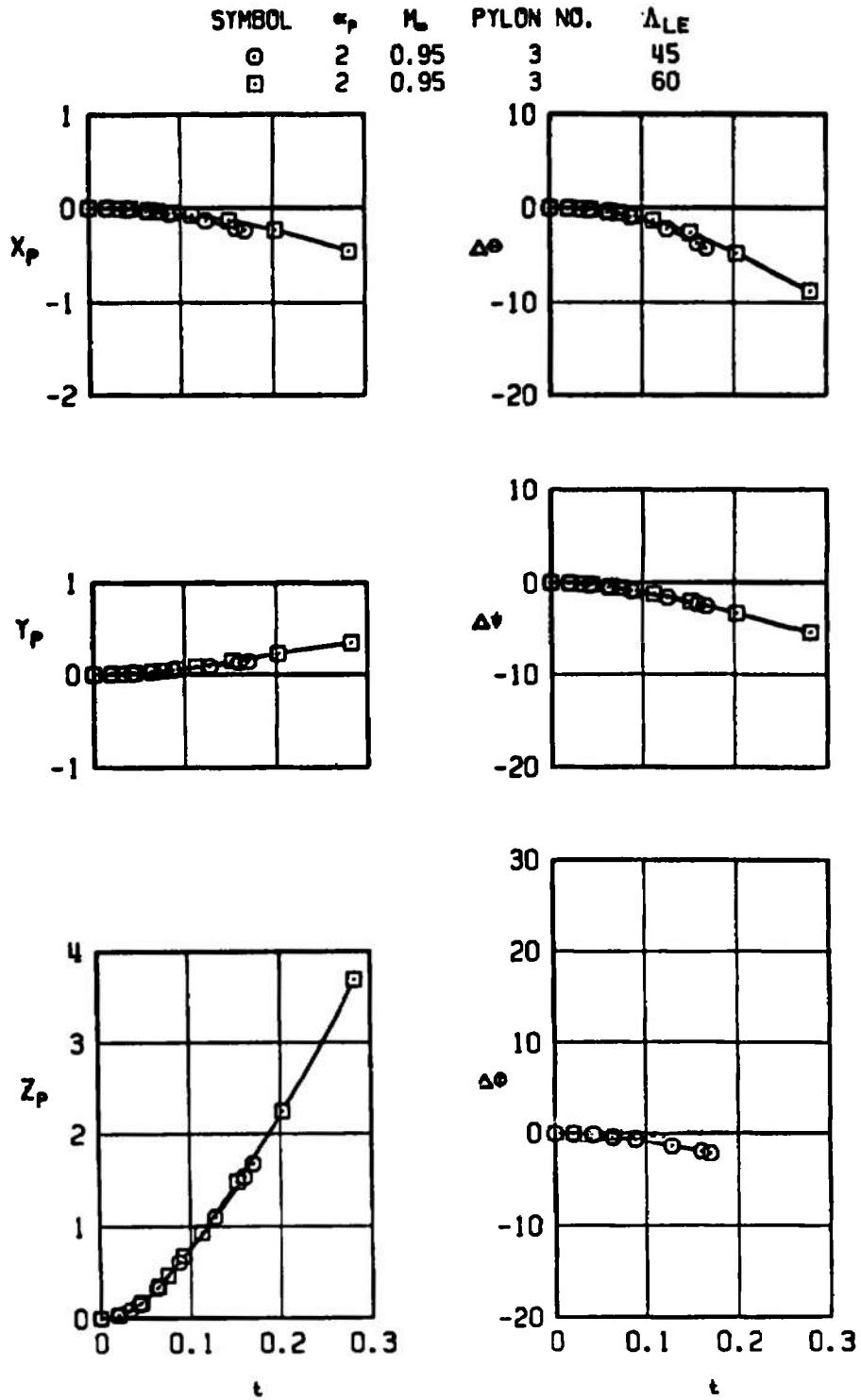
SYMBOL	α_p	M_∞	PYLON NO.	CANARDS
○	2	1.10	3	OFF
□	2	1.10	3	ON



b. $M_\infty = 1.10, \alpha_p = 2$
 Figure 16. Continued.

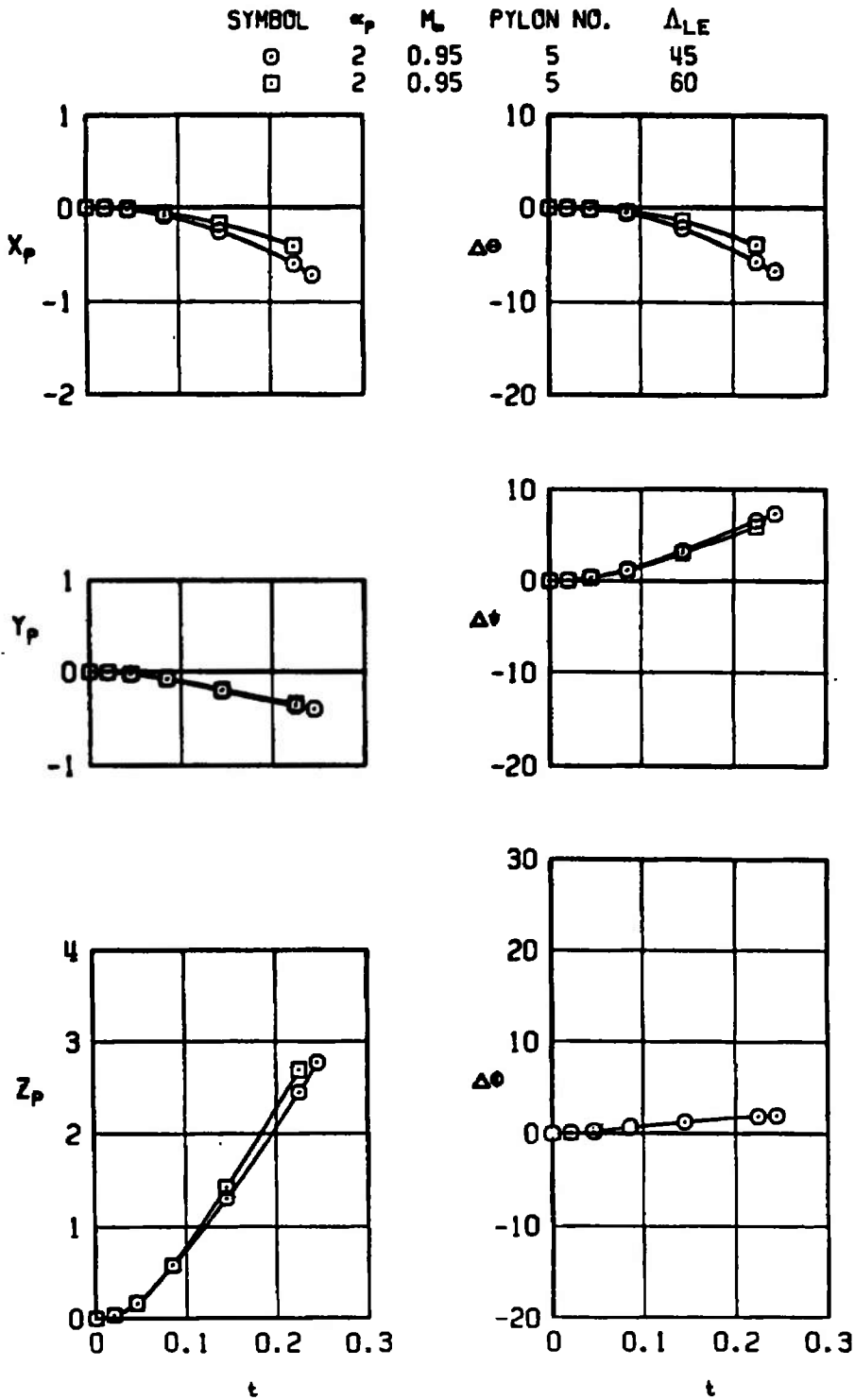


c. $M_\infty = 1.30, \alpha_p = 2$
 Figure 16. Concluded.



a. $M_\infty = 0.95$, pylon No. 3

Figure 17. Effects of the wing sweep angle on trajectory data for the MK-84 LGB; canards off, SCANA off, configuration 1.



b. $M_\infty = 0.95$, pylon No. 5
 Figure 17. Concluded.

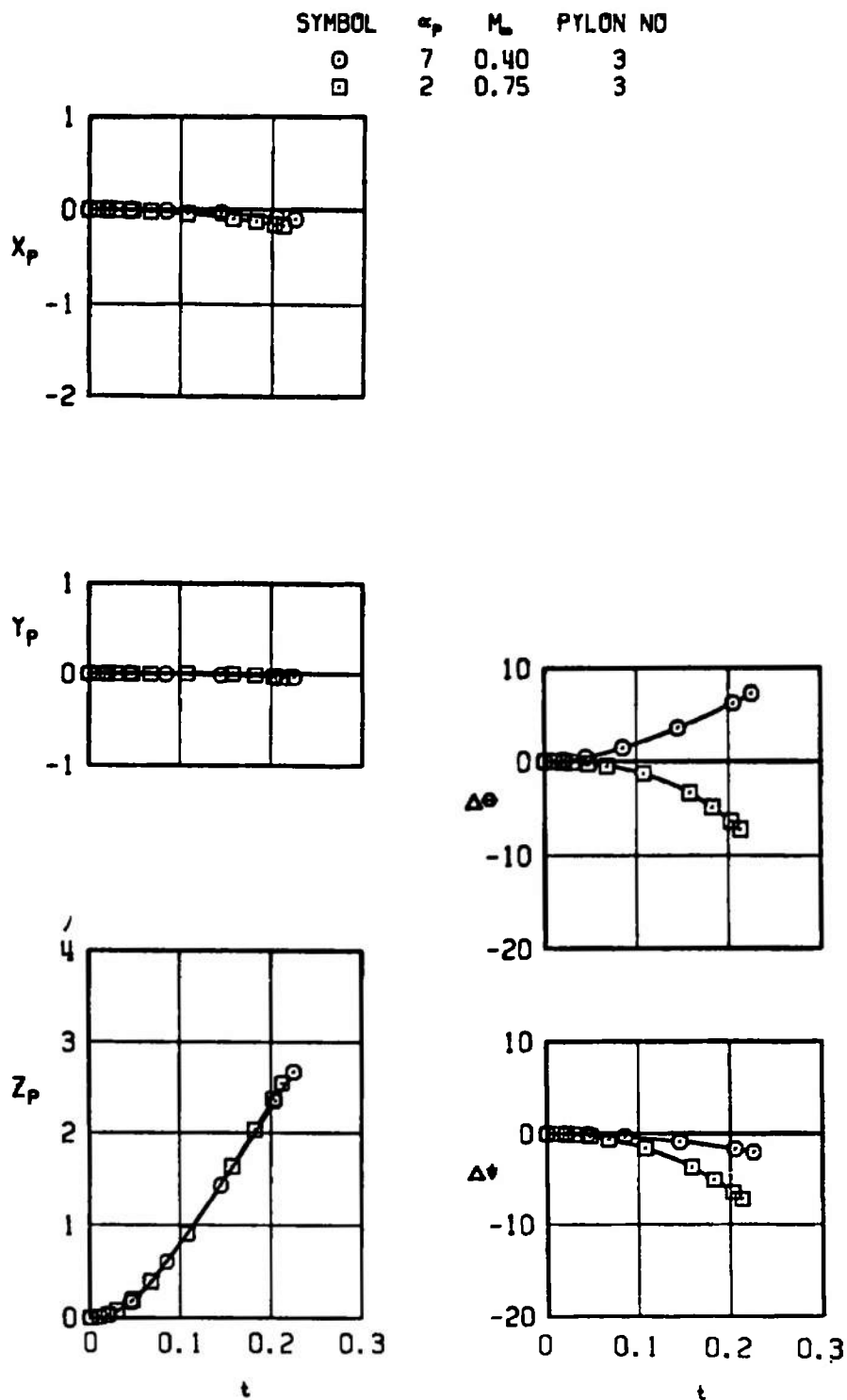


Figure 18. Effects of Mach number on trajectory data for the MK-84 LGB; canards on, SCANA on, $\Lambda_{LE} = 26$ deg, configuration 2.

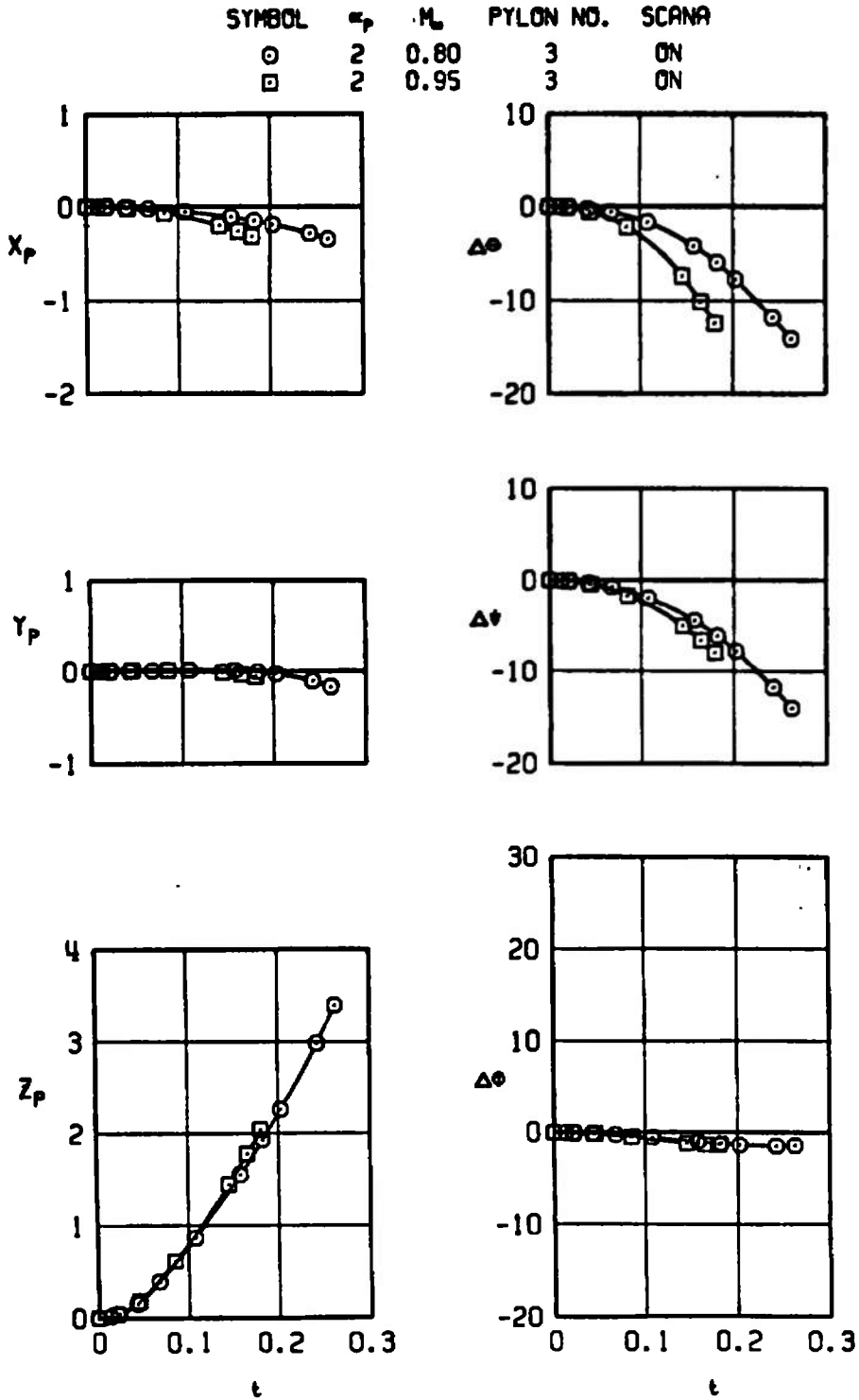


Figure 19. Effects of Mach number on trajectory data for the MK-84 LGB; canards on, SCANA on, $\Lambda_{LE} = 45$ deg, configuration 3.

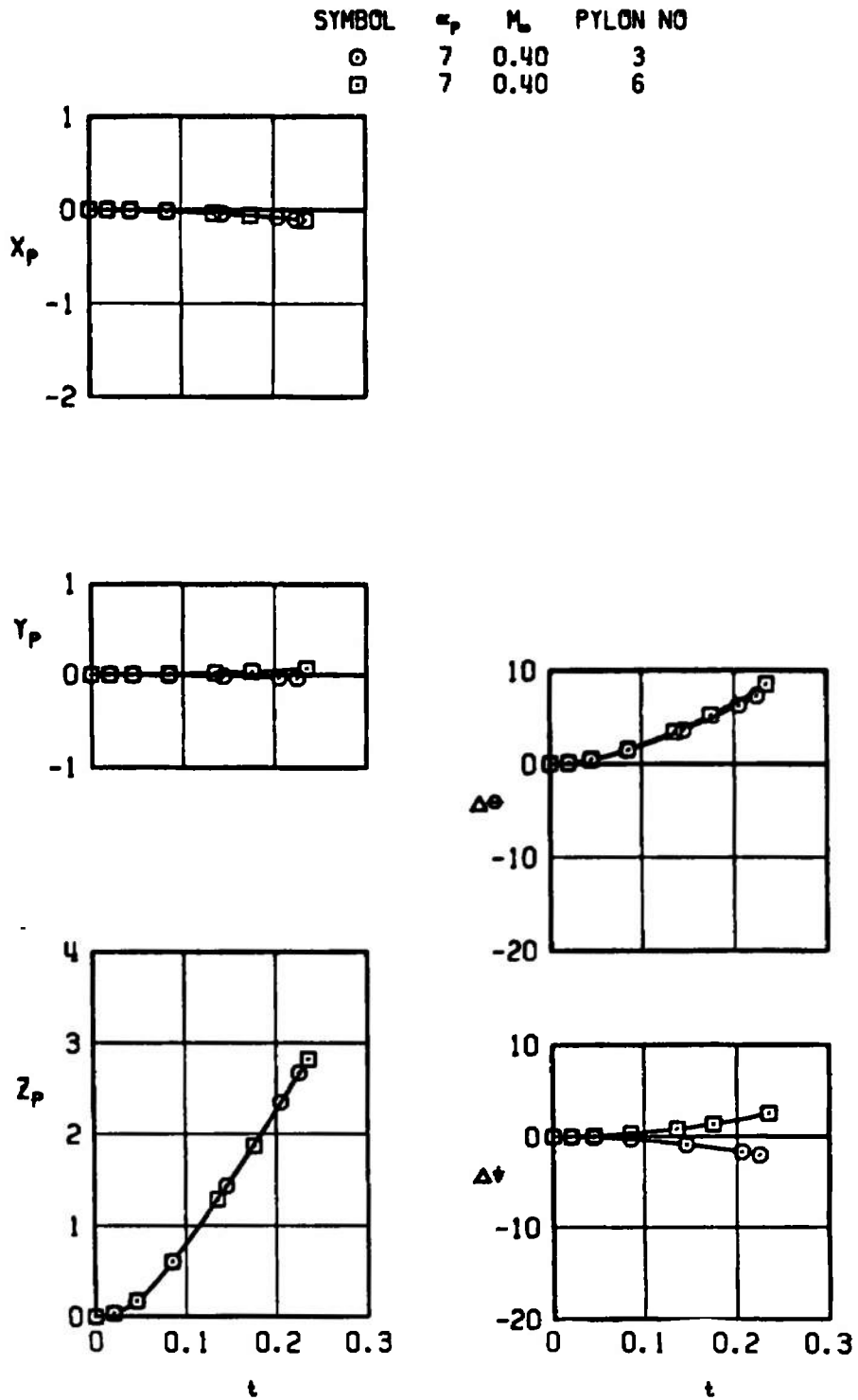


Figure 20. Effects of the carriage position on trajectory data for the MK-84 LGB; canards on, SCANA on, $\Lambda_{LE} = 26$ deg, configuration 2.

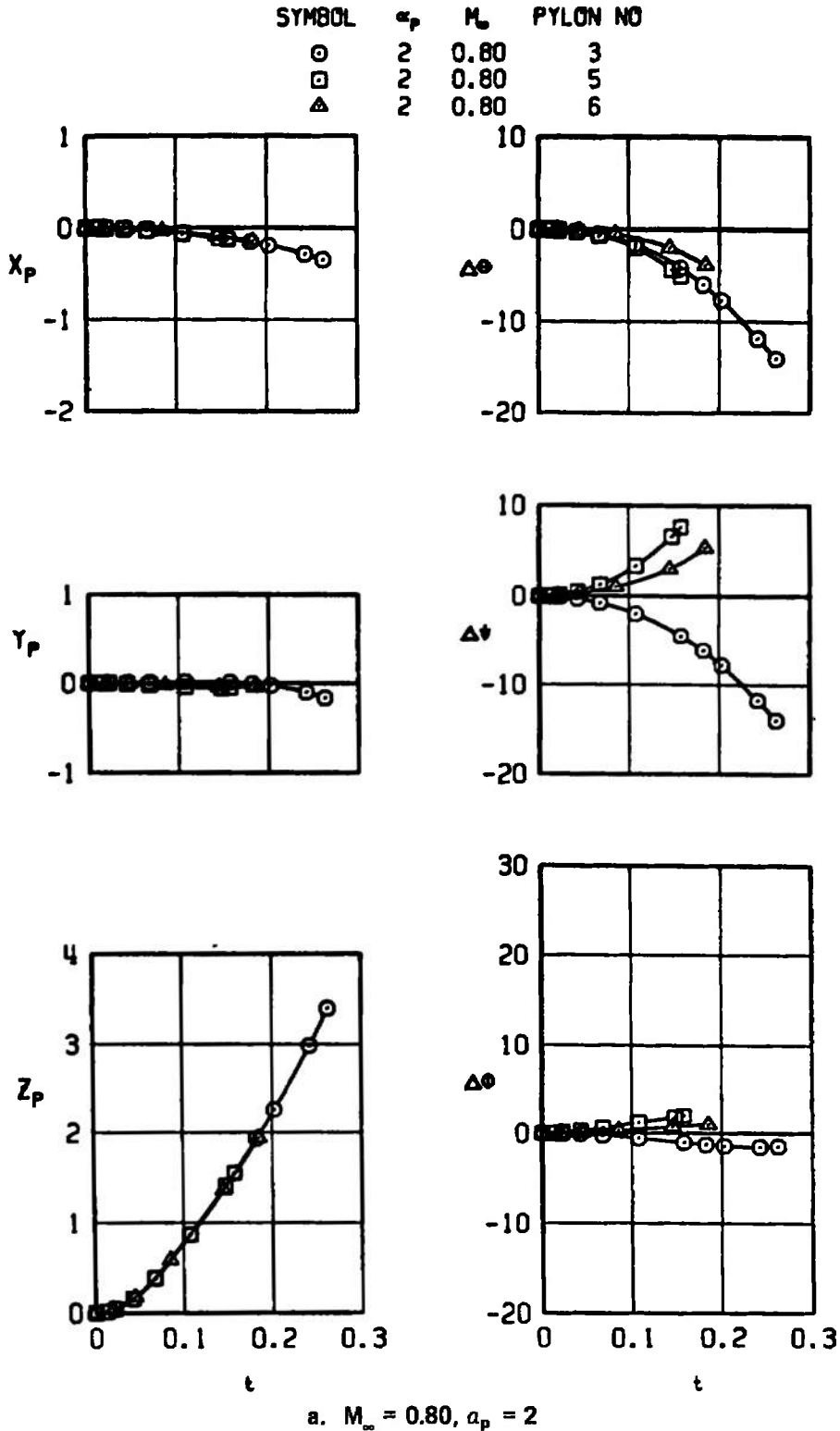
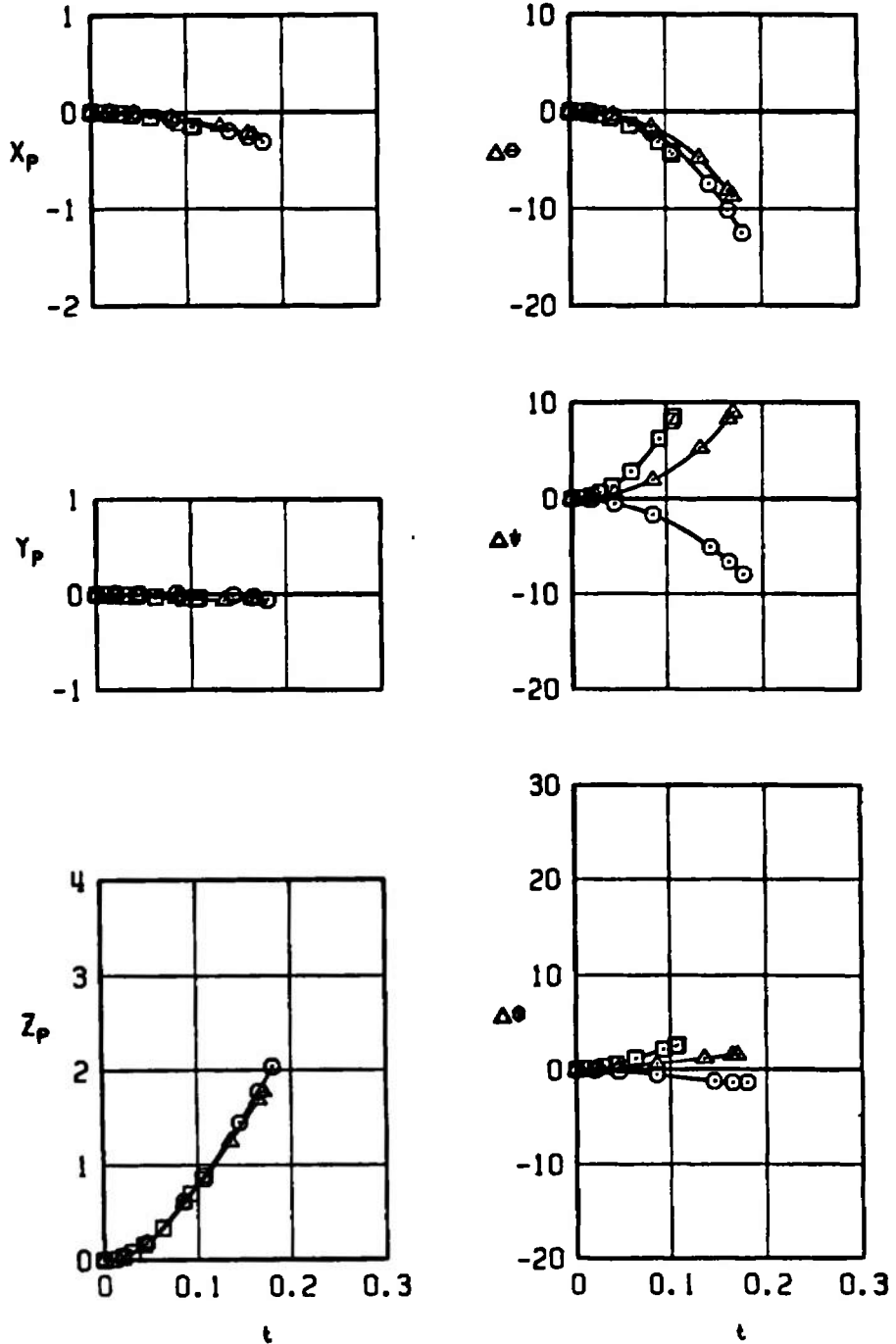


Figure 21. Effects of the carriage position on trajectory data for the MK-84 LGB; canards on, SCANA on, $\Lambda_{LE} = 45$ deg, configuration 3.

SYMBOL	a_p	M_∞	PYLON NO
○	2	0.95	3
□	2	0.95	5
△	2	0.95	6



b. $M_\infty = 0.95, a_p = 2$
 Figure 21. Concluded.

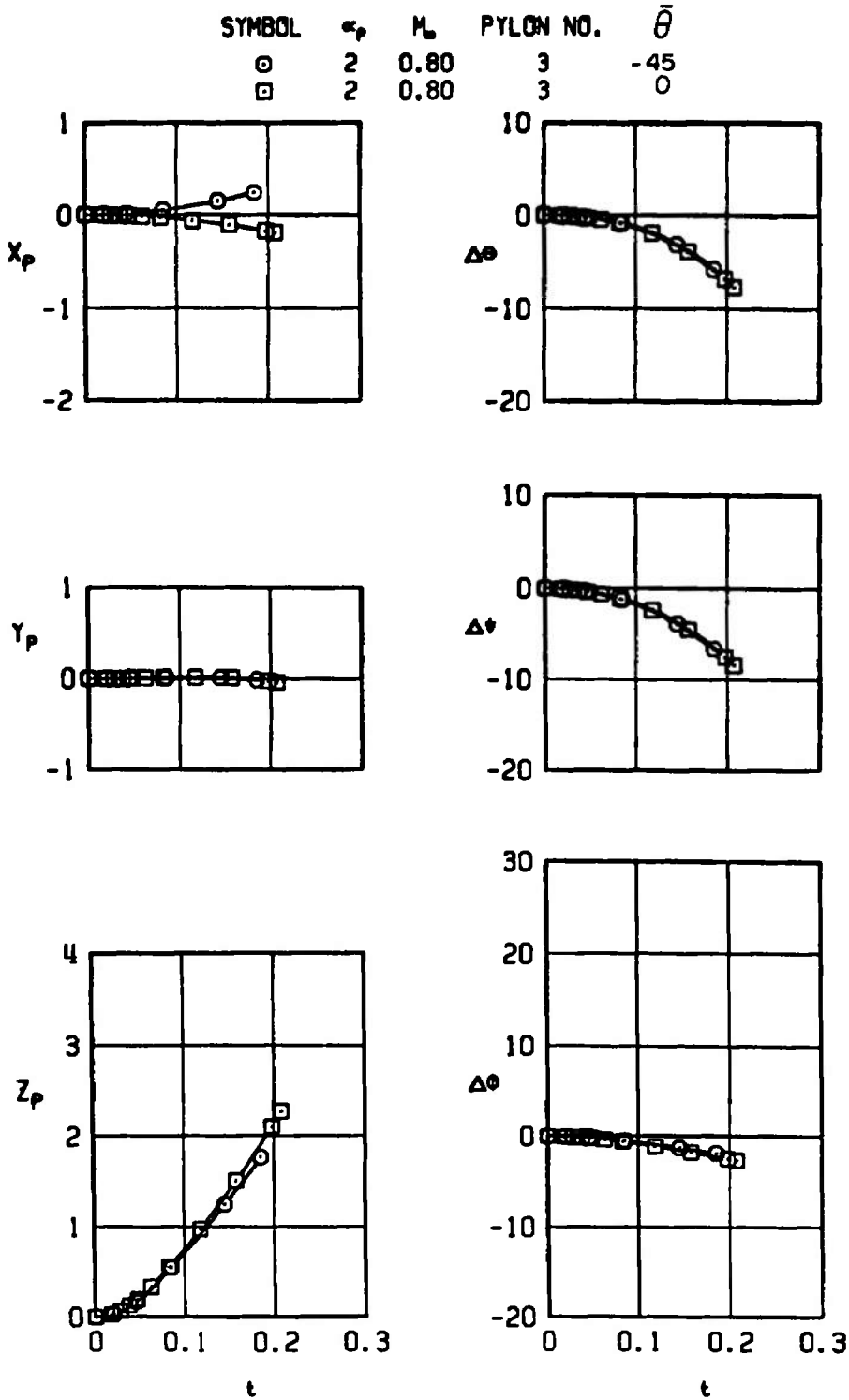
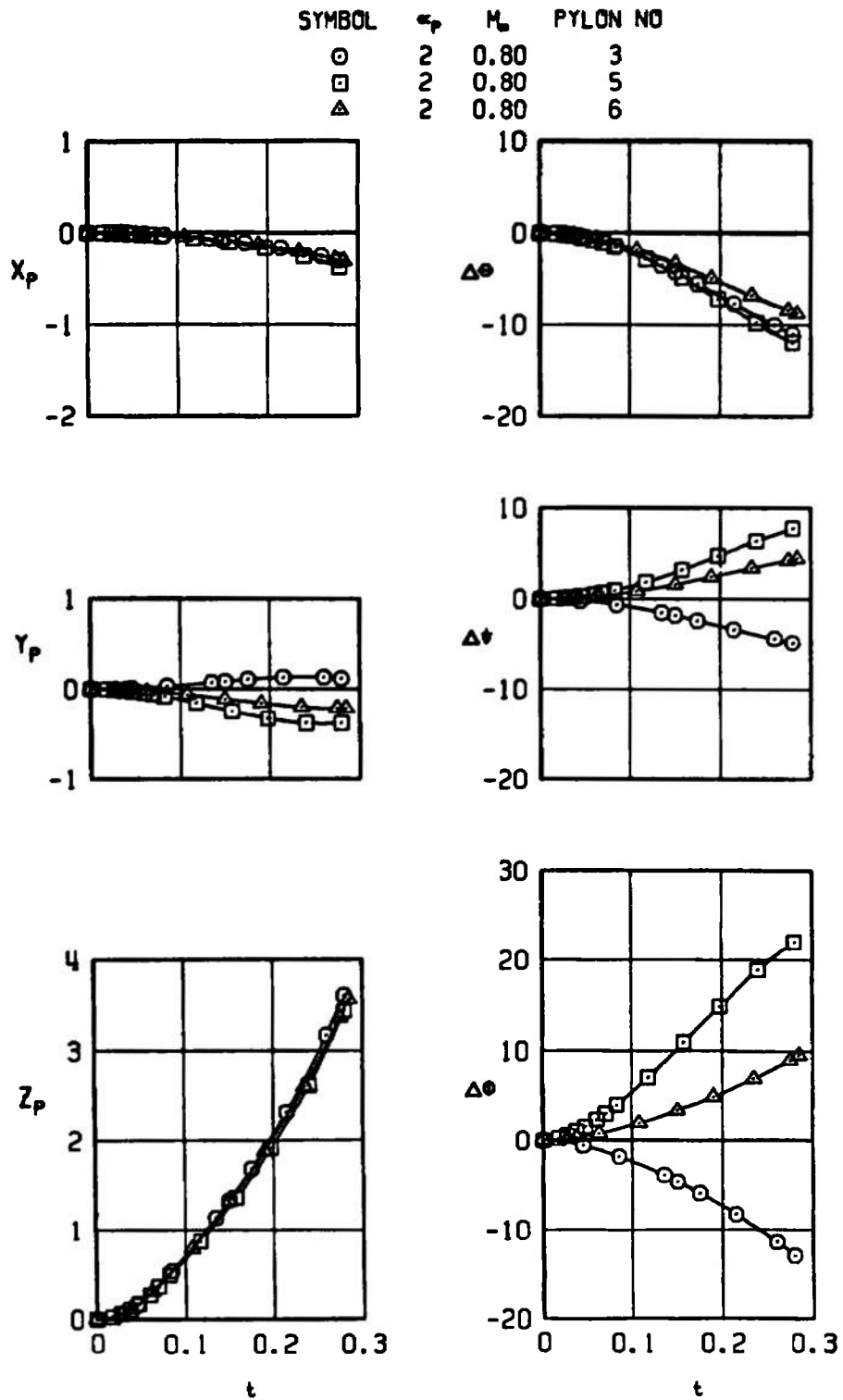


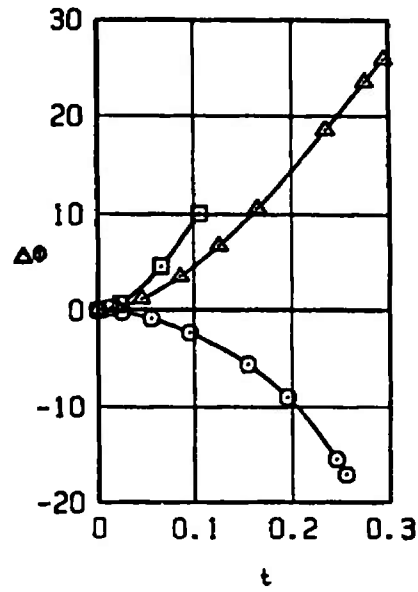
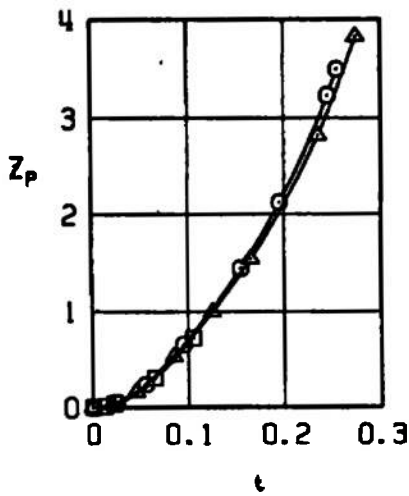
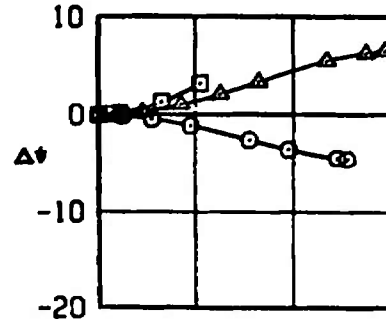
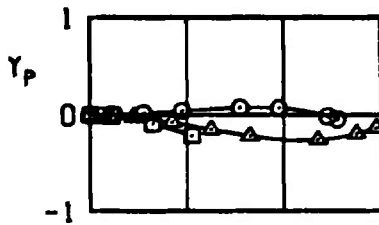
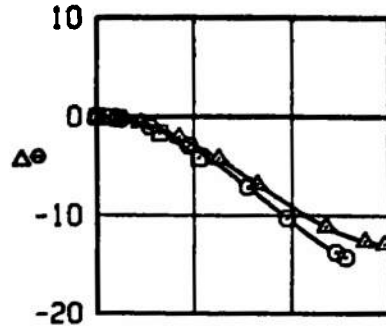
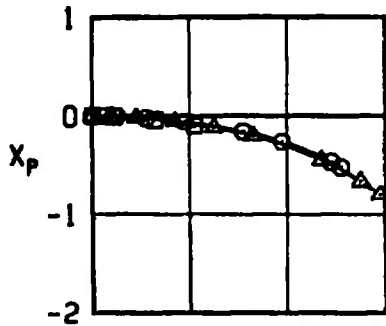
Figure 22. Effects of climb angle on trajectory data for the MK-84 LGB; canards on, SCANA off, $\Lambda_{LE} = 45$ deg, configuration 3.



a. $M_\infty = 0.80$

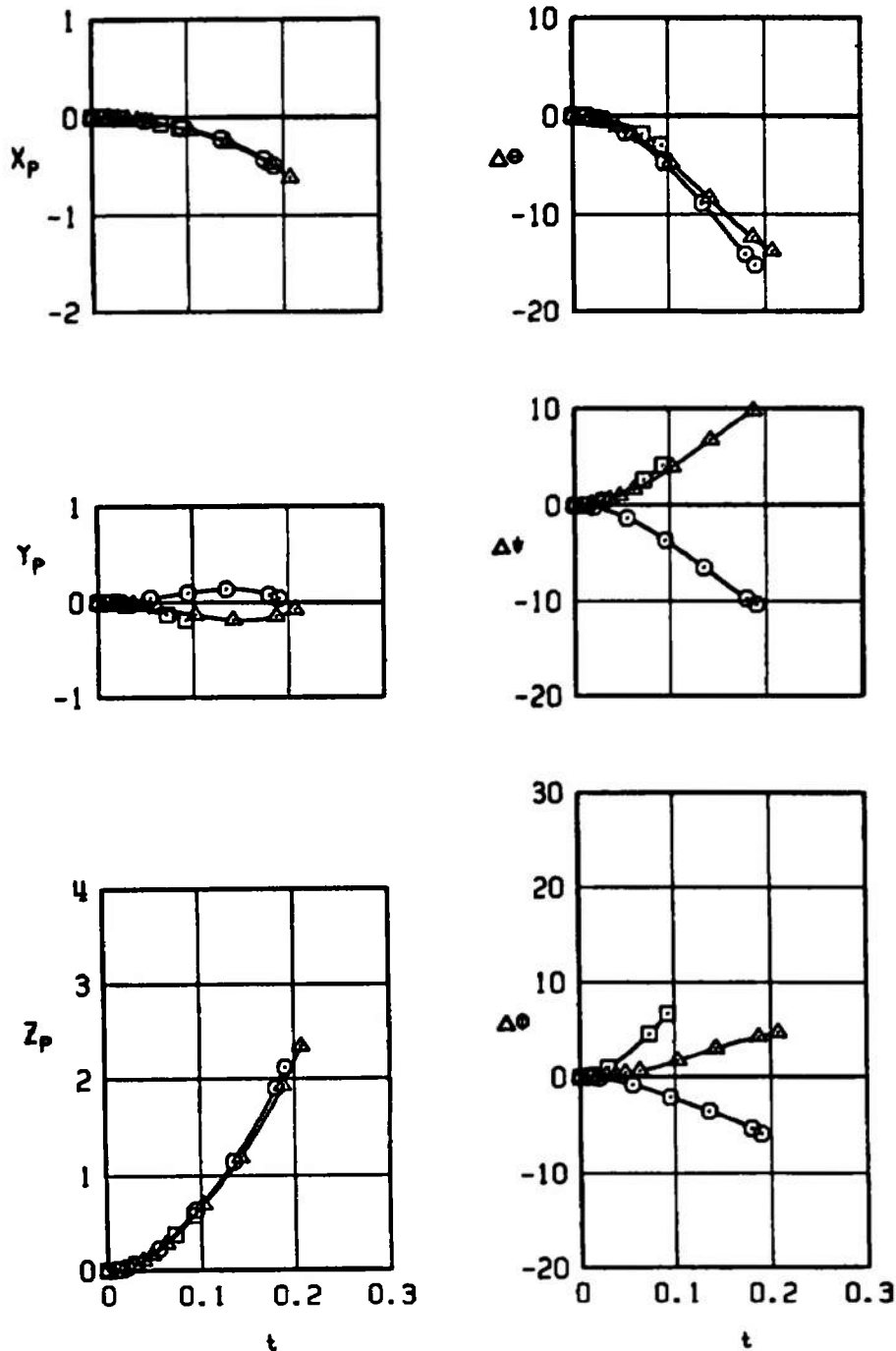
Figure 23. Effects of the carriage position on trajectory data for the MK-84 EOGB; SCANA on, $\Delta_{LE} = 60$ deg, configuration 4.

SYMBOL	κ_p	M_∞	PYLON NO
○	2	0.95	3
□	2	0.95	5
△	2	0.95	6

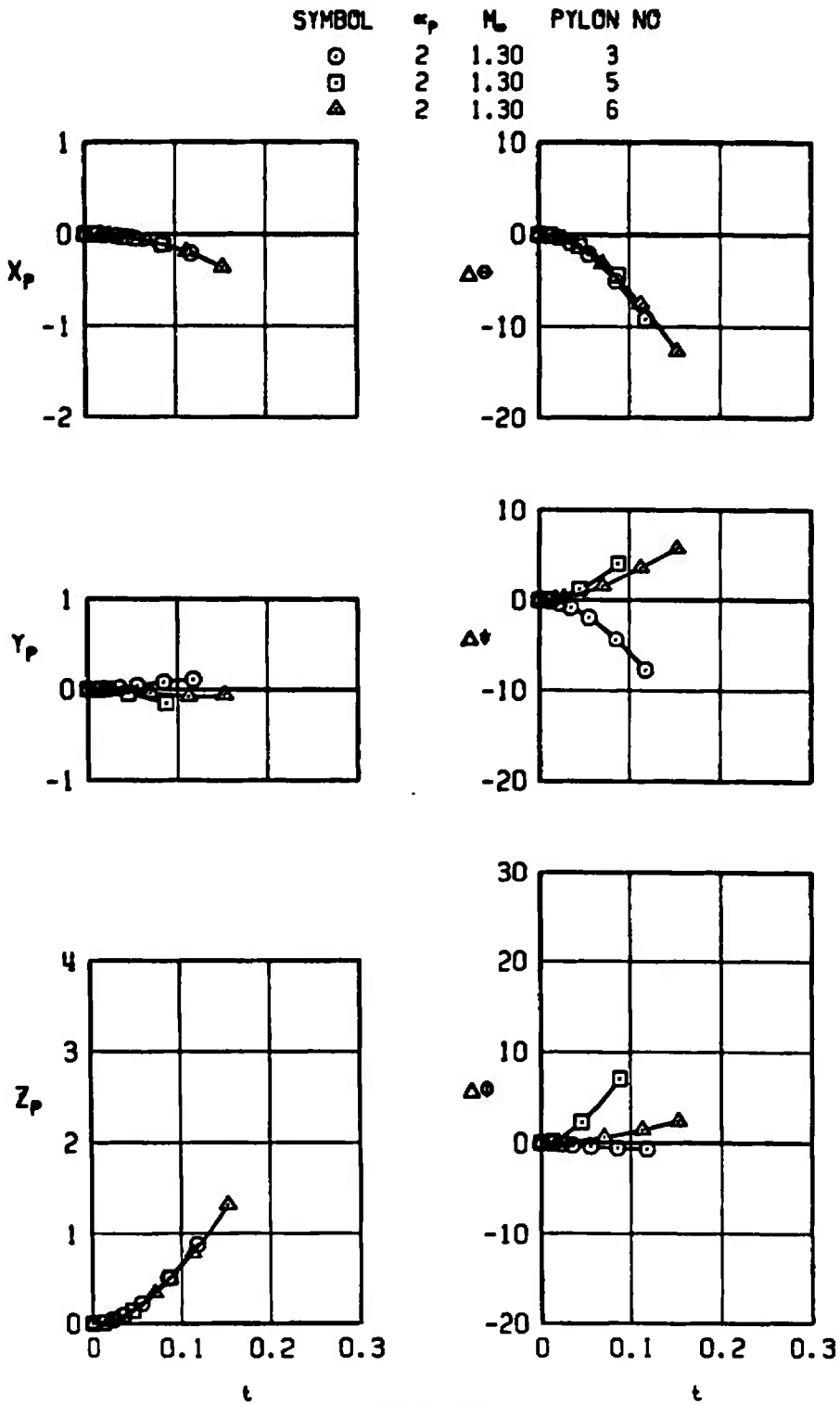


b. $M_\infty = 0.95$
 Figure 23. Continued.

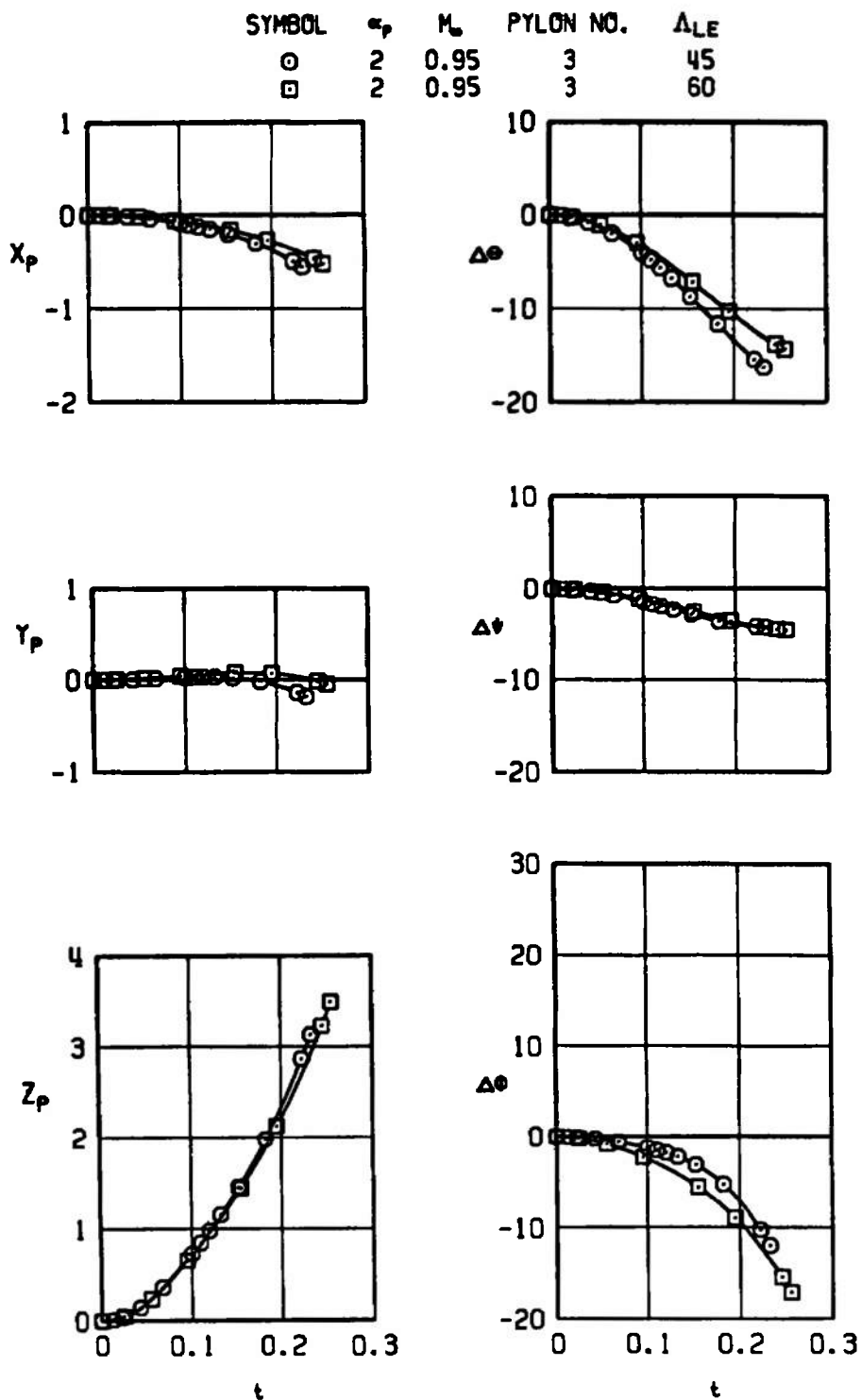
SYMBOL	α_p	M_∞	PYLON NO
○	2	1.10	3
□	2	1.10	5
△	2	6	



c. $M_\infty = 1.10$
 Figure 23. Continued.

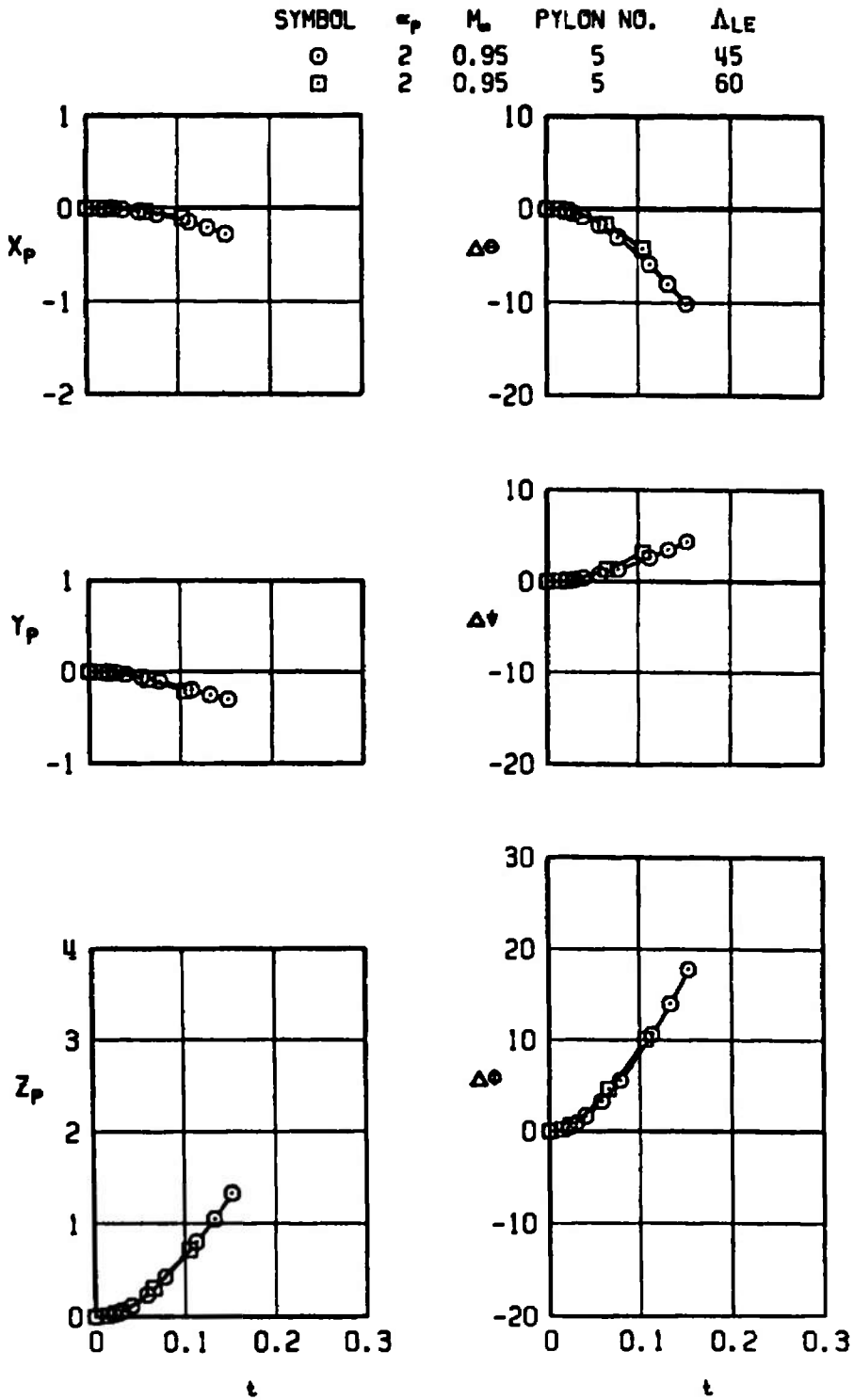


d. $M_\infty = 1.30$
 Figure 23. Concluded.

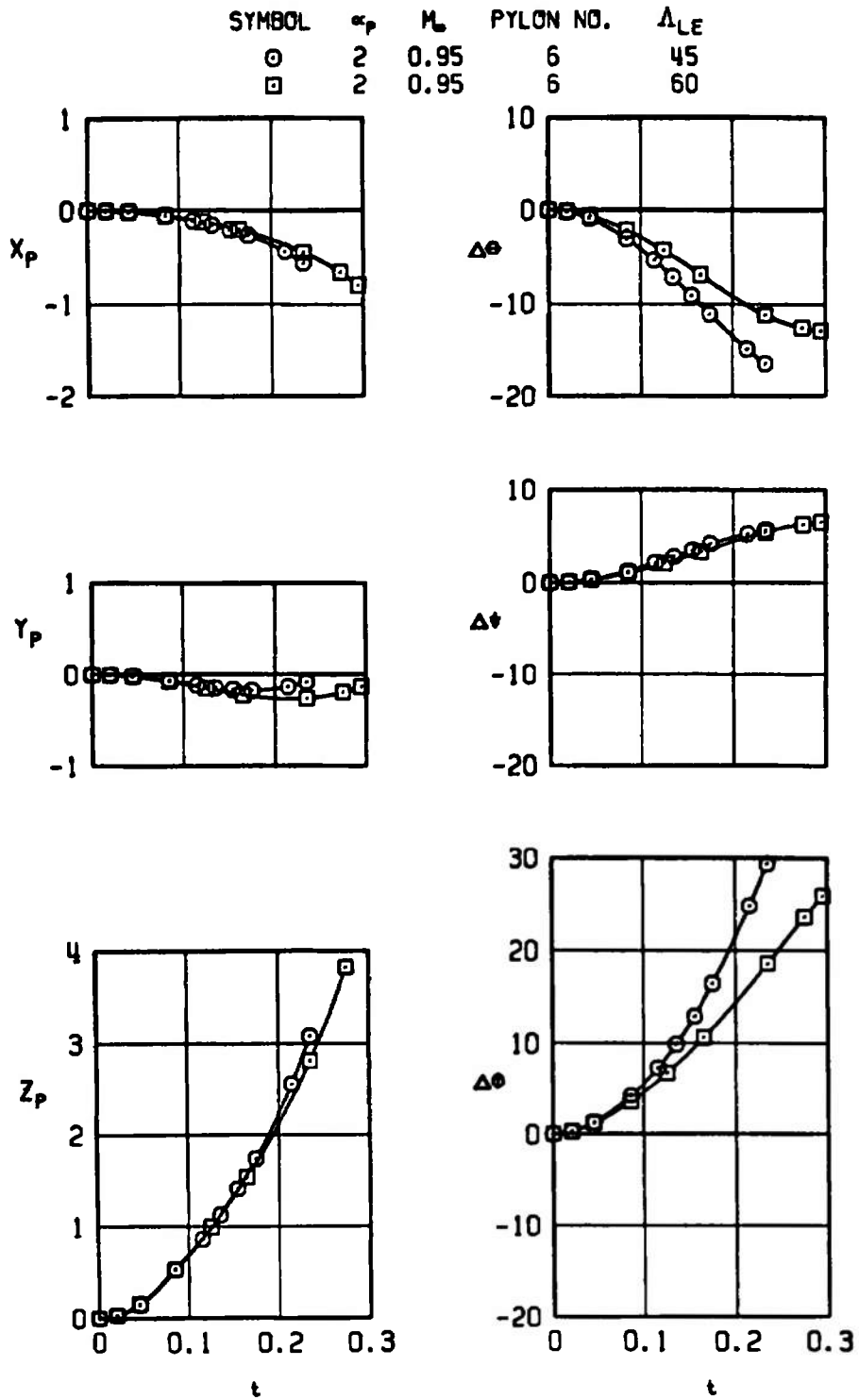


a. $M_\infty = 0.95$, pylon No. 3

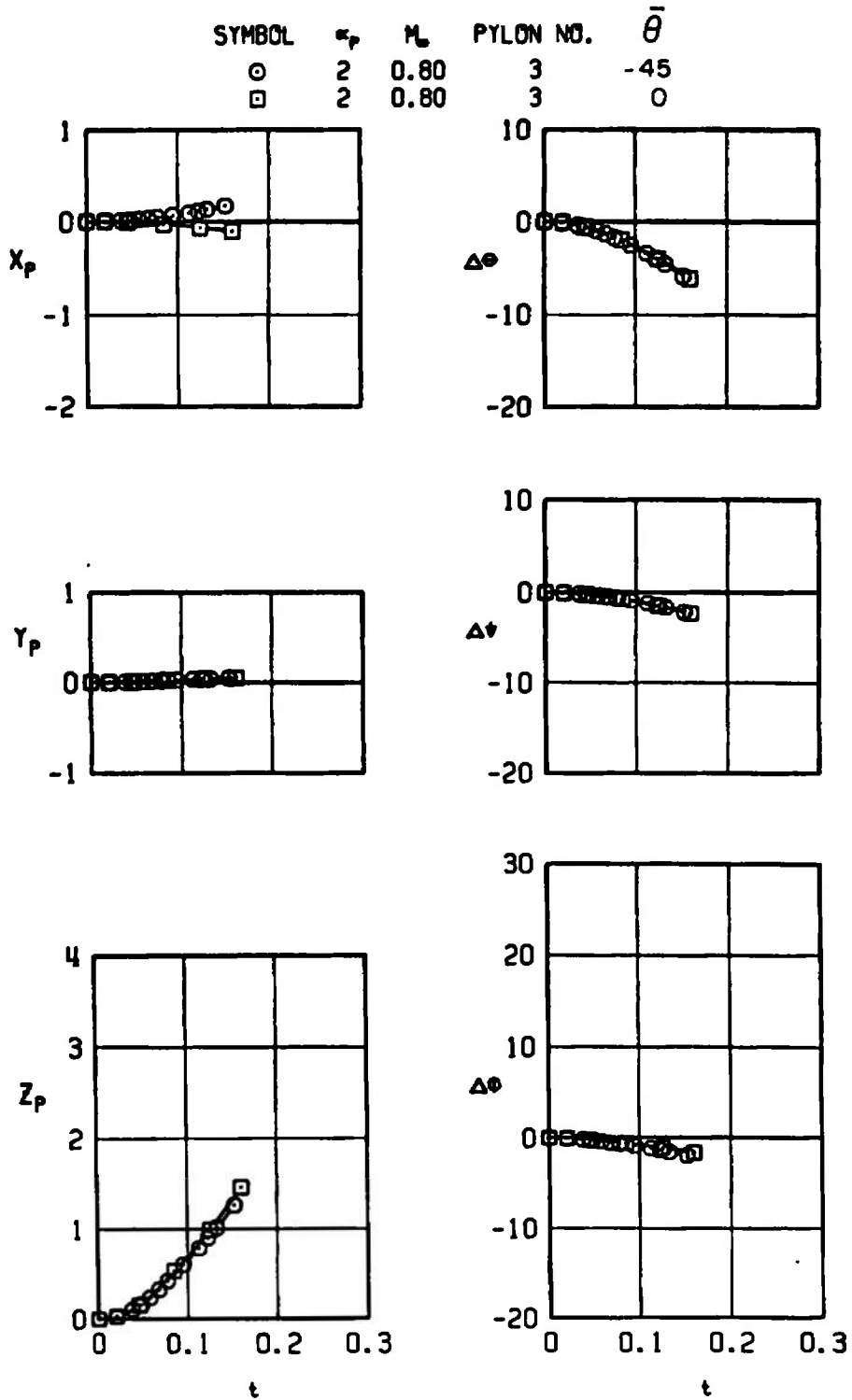
Figure 24. Effects of the wing sweep angle on trajectory data for the MK-84 EOGB; SCANA on, configuration 4.



b. $M_\infty = 0.95$, pylon No. 5
 Figure 24. Continued.

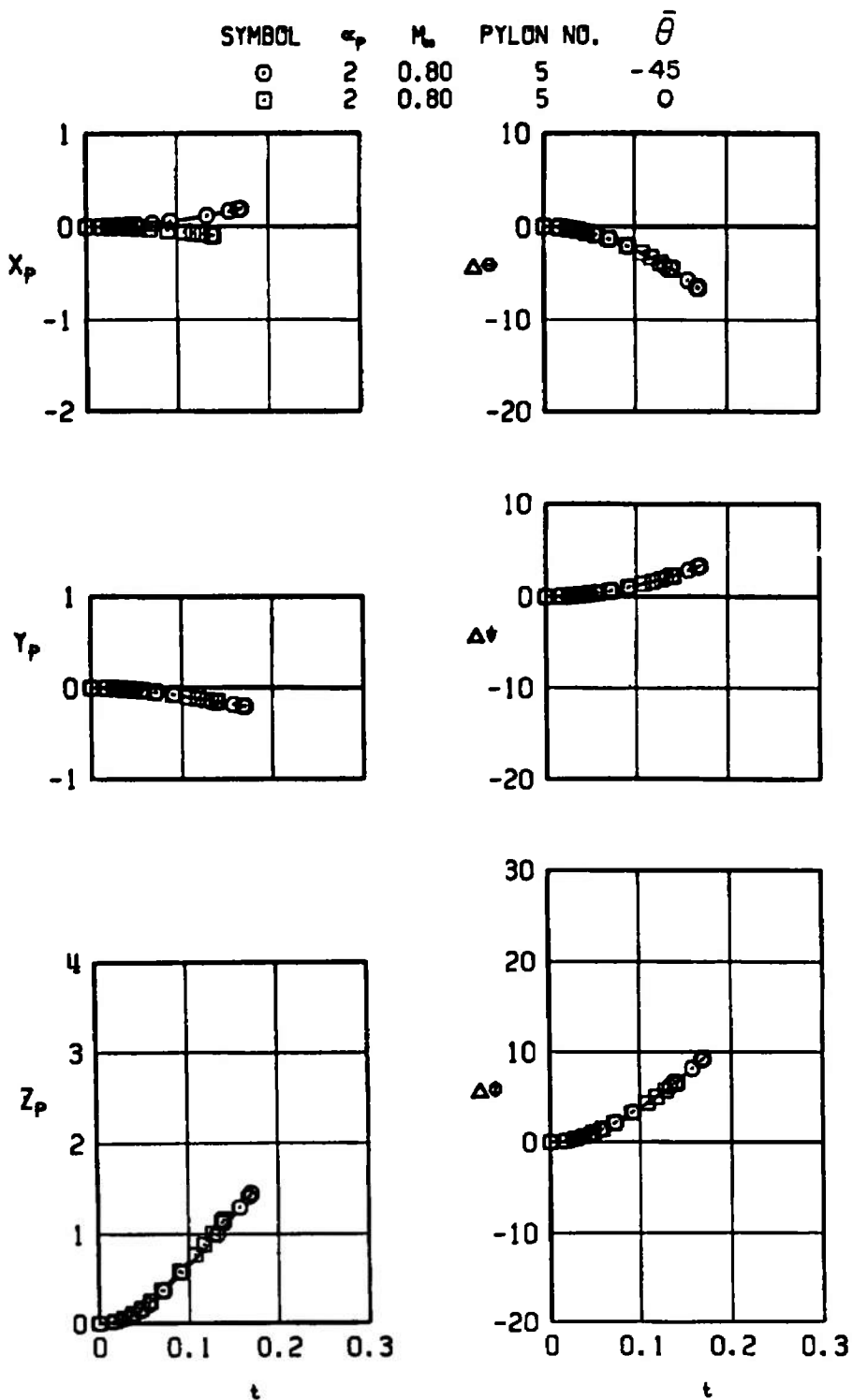


c. $M_\infty = 0.95$, pylon No. 6
 Figure 24. Concluded.

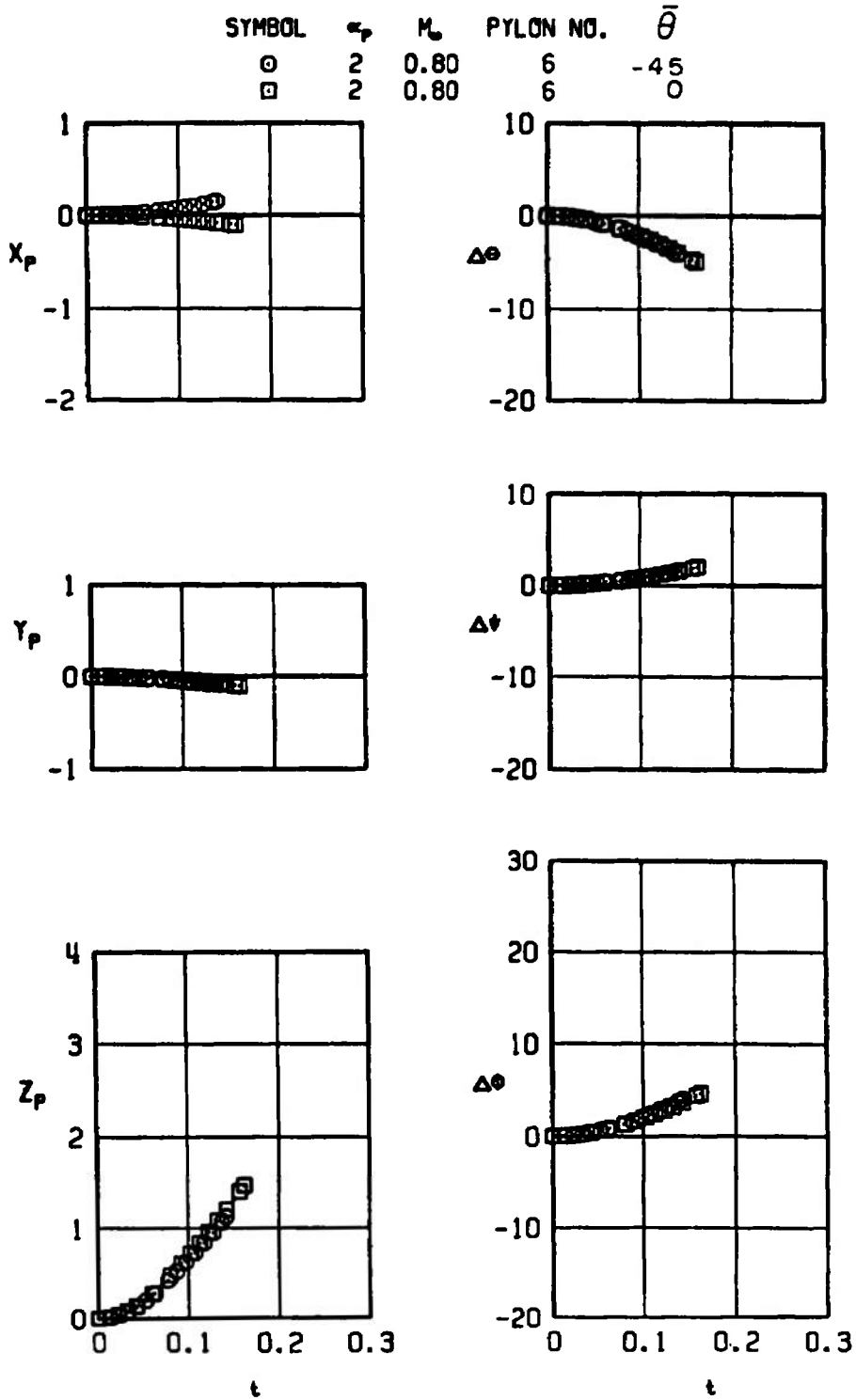


a. $M_\infty = 0.80$, pylon No. 3

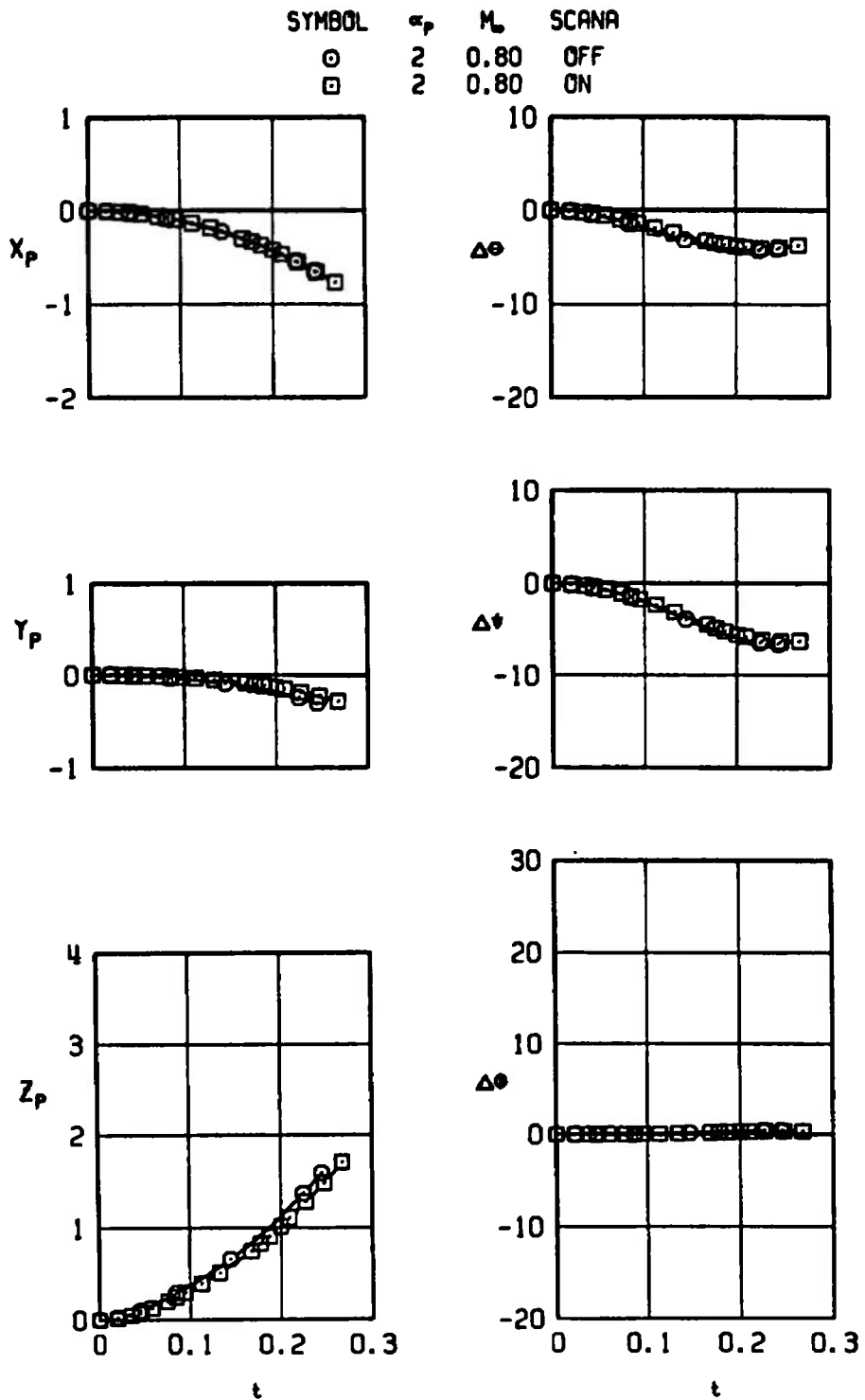
Figure 25. Effects of climb angle on trajectory data for the MK-84 EOGB; SCANA on, $\Lambda_{LE} = 45$ deg, configuration 4.



b. $M_w = 0.80$, pylon No. 5
 Figure 25. Continued.

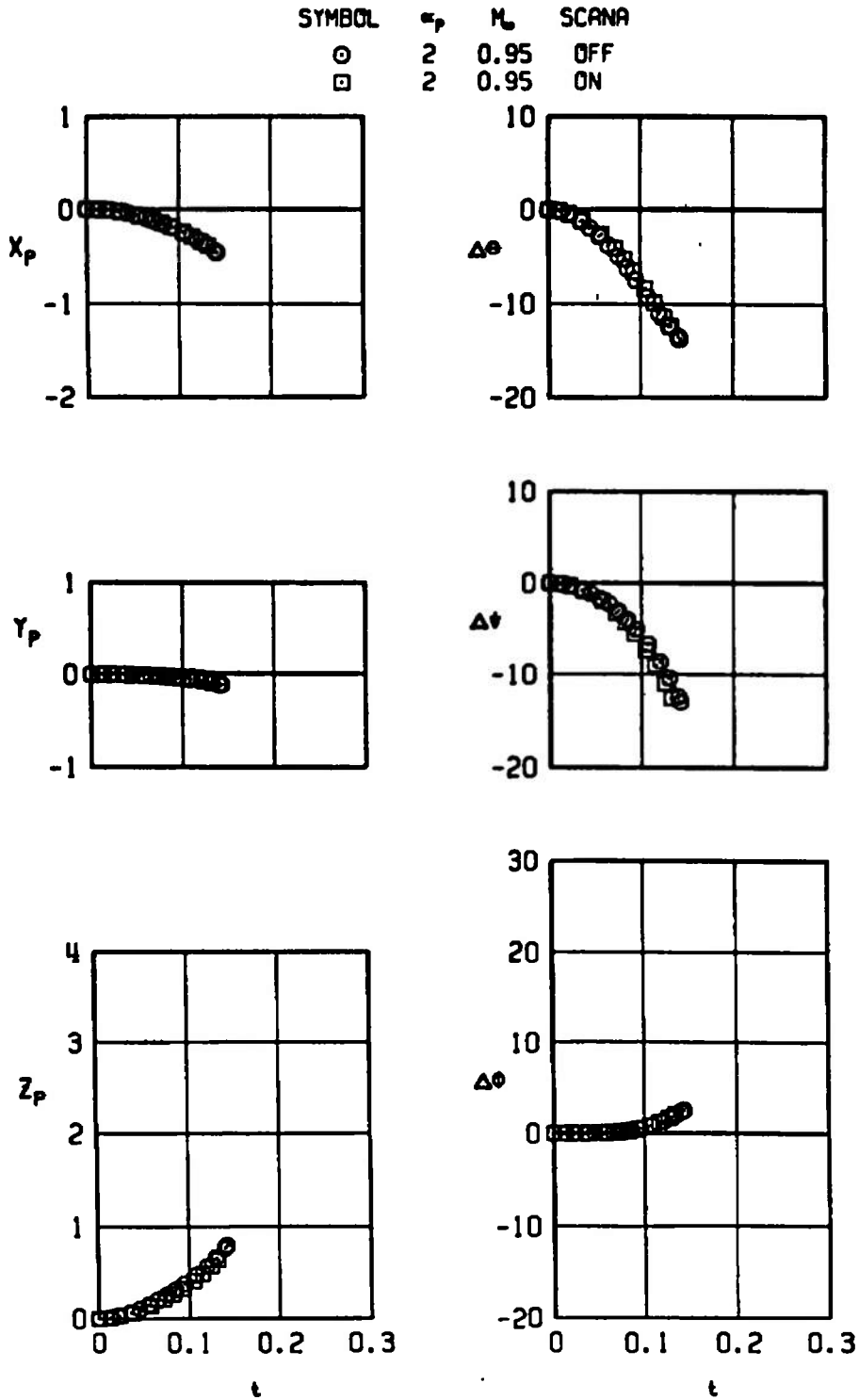


c. $M_u = 0.80$, pylon No. 6
 Figure 25. Concluded.



a. $M_\infty = 0.80$

Figure 26. Effects of the SCANA (shape No. 1) turret on trajectory data for the SUU-30 H/B; CG forward, BRU sta. 2, $\Lambda_{LE} = 45$ deg, configuration 7.



b. $M_\infty = 0.95$
 Figure 26. Concluded.

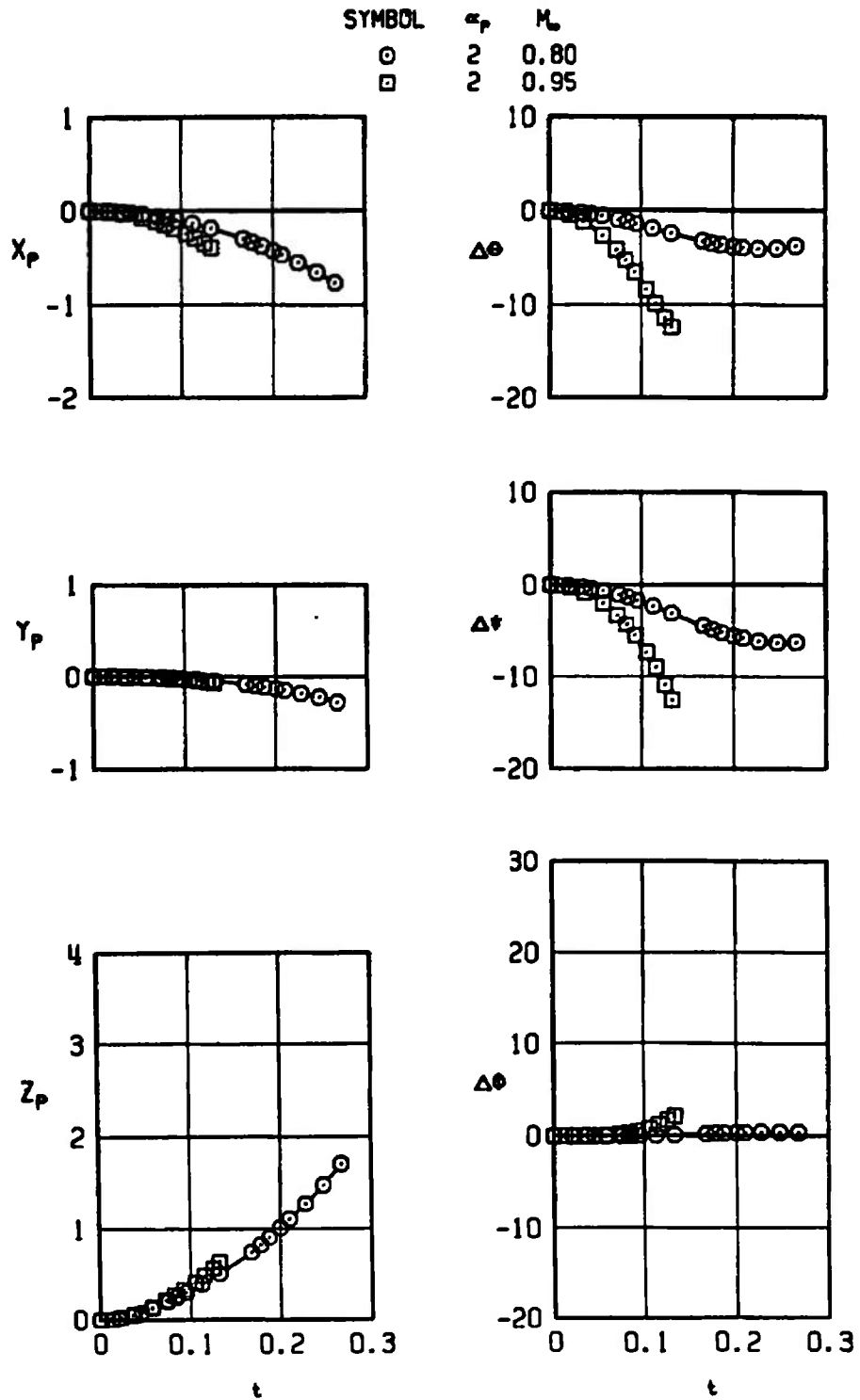
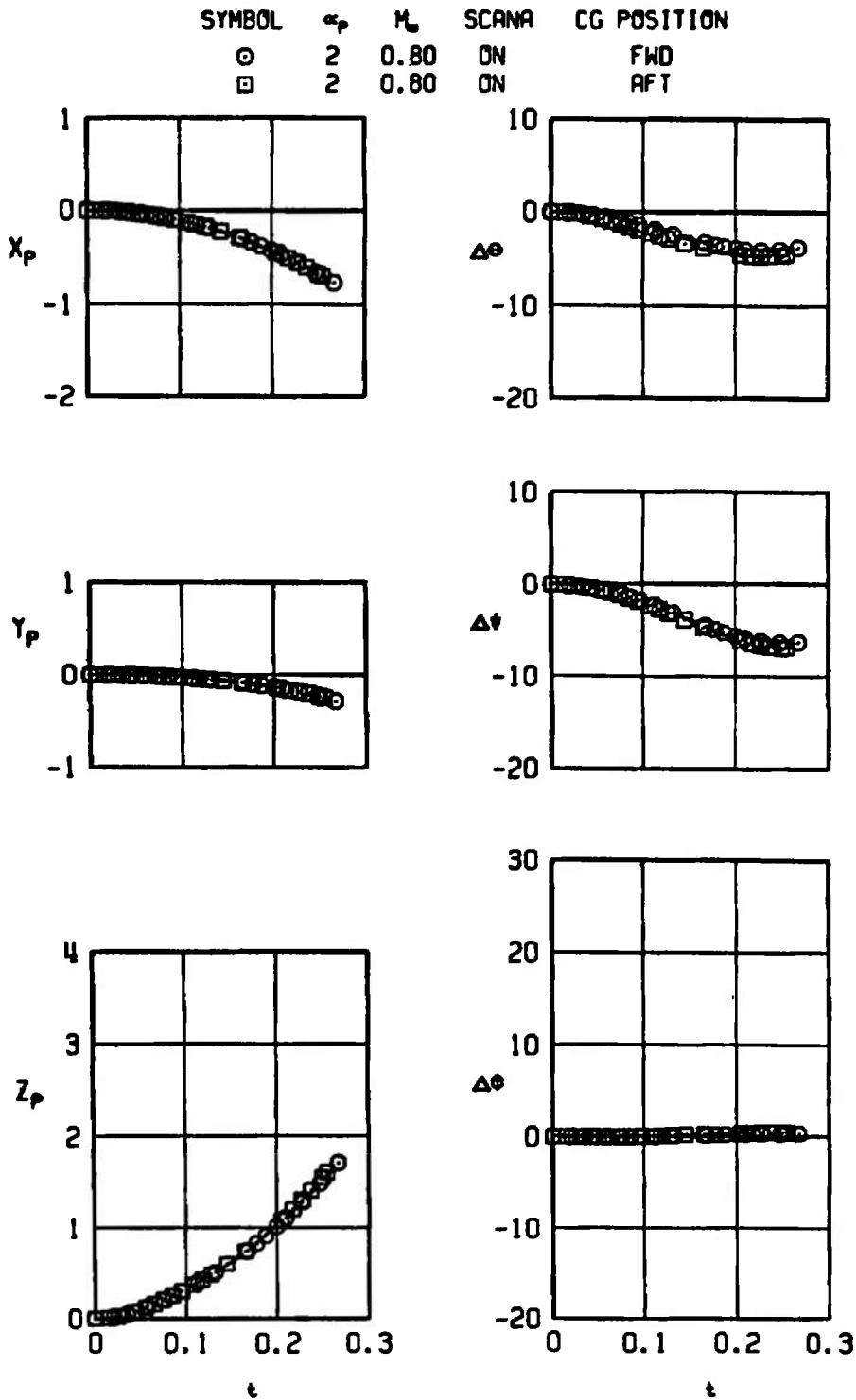
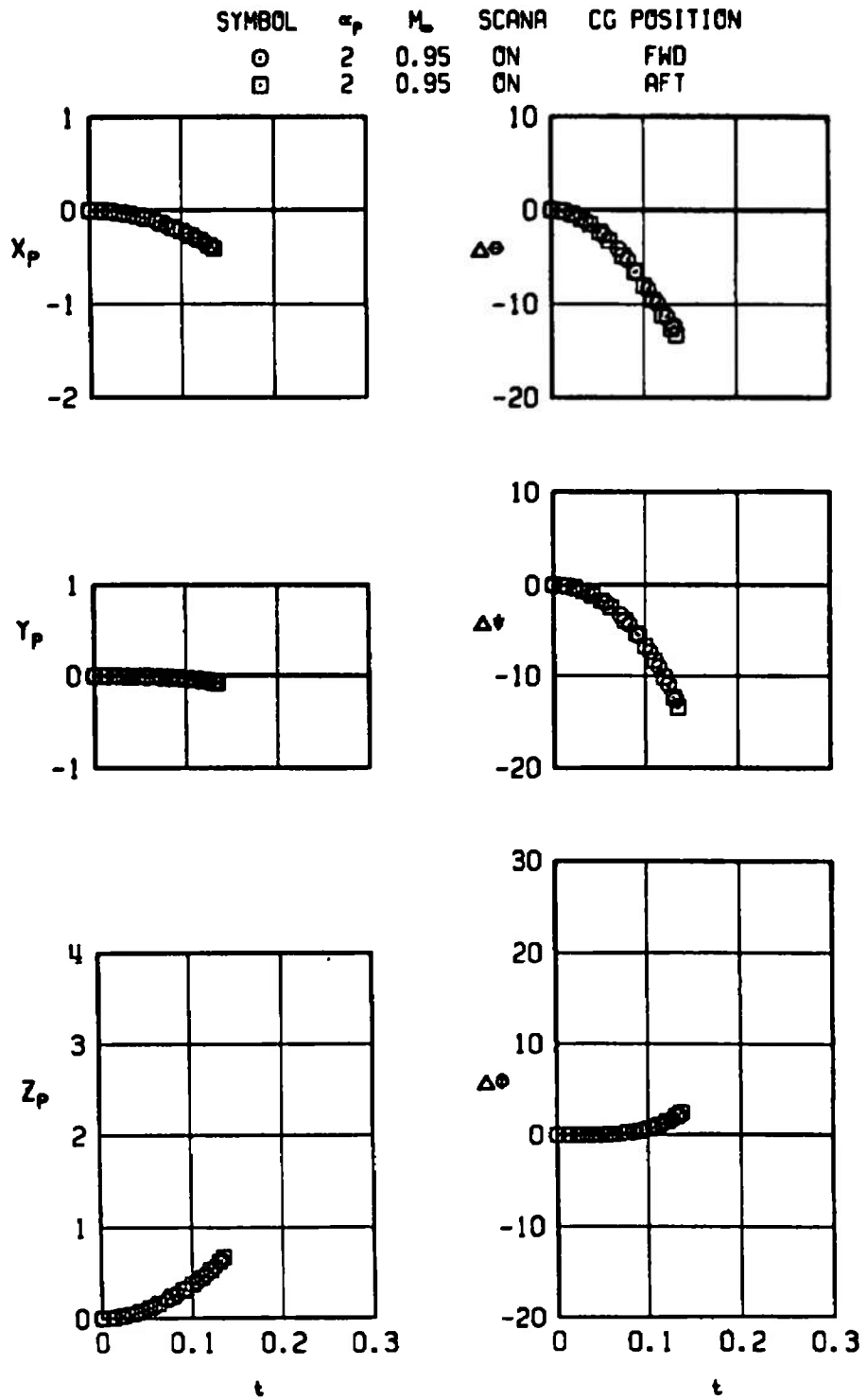


Figure 27. Effects of Mach number on trajectory data for the SUU-30 H/B; CG forward, BRU sta. 2, $\Delta_{LE} = 45$ deg, configuration 7.



a. $M_\infty = 0.80$

Figure 28. Effects of the CG position on trajectory data for the SUU-30 H/B; BRU sta. 2, $\Lambda_{LE} = 45$ deg, configuration 7.



b. $M_\infty = 0.95$
 Figure 28. Concluded.

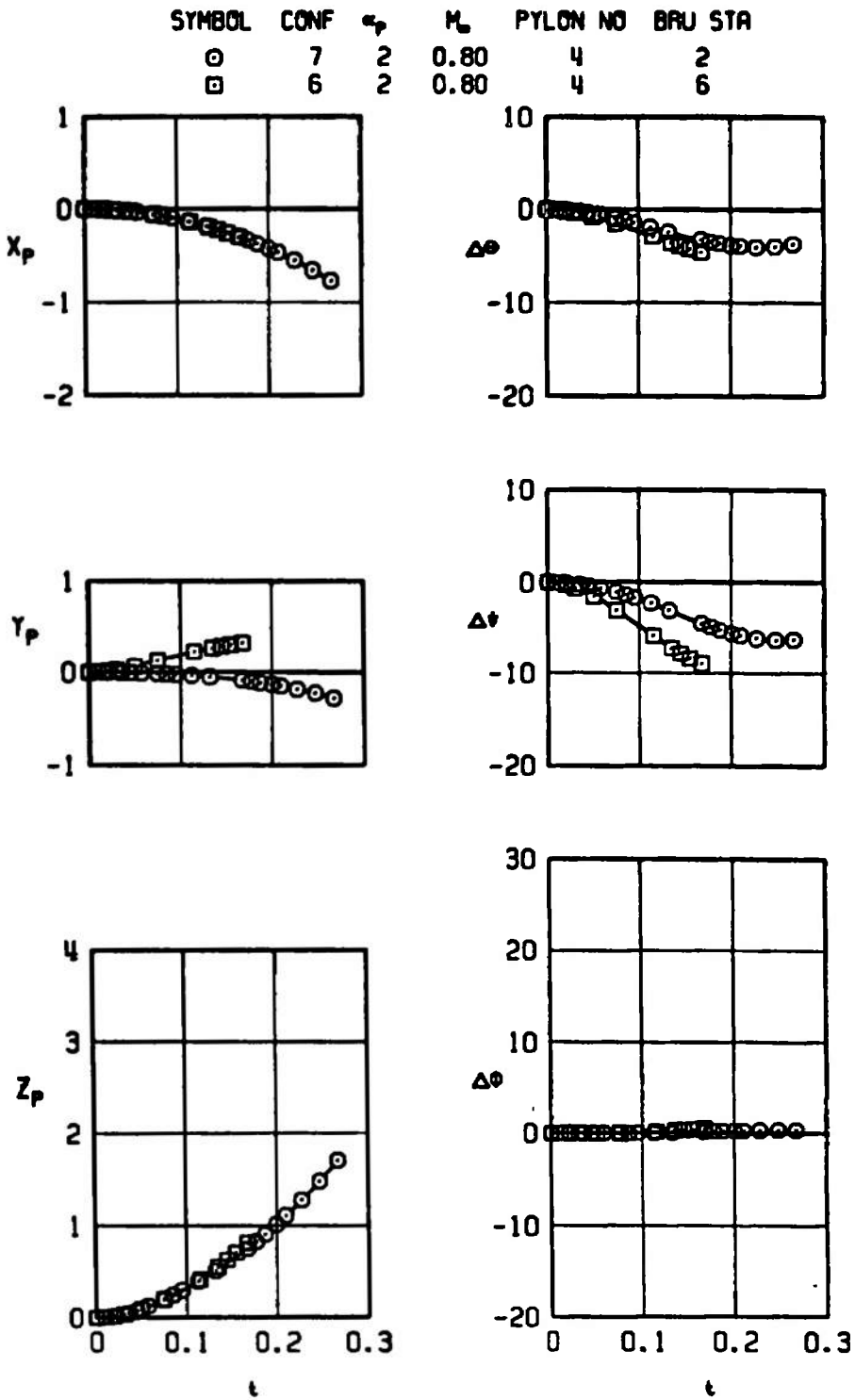
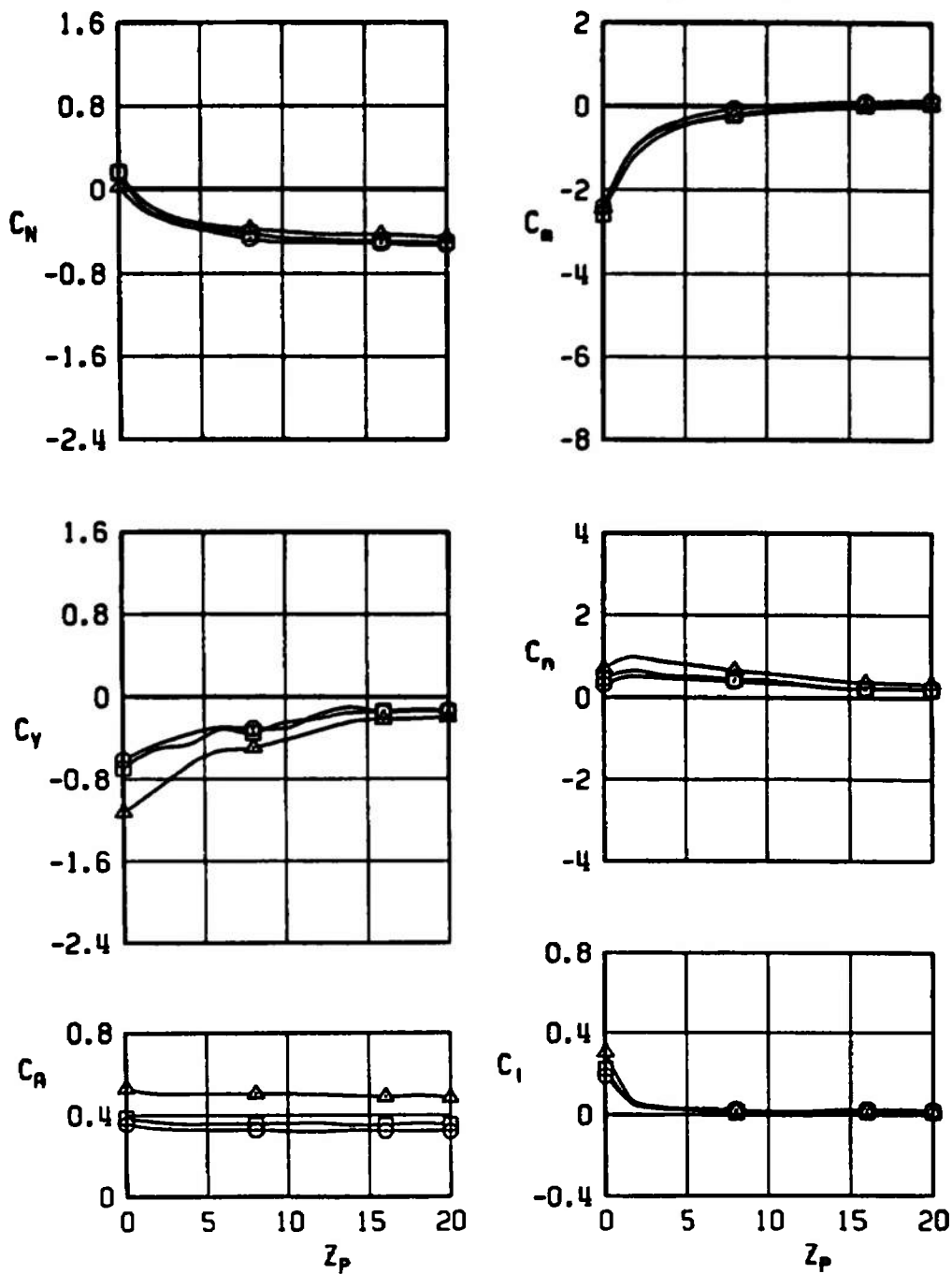


Figure 29. Effects of the carriage position on trajectory data for the SUU-30 H/B; CG forward, $\Lambda_{LE} = 45$ deg.

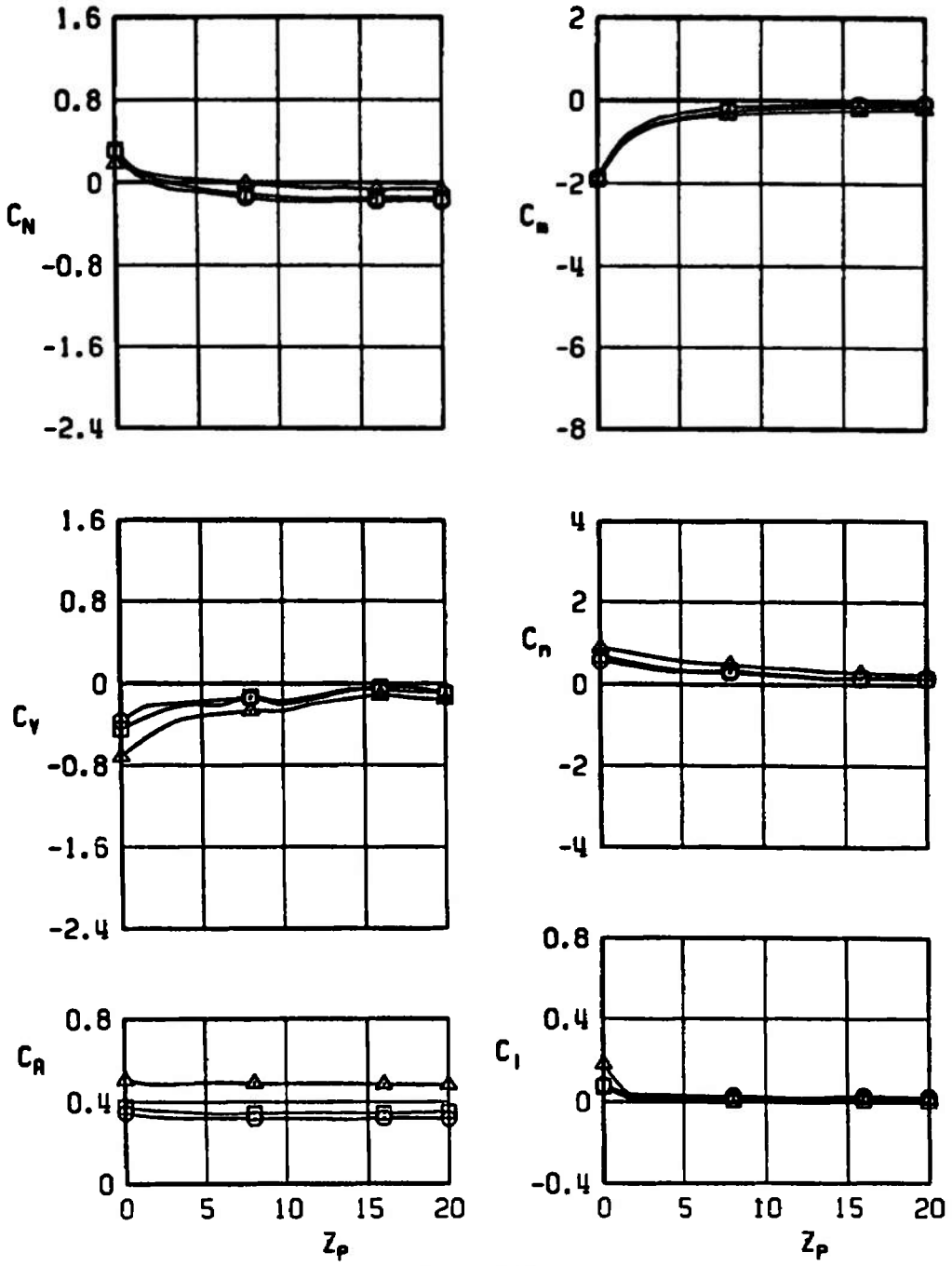
SYMBOL	α_p	M_∞	PYLON NO	Δ_{LE}
○	0	0.70	6	45
□	0	0.80	6	45
△	0	6	60	



a. $\alpha_p = 0$

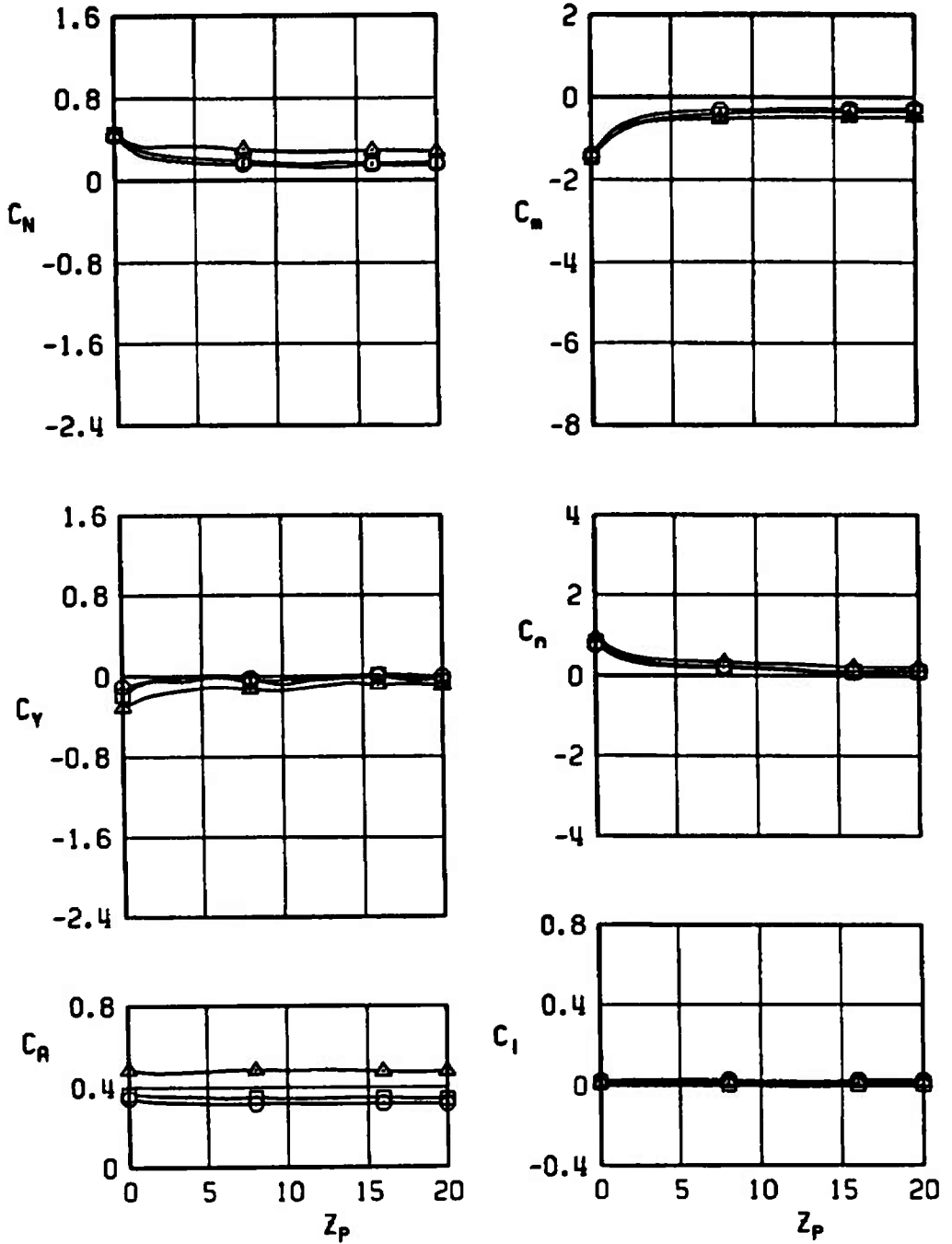
Figure 30. Effect of Mach number on aerodynamic coefficients for the MK-84 EOGB; SCANA on, configuration 4.

SYMBOL	α_p	M_∞	PYLON NO	Λ_{LE}
○	2	0.70	6	45
□	2	0.80	6	45
△	2	6	60	



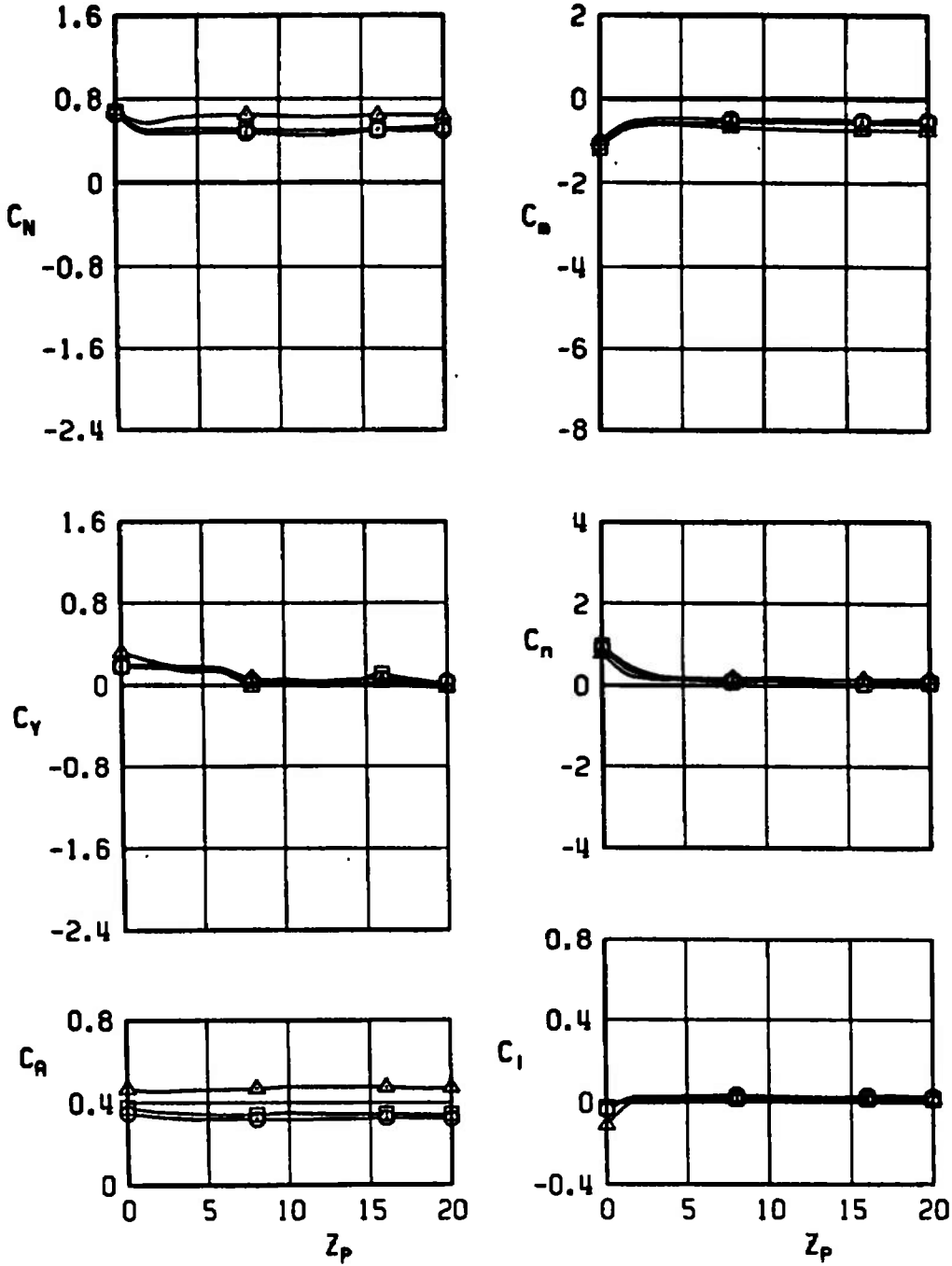
b. $\alpha_p = 2$
Figure 30. Continued.

SYMBOL	α_p	M_∞	PYLON NO	Δ_{LE}
○	4	0.70	6	45
□	4	0.80	6	45
△	4	0.95	6	60

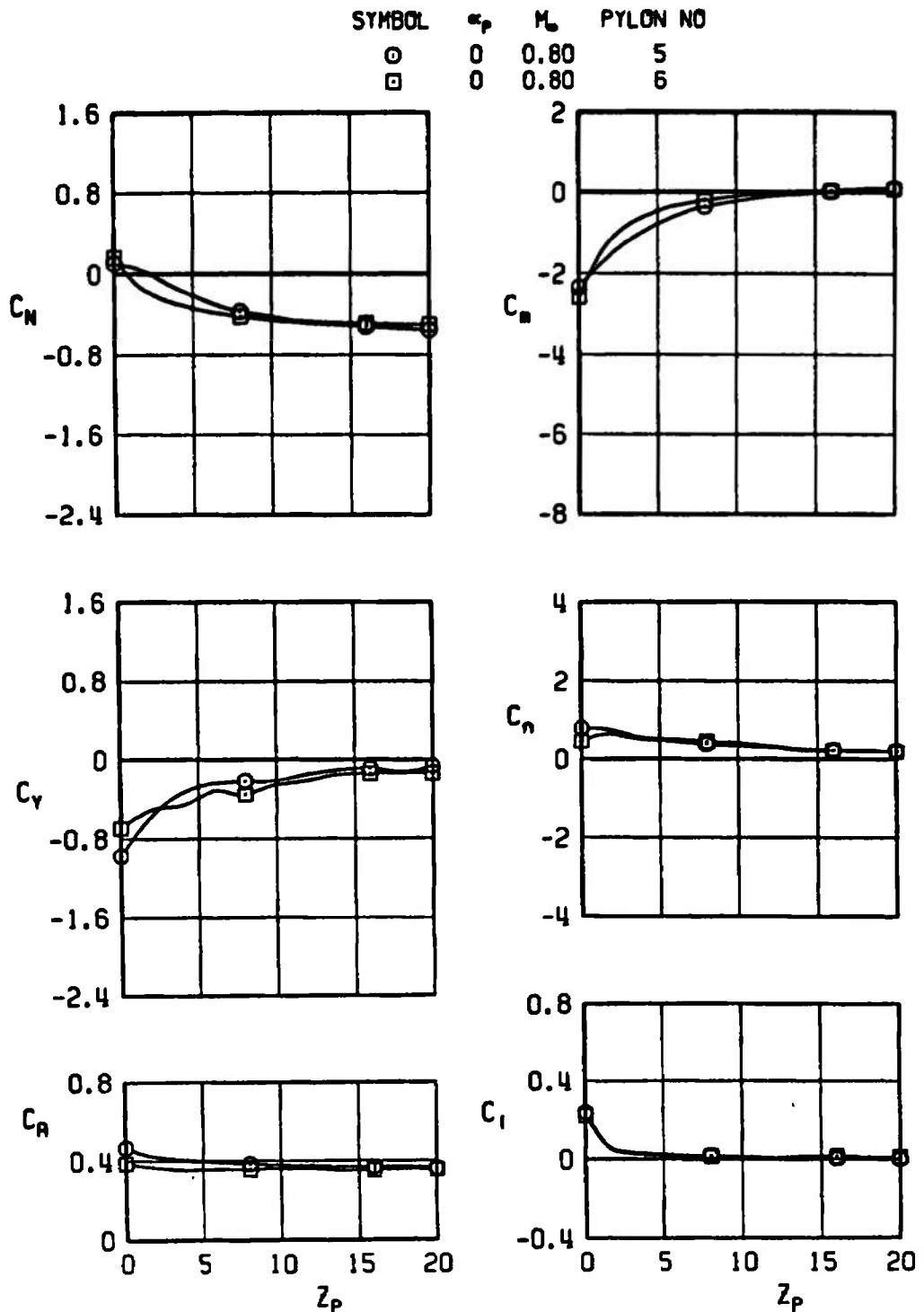


c. $\alpha_p = 4$
 Figure 30. Continued.

SYMBOL	a_p	M_∞	PYLON NO	Δ_{LE}
○	6	0.70	6	45
□	6	0.80	6	45
△	6	0.95	6	60

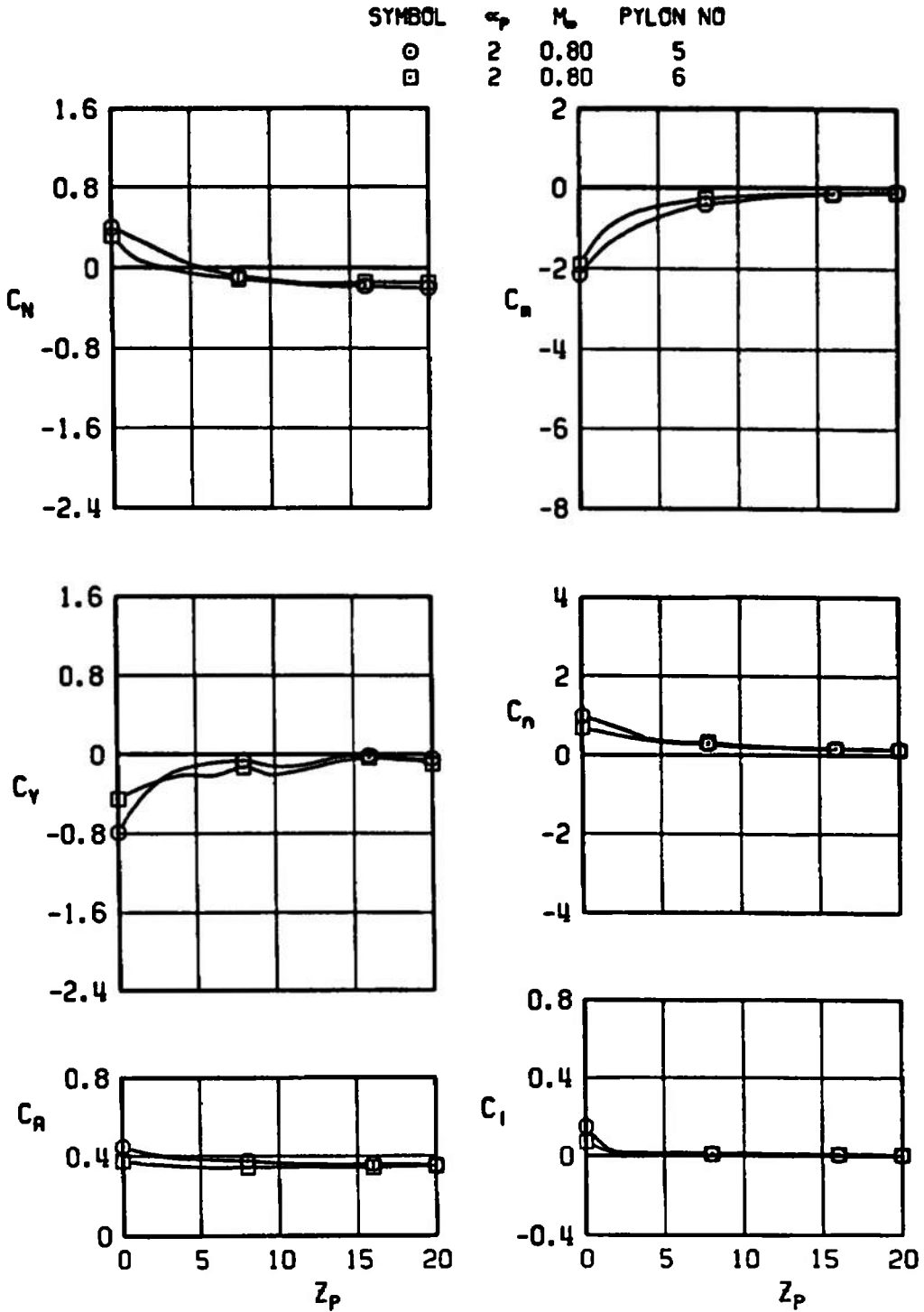


d. $a_p = 6$
 Figure 30. Concluded.

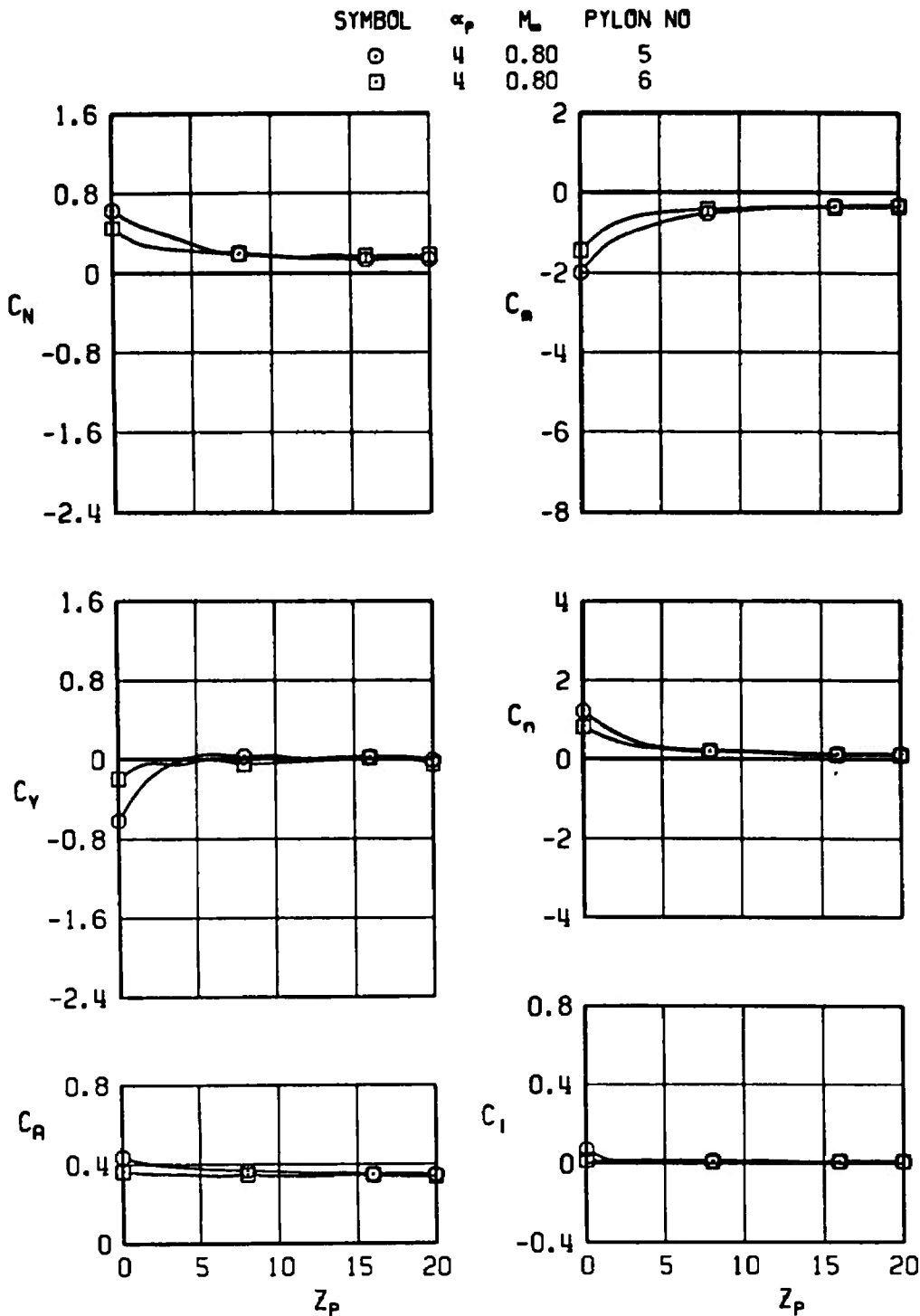


a. $\alpha_p = 0$

Figure 31. Effects of the carriage position on aerodynamic coefficients for the MK-84 EOGB; SCANA on, $\Lambda_{LE} = 45$ deg, configuration 4.

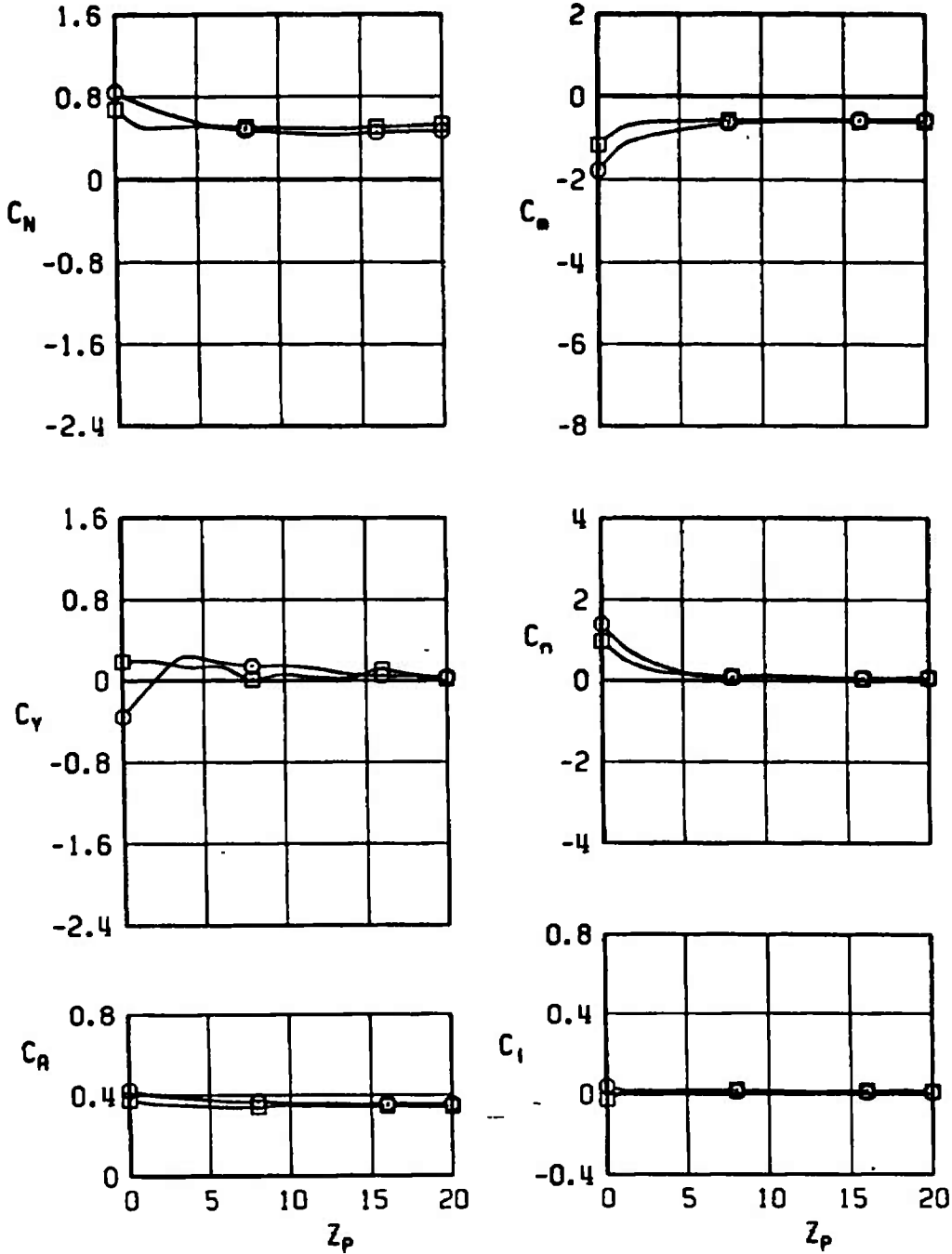


b. $\alpha_p = 2$
 Figure 31. Continued.

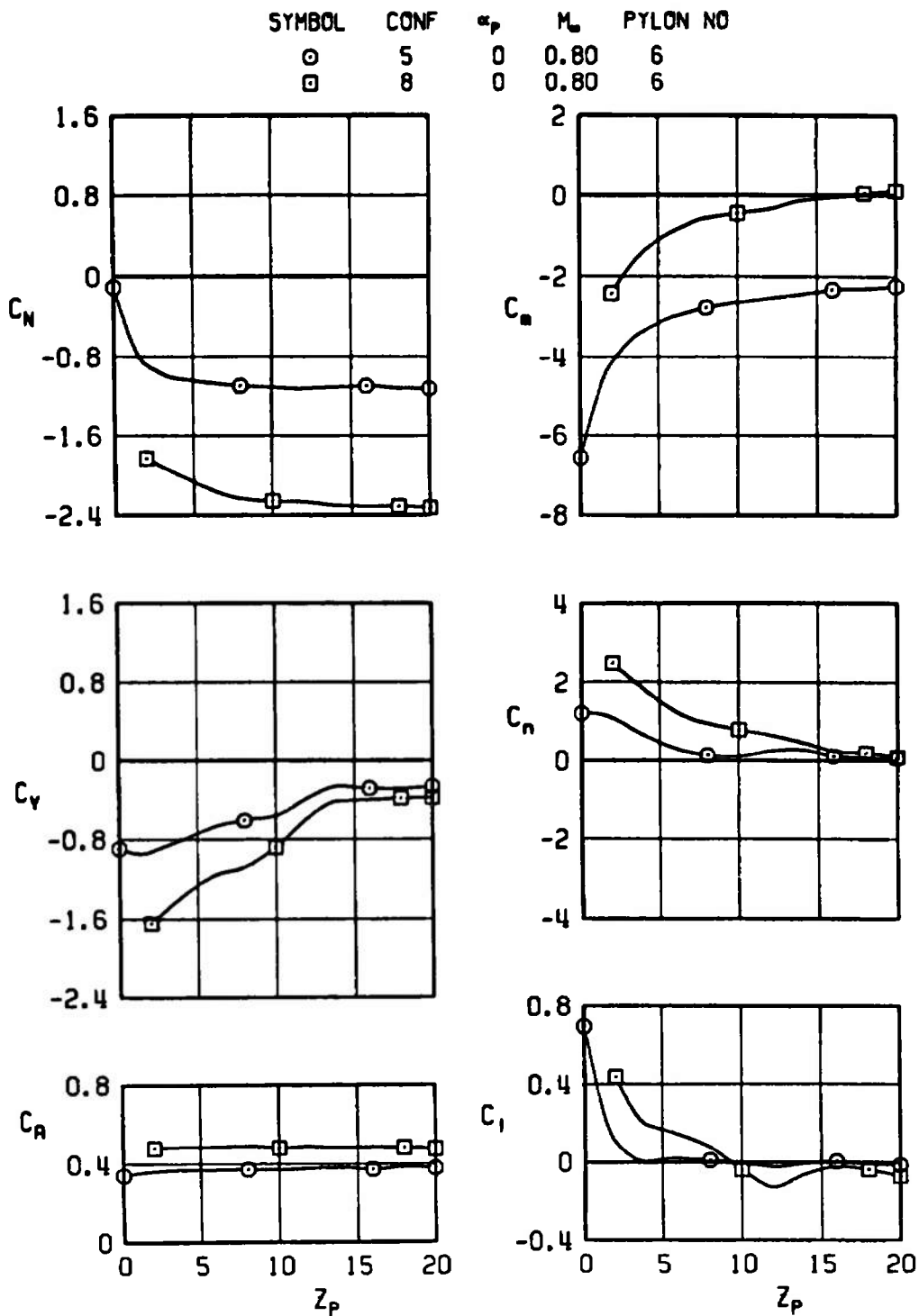


c. $\alpha_p = 4$
Figure 31. Continued.

SYMBOL	α_p	M_∞	PYLON NO
○	6	0.80	5
□	6	0.80	6

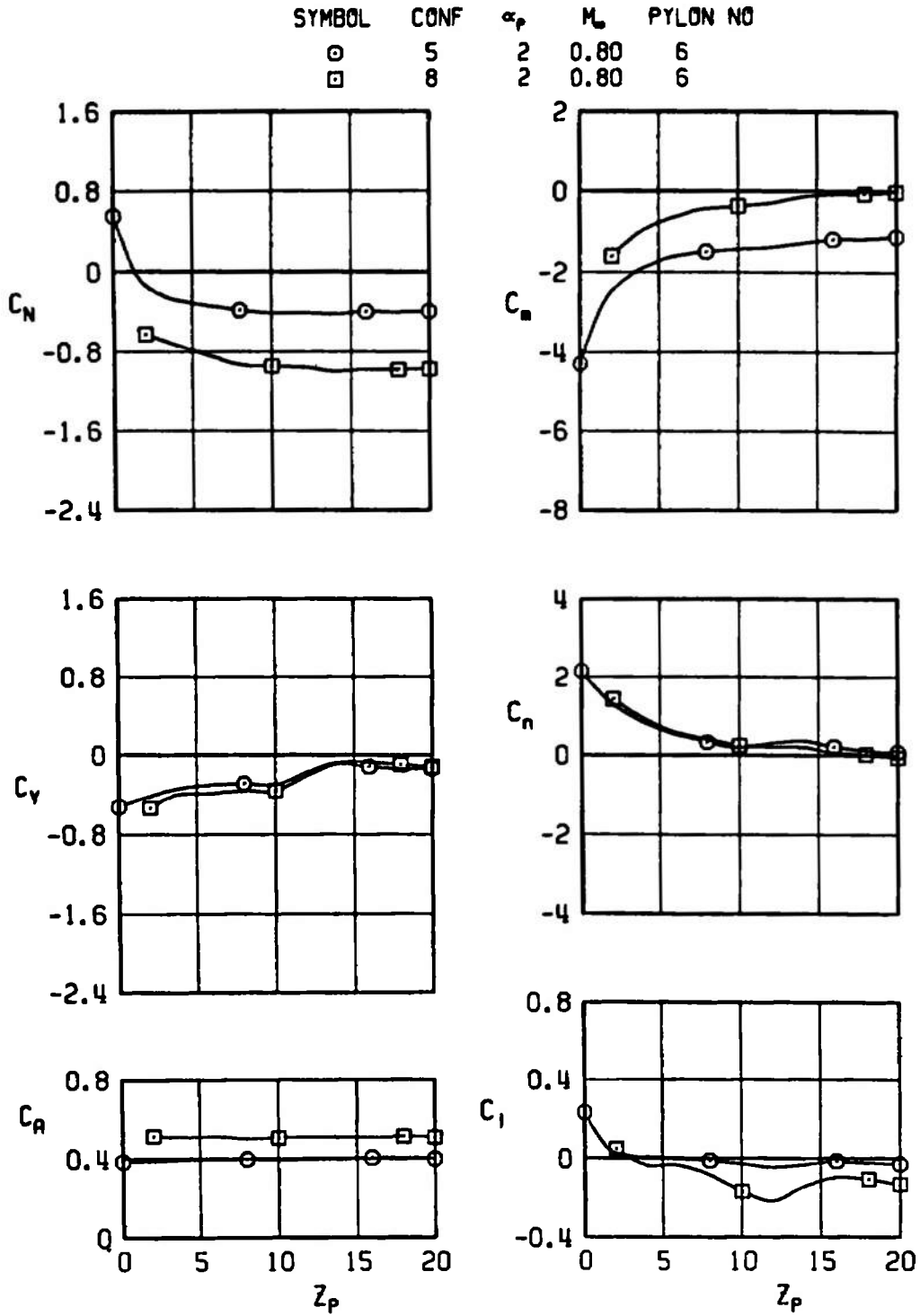


d. $\alpha_p = 6$
Figure 31. Concluded.

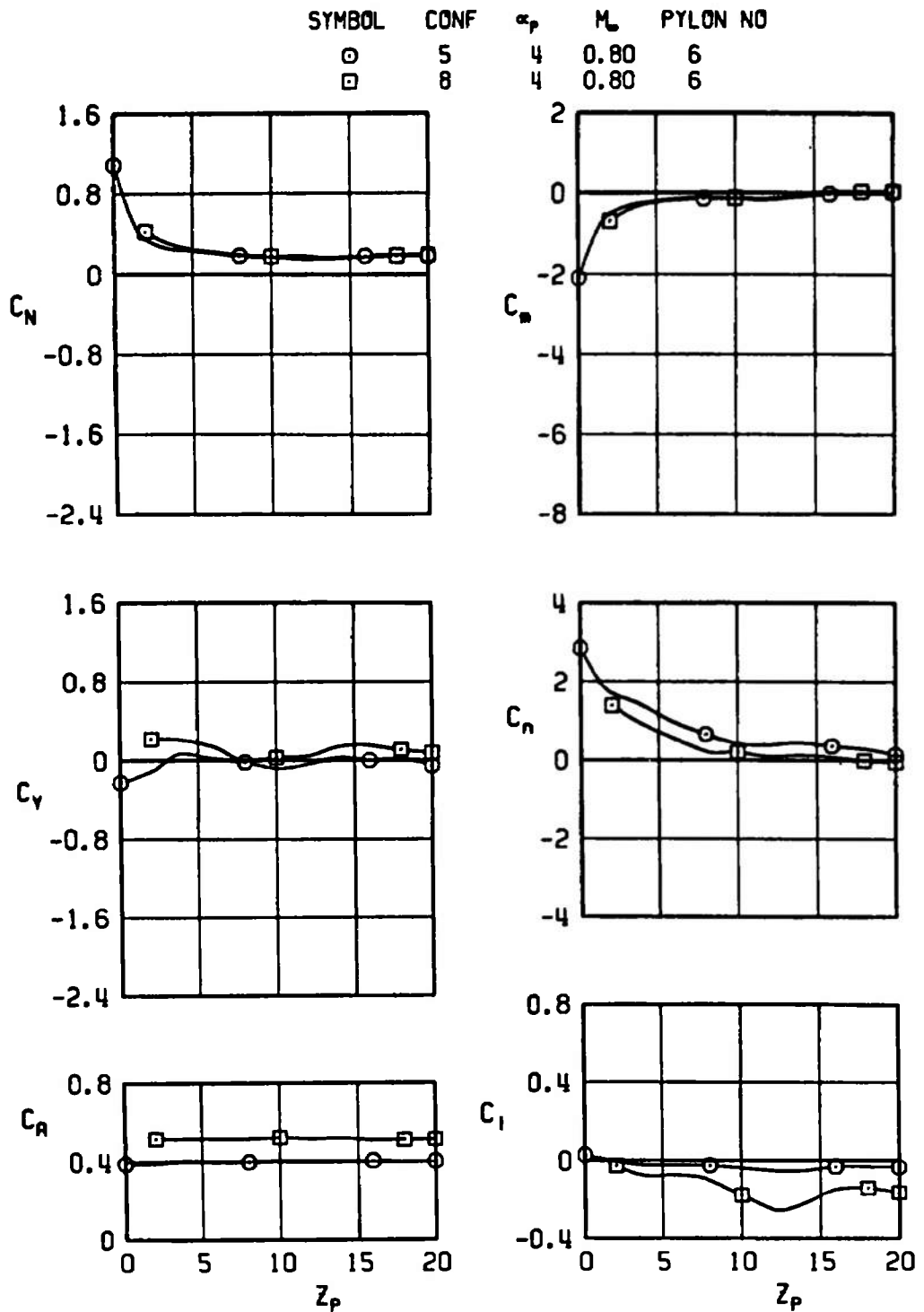


a. $\alpha_p = 0$

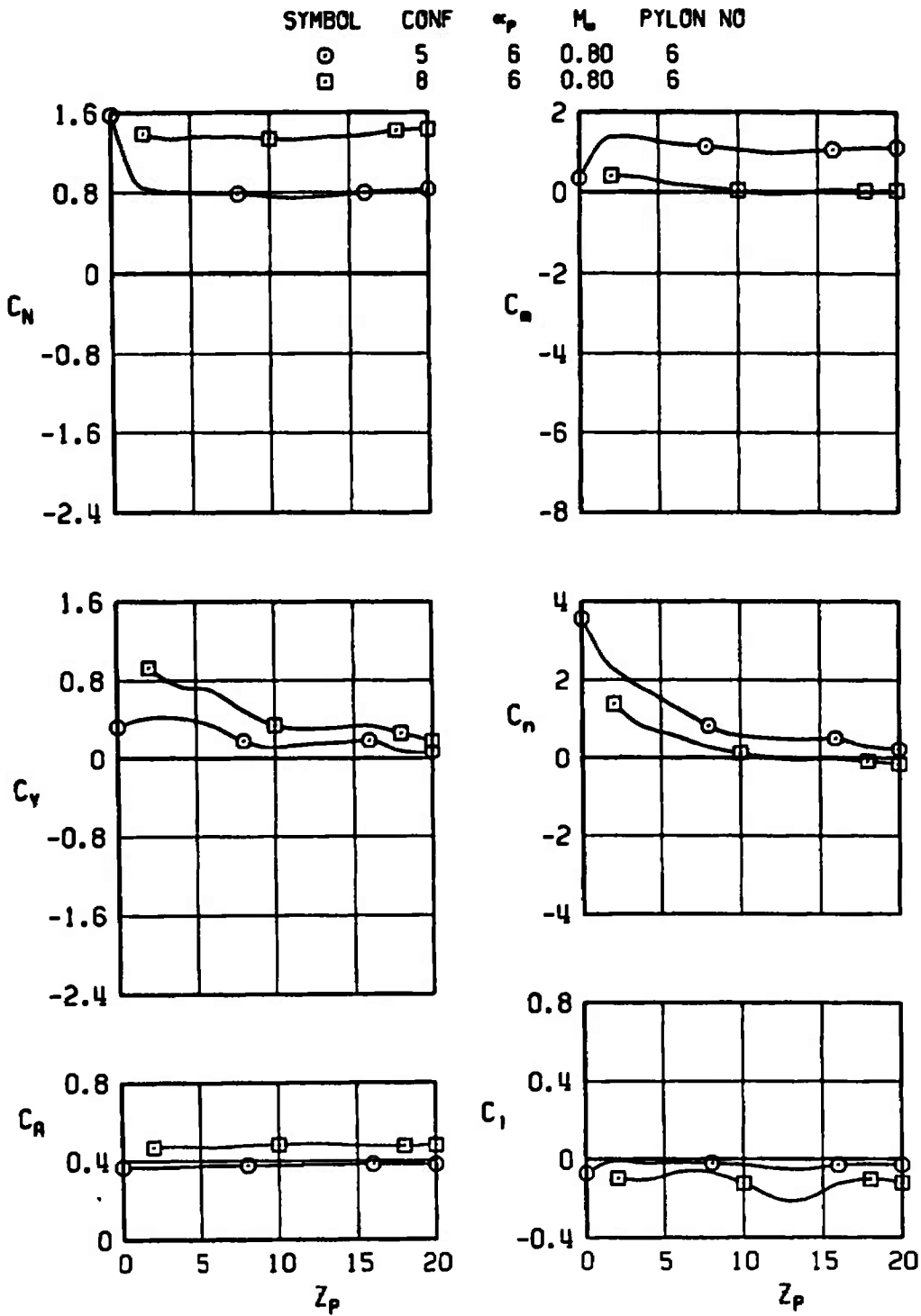
Figure 32. Effect of wing tip extensions on aerodynamic coefficients for the MK-84 Super HOBOS; SCANA on, $\Lambda_{LE} = 45$ deg.



b. $\alpha_p = 2$
 Figure 32. Continued.



c. $\alpha_p = 4$
Figure 32. Continued.



d. $\alpha_p = 6$
 Figure 32. Concluded.

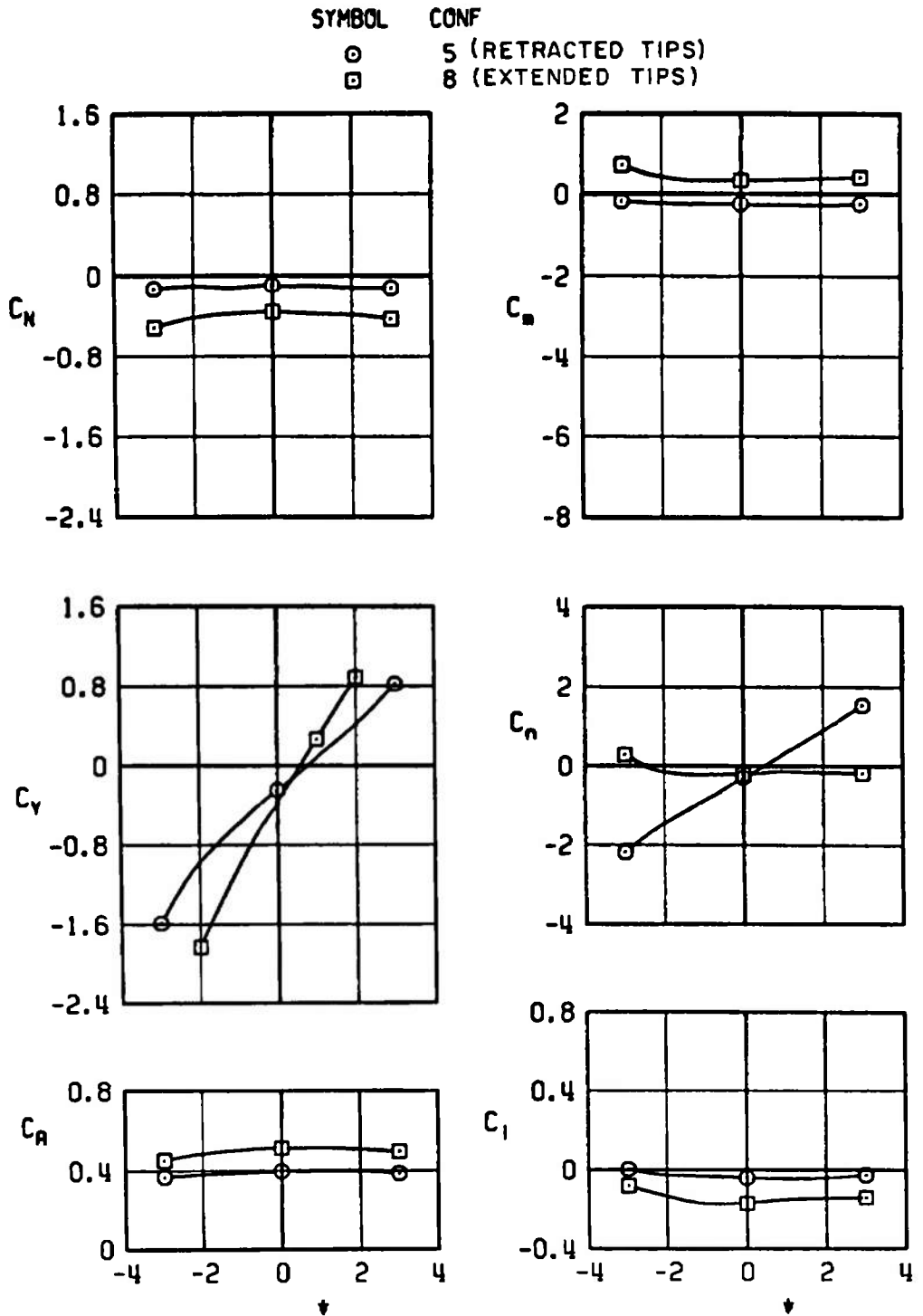


Figure 33. Free-stream data for the MK-84 Super HOBOS, $M_\infty = 0.80$.

Table 1. Identification of Test Conditions
a. Trajectory

 F-111				CONF. NO.	α_P	M_{∞}	ALT.	Δ_{LE}	CANARDS	CG POSITION	SCANA	$\bar{\theta}$
			● LGB	1	2°	0.75	5000	26°	OFF	NA	OFF	0
● LGB					↓	↓	↓					
↓					3°	0.60	0					
			● LGB		↓	↓	↓					
			↓		7°	0.40	3000					
● LGB					↓	↓	↓		↓			
↓									ON			
			● LGB		↓	↓	↓					
			↓		3	0.60	0					
● LGB					↓	↓	↓					
↓					2°	0.75	5000					
	● LGB				↓	↓	↓					
			● LGB		↓	↓	↓				↓	
	● LGB				7°	0.40	3000				ON	
			● LGB		↓	↓	↓	↓	↓	↓	↓	↓

Table 1. Continued
a. Continued

 F-111				CONF. NO.	α_P	M_{∞}	ALT.	Δ_{LE}	CANARDS	CG POSITION	SCANA	$\bar{\theta}$
●				1	2°	0.75	5000	26°	ON	NA	ON	0
	●					0.80	3000	45°	OFF		OFF	
●						↓	↓	↓				
↓						0.95						
			●			↓	↓	↓				
			↓			1.30	18000	60°				
●						↓	↓					
↓						1.10	12000					
			●			↓	↓					
			↓			0.95	3000					
●						↓	↓					
↓									ON			
			●			↓	↓					
			↓			1.10	12000					
●						↓	↓					
↓						1.30	18000					

Table 1. Continued
a. Continued

				CONF. NO.	α_P	M_{∞}	ALT.	Δ_{LE}	CANARDS	CG POSITION	SCANA	$\bar{\theta}$
			● LGB	1	2°	1.30	18000	60°	ON	NA	OFF	0
● LGB			● LGB	↓	↓	0.95	3000	↓	↓	↓	ON	↓
			↓	↓	↓	1.10	12000	↓	↓	↓	↓	↓
● LGB			↓	↓	↓	1.30	18000	↓	↓	↓	↓	↓
● LGB	○ LGB	SUU 30	● LGB	2	7°	0.40	3000	26°				
↓	↓	↓	● LGB	↓	↓	↓	↓	↓	↓	↓	↓	↓
↓	↓	↓	↓	↓	2°	0.75	5000	↓	↓	↓	↓	↓
			↓	3		0.80	3000	45°			OFF	↓
			↓	↓	↓	↓	↓	↓	↓	↓	↓	-45
● LGB			↓	↓	↓	↓	↓	↓	↓	↓	↓	0
↓	↓	↓	↓	↓	↓	0.95	↓	↓	↓	↓	↓	↓
↓	↓	↓	↓	↓	↓	↓	↓	↓	↓	ON	↓	↓
			● LGB	↓	↓	↓	↓	↓	↓	↓	↓	↓

Table 1. Continued
a. Continued

 F-111				CONF. NO.	α_P	M_{∞}	ALT.	Δ_{LE}	CANARDS	CG POSITION	SCANS	$\bar{\theta}$
● LGB			SUU 30	3	2°	0.95	3000	45°	ON	NA	ON	0
↓						0.80						
	● LGB											
● EGB				4					NA			↓
↓												-45
	● EGB											↓
	↓											0
												↓
												-45
						0.95						0
	● EGB											
● EGB												
						0.80						
	● EGB							60°				
	● EGB											
● EGB												

Table 1. Continued
a. Continued

				CONF. NO.	α_p	M_{∞}	ALT.	Λ_{LE}	CANARDS	CG POSITION	SCANA	$\bar{\theta}$
● EOGB		SUU 30	○ ○	4	2°	0.95	3000	60°	NA	NA	ON	0
	● EOGB			↓	↓	↓	↓	↓	↓	↓	↓	↓
			● EOGB	↓	↓	↓	↓	↓	↓	↓	↓	↓
			↓	↓	↓	1.10	12000	↓	↓	↓	↓	↓
	● EOGB			↓	↓	↓	↓	↓	↓	↓	↓	↓
● EOGB				↓	↓	↓	↓	↓	↓	↓	↓	↓
↓				↓	↓	1.30	18000	↓	↓	↓	↓	↓
	● EOGB			↓	↓	↓	↓	↓	↓	↓	↓	↓
			● EOGB	↓	↓	↓	↓	↓	↓	↓	↓	↓
	SUU 30	△	SUU 30	△	6	0.80	3000	45°		FWD		
	↓		↓		↓	↓	↓	↓		AFT	↓	
	SUU 30	△	SUU 30	△	7						OFF	
	↓		↓		↓	↓	↓	↓		FWD		
				↓	↓	↓	↓	↓		↓		
				↓	↓	0.95				↓		
				↓	↓	↓	↓	↓		AFT	↓	
				↓	↓	↓	↓	↓		FWD	ON	↓
				↓	↓	0.80				↓		

Table 1. Continued
 b. Aerodynamic Loads Survey

				CONF. NO.	α_P	M_{∞}	ALT.	Δ_{LE}	CANARDS	CG POSITION	SCANA	$\bar{\theta}$
EOGB			SUU 30	4	0°	0.80	NA	45°	NA	NA	ON	NA
↓					1°							
					2°							
					3°							
					4°							
					6°							
EOGB					0°							
					1°							
					2°							
					3°							
					4°							
					6°							
					0°	0.70						
					1°							
					2°							
					3°							

Table 1. Continued
b. Continued

 F-111				CONF. NO.	α_P	M_{∞}	ALT.	Δ_{LE}	CANARDS	CG POSITION	SCANA	$\bar{\theta}$
	● EOGB		SUU 30	4	4°	0.70	NA	45°	NA	NA	ON	NA
	↓				6°							
	● EOGB				0°							
					1°							
					2°							
					3°							
					4°							
					6°							
					0°	0.95		60°				
					1°							
					2°							
					3°							
					4°							
					6°							
	+ ● S. HOBOS			5	0	0.80		45°				
	↓				1°							

+ Retracted Tips

Table 1. Concluded
b. Concluded



 F-111				CONF. NO.	α_P	M_{∞}	ALT.	Δ_{LE}	CANARDS	CG POSITION	SCANA	$\bar{\theta}$
+ ●	S. HOBOS	SUL	30	5	2°	0.80	NA	45°	NA	NA	ON	NA
↓		↓		↓	3°							
↓		↓		↓	4°							
↓		↓		↓	6°							
* ●	S. HOBOS			8	0°							
↓		↓		↓	1°							
↓		↓		↓	2°							
↓		↓		↓	3°							
↓		↓		↓	4°							
↓		↓		↓	6°							

+ Retracted Tips
* Extended Tips

Table 2. Identification of Full-Scale Store Parameters

Parameter	MK-84 LGB	MK-84 EOGB	MK-84 Super HOBOS	SUU-30 Forward CG	SUU-30 Aft CG
\bar{m}	63.447	70.341	NA	25.5	25.5
X_{CG}	8.267	6.604	7.224	3.208	3.333
Suspension	30-in.	30-in.	30-in.	14-in.	14-in.
I_{yy}	406	524	NA	60.350	60.350
I_{zz}	406	524	↓	60.770	60.770
I_{xx}	24	25	↓	5.70	5.70
b	1.5	1.5	1.5	1.343	1.343
s	1.767	1.767	1.767	1.417	1.417
F_{Z1}	4400	4400	NA	900	900
F_{Z2}	4400	4400	↓	500	500
Z_E	0.343	0.343		0.25	0.25
X_{L1}	0.592	0.813		0.375	0.500
X_{L2}	-1.075	-0.853		-0.792	-0.667
C_{mq}	-100	-110		-54	-54
C_{nr}	-100	-110		-54	-54
C_{lp}	-0.71	-10	↓	-2	-2

Table 3. Store Positions and Orientations for the Aerodynamic Loads Survey Data

$$X_p = 0$$

$$Y_p = 0$$

$$Z_p = 0, 2, 4, 6, 8, 10, 12, 14, 16, 18, 20$$

$$\Delta\theta = -3, -2, -1, 0, 1, 2, 3$$

$$\Delta\psi = 0$$

$$\Delta\phi = 0$$

Note: The MK-84 Super HOBOS with extended tips was tested at the above positions with the exception of $Z_p = 0$.

NOMENCLATURE

BL	Aircraft buttock line from plane of symmetry, in., model scale
b	Store reference dimension, ft full scale
C_A	Store axial-force coefficient, axial force/ $q_\infty S$
C_ℓ	Store rolling-moment coefficient, rolling moment/ $q_\infty S b$
$C_{\ell p}$	Store roll-damping derivative, $dC_\ell/d(pb/2V_\infty)$
C_m	Store pitching-moment coefficient, referenced to the store cg, pitching moment/ $q_\infty S b$
$C_{m q}$	Store pitching-damping derivative, $dC_m/d(qb/2V_\infty)$
C_N	Store normal-force coefficient, normal force/ $q_\infty S$
C_n	Store yawing-moment coefficient, referenced to the store cg, yawing moment/ $q_\infty S b$
$C_{n r}$	Store yaw-damping derivative, $dC_n/d(rb/2V_\infty)$
C_y	Store side-force coefficient, side force/ $q_\infty S$
FS	Aircraft fuselage station, in., model scale
F_{z_1}	Forward ejector force, lb
F_{z_2}	Aft ejector force, lb
I_{xx}	Full-scale moment of inertia about the store X_B axis, slug-ft ²
I_{yy}	Full-scale moment of inertia about the store Y_B axis, slug-ft ²
I_{zz}	Full-scale moment of inertia about the store Z_B axis, slug-ft ²
M_∞	Free-stream Mach number
m	Full-scale store mass, slugs
p	Store angular velocity about the X_B axis, radians/sec
p_∞	Free-stream static pressure, psfa

q	Store angular velocity about the Y_B axis, radians/sec
q_∞	Free-stream dynamic pressure, psf
r	Store angular velocity about the Z_B axis, radians/sec
S	Store reference area, ft^2 , full scale
t	Real trajectory time from initiation of trajectory, sec
V_∞	Free-stream velocity, ft/sec
WL	Aircraft waterline from reference horizontal plane, in., model scale
X_p	Separation distance of the store cg parallel to the pylon axis system X_p direction, ft, full scale measured from the prelaunch position
X_{cg}	Full-scale cg location, ft from nose of store
X_{L1}	Forward ejector piston location relative to the store cg, positive forward of store cg, ft, full scale
X_{L2}	Aft ejector piston location relative to the store cg, positive forward of store cg, ft, full scale
Y_p	Separation distance of the store cg parallel to the pylon axis system Y_p direction, ft, full scale measured from the prelaunch position
ZE	Ejector stroke length, ft, full scale
Z_p	Separation distance of the store cg parallel to the pylon axis system Z_p direction, ft, full scale measured from the prelaunch position
α_p	Parent-aircraft model angle of attack relative to the free-stream velocity vector, deg
$\Delta\theta$	Angle between the store longitudinal axis and its projection in the X_p - Y_p plane, positive when store nose is raised as seen by pilot, deg
$\Delta\phi$	Angle between the projection of the store lateral axis in the Y_p - Z_p plane and the Y_p axis, positive for clockwise rotation when looking upstream, deg
$\Delta\psi$	Angle between the projection of the store longitudinal axis in the X_p - Y_p plane and the X_p axis, positive when the store nose is to the right as seen by the pilot, deg

- θ Simulated parent-aircraft climb angle, angle between the flight direction and the earth horizontal, deg. positive for increasing altitude
- Λ_{LE} Angle between the leading edge of the wing and a line perpendicular to the aircraft plane of symmetry
- ψ Angle between the wind axis and the projection of this axis on the model Z_B - X_B plane

PYLON AXIS SYSTEM COORDINATES

Directions

- X_p Coincident with the store longitudinal axis at the carriage position, positive is forward as seen by the pilot
- Y_p Perpendicular to the aircraft plane of symmetry, positive is to the right as seen by the pilot
- Z_p Perpendicular to both the X_p and Y_p axes, positive direction is downward

STORE BODY-AXIS SYSTEM COORDINATES

Directions

- X_B Parallel to the store longitudinal axis, positive direction is upstream in the prelaunch position
- Y_B Perpendicular to the store longitudinal axis and parallel to the pylon-axis system X_p - Y_p plane when the store is at zero roll angle, positive direction is to the right looking upstream when the store is at zero yaw and roll angles
- Z_B Perpendicular to both the X_B and Y_B axes, positive direction is downward as seen by the pilot when the store is at zero pitch and roll angles

The store body-axis system origin is coincident with the store cg and moves with the store during separation from the parent airplane. The X_B , Y_B , and Z_B coordinate axes rotate with the store in pitch, yaw, and roll so that mass moments of inertia about the three axes are not time-varying quantities.